1-1-2013

Characterization of a Test Stand for Evaluating Performance and Qualifying Metal Media Filters under ASME AG-1

John Andrew Wilson

Characterization of a test stand for evaluating performance and qualifying metal media filters under ASME AG-1

By

John A. Wilson

A Thesis
Submitted to the Faculty of
Mississippi State University
in Partial Fulfillment of the Requirements
for the Degree of Masters of Science
in Mechanical Engineering
in the Department of Mechanical Engineering

Mississippi State, Mississippi

December 2013

Characterization of a test stand for evaluating performance and qualifying metal media filters under ASME AG-1

By

John A. Wilson

Approved:

_____

Charles A. Waggoner
(Major Professor)

_____

W. Glenn Steele Jr.
(Committee Member)

_____

Pedro J. Mago
(Committee Member)

_____

Kalyan K. Srinivasan
(Graduate Cooridnator)

_____

Achille Messac
Dean of
Bagley College of Engineering

Name: John A. Wilson

Date of Degree: December 14, 2013

Institution: Mississippi State University

Major Field: Mechanical Engineering

Major Professor: Charles A. Waggoner

Title of Study: Characterization of a test stand for evaluating performance and qualifying metal media filters under ASME AG-1

Pages in Study: 196

Candidate for Degree of Masters of Science

The Institute of Clean Energy Technology (ICET) at Mississippi State University was awarded a contract by the DOE to design, fabricate, assemble, and characterize a research grade test stand to assist in the development of ASME AG-1 Section FI Metal Media Filters. The major barriers to completing the code section is development of a test stand for collecting data necessary to specify performance requirements for use and for filter qualification. Currently there is not a test stand capable of performing this testing. Performance criteria for the FI test stand were developed by the Section FI project team and ICET. These performance criteria were used to create a test stand to collect the data necessary to get Section FI balloted and approved.

DEDICATION

This thesis is dedicated to my parents Jett and Anne Wilson. They raised me in a Christian home and always provided a good example of how to live my life. Their support throughout my undergraduate and graduate career has been invaluable in my success.

ACKNOWLEDGEMENTS

I would like to thank my advisor Dr. Charles Waggoner for his help and guidance during this project. Much thanks is due to the staff at The Institute for Clean Energy Technology for making completion of this project possible.

I would like to acknowledge the International Society for Nuclear Air Treatment Technologies for providing initial funding for this project as well as the Department of Energy and the National Nuclear Security Administration for funding for this project.

TABLE OF CONTENTS

LIST OF TABLES

LIST OF FIGURES

CHAPTER I

INTRODUCTION

Project overview

High efficiency particulate air (HEPA) filters are routinely employed in the United States (U.S.) to control particulate matter (PM) emissions from processes that involve management or treatment of radioactive materials. Facilities within the US Department of Energy (DOE) complex are particularly likely to make use of HEPA filters in the processing of exhaust gases prior to release to the environment [1].

Hazards associated with radioactive materials involved in nuclear applications necessitate specialized containment systems to provide safety for employees, the general public, and the environment. Nuclear grade HEPA filters are used in these specialized containment systems as the last line of defense against the release of very small radioactive particles. A nuclear grade HEPA filter is considered to be a throwaway, extended-medium, dry-type filter with: (1) a minimum particle removal efficiency of 99.97% for a 0.3 μm monodisperse particle cloud, (2) a maximum clean filter resistance of 1 inch water column (w.c.) when operated at rated airflow capacity and (3) a rigid frame extending the full depth of the medium. [2]. Current nuclear grade HEPA filters are constructed of glass fiber media and are one time use filters that must be disposed of safely when they reach their usable limit.[2]

The usable limit for glass fiber HEPA filters is specified as when the filter reaches 3 to 5 inches w.c. greater than the initial differential pressure across the filter [1]. The American Society of Mechanical Engineers (ASME) standard AG-1 lays out requirements for filters that may be used for HEPA filtration in containment ventilation systems. AG-1 contains two sections dealing with nuclear grade HEPA filters. These sections are the standard for glass fiber media filters. AG-1 is currently in the process of adding a non mandatory service life for fibrous glass HEPA filters as well as additional sections to broaden the filter types available for nuclear applications [3].

Statement of need

The Institute for Clean Energy Technology (ICET) was awarded a contract by the Department of Energy (DOE) to facilitate the necessary tasks for balloting ASME AG-1 Code on Nuclear Air and Gas Treatment Section FI for metal media filters. Development of Section FI requires infrastructure to qualify FI filters and generation of performance data to complete the code section. Initial funding for this project was provided by the International Society for Nuclear Air Treatment Technologies (ISNATT). Additional funding was provided by the U.S. DOE under cooperative agreement DE-FC01-06EW07040 and the National Nuclear Security Administration (NNSA) under contract number DE-FC01-06EW07040-06040310.

Objectives

The objective of this project was to develop a research grade test stand capable of achieving data needs to complete Section FI. Tasks for this project included:

- Identify performance criteria of the research grade test stand.

- Test stand design, fabrication, assembly, and characterization
- Development of qualification protocols
- Collection of data to facilitate code development

CHAPTER II

HISTORY OF HEPA FILTRATION

Origins of HEPA filtration

Development of HEPA filtration technology was triggered by the need for protection against chemical agents used in World War I and II [4]. British and American forces used gas masks with filter media composed of resin coated-wool [5]. British troops captured several German made gas masks during World War II and sent them to the U.S. Army Chemical Warfare Service Laboratory (CSW) for analysis [5]. The captured filters used a medium composed of a blend of fine asbestos fibers and cellulose fibers [4]. The asbestos and cellulose fiber filters were found to be superior to media used by the United States or Britain because of their high particle retention characteristics, acceptable resistance to airflow, good dust storage, and resistance to plugging from oil-type screening smokes [1]. Media modeled after the captured German product was adapted by US and British military [4].

The threat of chemical warfare directed against army operational headquarters resulted in using the filter medium for large scale filters capable of higher flow rates [1]. Filters were constructed with deep pleats of continuous medium separated by spacer panels and sealed into a rigid rectangular frame using rubber cement [2].

Filters, originally designed to keep harmful particulate matter out of army operational head quarters were used to contain radioactive particulate matter during the

Manhattan Project. The U.S. Army Chemical Corps was the sole supplier of high performance filters for the Manhattan Project [5]. In 1948, the graphite moderated, air cooled nuclear reactor at Oak Ridge National Laboratory was fitted with the army designed filters after radioactive particles up to 600 μm in diameter were discovered on the ground near the exhaust stacks [1]. These actions laid initial groundwork for containment ventilation systems.

In the late 1940s HEPA filters were known as Atomic Energy Commission (AEC) filters, nuclear filters, absolute, super-inception, or super-efficiency filters [1]. The term absolute used to describe high efficiency filters is misleading because the media, although highly efficient, does not stop all particles. The term absolute was dropped and the filters began being known as high efficiency particulate air filters (HEPA). The term HEPA became popular from an AEC report by Humphrey Gilbert titled, "High-Efficiency Particulate Air Filter Units, Inspection, Handling, Installation" in 1961 [1].

Regulation of filters used exclusively in nuclear facilities became necessary to ensure consistency among manufacturers. The U.S. military developed two military codes for nuclear HEPA filters. The codes MIL-F-51068 Filter, Particulates, High-Efficiency, Fire Resistant for fire-resistant filters and MIL-F-51079 Filter Medium, Fire-Resistant, High-Efficiency, for glass fiber medium were issued in 1962 and 1963 respectively [1]. Nuclear power plants began to be seen as huge liabilities at the end of the Cold War with realization of the problems associated with cleaning up radioactive waste and the wide spread contamination at Chernobyl [6].Advancements in materials, instruments, and changing requirements made it rational for standards to be consolidated. ASME issued AG-1, Code on Nuclear Air and Gas Treatment, 1st Edition in 1984 to

provide standards to the nuclear industry [2]. The standards for HEPA filters patterned after MIL-SPEC standards were incorporated into Section FC of AG-1 in 1997. Section FC was added to AG-1 to better establish performance requirements for the nuclear industry [1]. The U.S. Department of Defense (DOD) consensus standards MIL-F-51068 and MIL-F-51079 became obsolete and were superseded in 1997 by AG-1 Section FC [6].

ASME AG-1 addresses more filtration elements than just final stage HEPA filters since different types of filters are used in nuclear applications. Nuclear grade HEPA filters are described in ASME AG-1 Sections FC and FK [2]. Filters with lower efficiencies are used before the final stage of HEPAs to prolong life and protect the HEPA filters from damage [2]. Section FA discusses moisture separators that are used to remove liquid droplets from the air. However, they are not high efficiency filtration devices. Section FB and FJ discuss medium and low efficiency filters respectively that are used in nuclear facilities to reduce particulate matter loading on HEPA filters [2]. A final type of stage filters with HEPA efficiency that can be used are deep bed sand filters as described in Section FL [2].

Filtering efficiency

Filtration efficiency is the comparison of the upstream concentration of aerosols to the downstream concentration. Testing high efficiency filters typically involves two types of efficiency measurements. The overall filtering efficiency for all particle sizes measured is computed by simply comparing the total upstream concentration to the total downstream concentration. The second type of efficiency measurement is based on particle size. Overall efficiency gives a representation of the total efficiency of the filter

but does not demonstrate compliance to HEPA standards. HEPA standards require the filter to have a filtering efficiency of 99.97% for particles of diameter 0.3 μm or greater [2]. The total efficiency for particles greater than 0.3 μm may be less than 99.97%. Therefore, the filter is not considered a HEPA filter even though the overall efficiency is greater than 99.97% and appear to exceed the required efficiency. A filtering efficiency curve is a plot of efficiencies as a function of particle size. The penetration curve is the plot of 1-FE as a function of particle size. This is effectively the normalized fraction of particles of a given diameter failing to be captured by the medium. The penetration curve gives a more comprehensive representation of the filtering efficiency and performance of the filter.

During the 1940s and 1950s significant advancements were made in filtration theory by multiple contributors. Three names in particular stand out: Langmuir, Ramskill, and Anderson [7].

Early air filtration theory focused on particle capture by a single fiber in an air flow. These studies resulted in a greater understanding of factors affecting particle capture by a fiber. Improved concepts of aerosol behavior have led to improvement in HEPA filter designs to better serve the nuclear industry. The most penetrating particle size (MPPS) was an important discovery that directly influenced the current definition of HEPA filtering efficiency. Mechanisms that cause a MPPS were discovered by Langmuir and later updated by Ramskill and Anderson [7]. Filtration studies determined that decreasing fiber diameters produces, increased filtering efficiency without increasing the pressure drop of the filter [6]. The theoretical MPPS was initially predicted to be 1.0 μm by Irving Langmuir [1]. However, Langmuir's studies of particle retention on filter fibers

focused on interception and diffusion as collection mechanisms. Research conducted by Ramskill and Anderson modified Langmuir's findings to include inertial effects also known as impaction [1]. Combination of these three removal mechanisms resulted in a predicted MPPS 0.3 μm. The standard particle size of HEPA testing remains 0.3 μm as a result of this study even though the MPPS for most HEPA filters is closer to 0.150 μm [2].

Hinds gives detailed theoretical equations for determining filtering efficiency due the five collection mechanisms for filtration. These filtration mechanisms include: inertial impaction, interception, diffusion, gravitational settling and electrostatic attraction [7]. Four of the five collection mechanisms for filtration are discussed in detail in the following paragraphs. Electrostatic filtration will not be discussed because it is not applicable to this project.

Air flow through a filter is considered to be laminar and therefore predicting the single fiber efficiency is highly dependent on streamlines and boundary layers. The single fiber efficiency mechanisms were developed from the solution to the Navier-Stokes equations for flow around a system of cylinders using the stream function for Kuwabara flow [8]. Dimensionless parameters such as the Reynolds number, Stokes number, and Peclet number play an important factor in filtration theory. The parameter known as solidity is another important parameter in the performance of a filter. Solidity is essentially the volume displaced by media fibers. Solidity (α) is defined in Equation 1. The solidity of fibrous filters is typically between 0.01 and 0.3 [7].

$$\alpha = \frac{\text{Fiber Volume}}{\text{Total Volume}} \quad (1)$$

Collection by interception occurs when a particle follows a gas streamline that comes within one particle radius of the surface of a fiber. The single-fiber efficiency for interception is dependent on the parameter R. R is the ratio of the diameter of the particle to the diameter of the collection fiber [8]. Interception is the only collection mechanism that is not a function of velocity. Dimensionless parameter R is shown in Equation 2. For the following equations α is the solidity of fibers in a filter, d_p is the particle diameter, and d_f is the fiber diameter.

$$R = \frac{d_p}{d_f} \tag{2}$$

The variable R predicts the increase in collection efficiency by interception as particle diameter increases and fiber diameter decreases. The Kuwabara hydrodynamic factor (Ku) variable is used in calculation of single fiber filtering efficiency. Ku is a function of the solidity of the filter and is defined in Equation 3.

$$Ku = -\frac{\ln(\alpha)}{2} - \frac{3}{4} + \alpha - \frac{\alpha^2}{4} \tag{3}$$

The single fiber efficiency for interception is given by Equation 4 [8].

$$E_R = \frac{(1-\alpha)R^2}{Ku(1+R)} \tag{4}$$

The second mechanism Langmuir defined for collection was diffusion. Diffusion is the result of Brownian motion of small particles. Brownian motion was observed by Robert Brown as irregular motion of particles in gases due to collisions between gas molecules. This motion causes very small particles to deviate from streamlines and increases the probability of a particle hitting a fiber [9]. The single fiber efficiency due to diffusion is a function of the dimensionless Peclet number shown in Equation 5 as

developed by Jean Claude Eugene Peclet. The particle diffusion coefficient D is highly dependent on particle size because of Brownian motion. U_0 is the media velocity and d_f is the diameter of the fiber.

$$\mathrm{Pe} = \frac{d_f U_0}{D} \tag{5}$$

The Peclet number is predicted to increase with an increase in fiber diameter and reduction in the particle diameter. The single fiber efficiency for diffusion is reduced to a function of only the Peclet number as seen in Equation 6 [10].

$$E_D = 2Pe^{-2/3} \tag{6}$$

The efficiency due to diffusion is shown to decrease as Pe increases. Therefore, E_D decreases with increasing particle size, increasing fiber diameter, and increasing velocity. Ku is required to account for enhanced collection due to interception of the diffusing particles when the single-fiber efficiency approaches minimum [8]. Lee and Liu developed a multiple-cylinder model to account for flow interference effect of other fibers. This corrected efficiency using the Ku is defined in Equation 7 [7].

$$E_{DR} = \frac{1.24R^{2/3}}{(KuPe)^{1/2}} \tag{7}$$

Ramskill and Anderson modified Langmuir's findings to include inertial effects of particle motion, known as impaction [11]. Impaction is the result of inertia of the particle causing it to stray from the stream line and contact the filter fiber. Collection efficiency of impaction will increase as the velocity or particle size increase. This modification changed the predicted most penetrating particle size to 0.3 μm. The standard particle size for HEPA testing still remains 0.3 μm [2].

The Stokes number governs impaction collection and is a dimensionless characterization of curvilinear motion. A the particle is more likely to stray from streamlines as the Stokes number increases and be collected on the filter fibers due to impaction or interception. The Stokes number is given in Equation 8 where ρ_p is the particle density, C_c is the Cunningham Correction Factor and η is the dynamic viscosity.

$$Stk = \frac{\rho_p d_p^2 C_c U_0}{18\eta d_f} \tag{8}$$

The Stokes number increases with increasing particle diameter and velocity and decreases with increasing fiber diameter. Because the particle diameter is squared it has much more effect on the change in the Stokes number. Variable J developed by Adolf Fick is known as the flux and this relationship is known as *Fick's first law of diffusion*. This variable is defined in Equations 9 and 10 [7].

$$J = (29.6 - 28\alpha^{0.62}) * R^2 - 27.5R^{2.8} \quad for\ R < 0.4 \tag{9}$$

$$J \cong 2.0\ for\ R > 0.4 \tag{10}$$

Single fiber efficiency for impaction is shown in Equation 11 [10]. As can be seen from the Stokes number the collection efficiency of impaction increases with increasing velocity, particle density and particle diameter.

$$E_I = \frac{(Stk)J}{(2Ku)^2} \tag{11}$$

Particle deposition due to gravity is dependent on the dimensionless variable G as defined in Equation 12 [7]. This equation includes the gravitational acceleration g.

$$G = \frac{\rho_g d_p^2 C_c g}{18\eta U_0} \tag{12}$$

The single fiber efficiency for gravitational deposition is found using Equation 13 for E_G [7]. The sign for gravitational collection efficiency is dependent on the direction of the flow.

$$E_G = \pm G(1 + R) \tag{13}$$

The overall theoretical filtering efficiency is the summation of the single fiber efficiencies of each collection mechanism. This is shown in Equation 14 [7].

$$E_\Sigma = 1 - (1 - E_R)(1 - E_I)(1 - E_D)(1 - E_{DR})(1 - E_G) \tag{14}$$

It can be seen from the above equations that the individual fiber efficiency for each mechanism contains multiple parameters and each filtering mechanism is independent of others. If a single parameter in the filtering process is changed the overall filtering efficiency will change. Penetration of HEPA filters by very small particles, less than 1 μm, is directly velocity-dependant and increase significantly at very high airflow rates. Diffusion is a time dependant phenomena and the longer the particles dwell near a fiber the greater the possibility of capture. Penetration of HEPA filters by particles larger than 1 μm may increase at very low flow rates due to the reduction in effectiveness of the impaction mechanism. The design of the filter is important but also the design of the filtration system as a whole effects filter performance.

The single fiber efficiency equations do not account for the thickness of the filter. To predict the efficiency of a filter the fibrous filters can be considered as made from many thin layers of filter fibers. The equation for efficiency as a function of thickness is shown in Equation 15 where t is filter thickness [12]. This equation predicts filter efficiency will increases exponentially with filter thickness.

$$E = 1 - \exp(\frac{-4\alpha E_\Sigma t}{\pi d_f}) \quad (15)$$

The experimental efficiency of a filter can be calculated or determined with respect to either number collection efficiency or mass collection efficiency [7]. The number collection efficiency is a comparison of the upstream and downstream concentration. The mass efficiency is a comparison of the upstream mass to the downstream mass.

The volume of a sphere increases as the cube of its radius. Therefore, as particles increase in size by a factor of 10 their mass increases by a factor of 1000. Thus mass removal efficiency is heavily weighted to removal of large particles. Number concentration is shown in Equation 16. Where N represents the number of particles counted. The mass collection efficiency is calculated using Equation 17. Where N and C represent the number of particles and the mass of the sample collected respectively.

$$\mathrm{E} = \frac{\mathrm{N_{in}} - \mathrm{N_{out}}}{\mathrm{N_{in}}} \quad (16)$$

$$\mathrm{E_m} = \frac{\mathrm{C_{in}} - \mathrm{C_{out}}}{\mathrm{C_{in}}} \quad (17)$$

Pressure drop is an important parameter in the function of HEPA filters. The pressure drop across a filter is the result of net drag forces from each fiber in the medium as airflows past it. The equation for predicting pressure drop is shown in Equation 18 [7]. Where η is the viscosity of the working fluid.

$$\Delta p = \frac{64\eta t U_0 \alpha^{1.5}(1+56\alpha^3)}{d_f} \quad (18)$$

The dimensionless parameter q_f represents filter energy efficiency. This quantity is the ratio of efficiency over the pressure drop of a filter. The equation for filter energy quality is given by Equation 19 [7].

$$q_f = \frac{\ln(1/(1-E))}{\Delta p} \tag{19}$$

Media

Development of HEPA media began with the gas mask filters used during WWII and has been improved to include a number of current media types. The basis for HEPA filtration was laid during the early 1940s [1].

Filter media falls into two broad categories. The first is fibrous media which includes glass, sintered metal, or plastic fibers. The second is granular media that includes sintered metal powder, sand, and ceramic media. The most common type of filter used current in the US the fibrous glass filter. Glass fiber filters offer high efficiency with low pressure drop. Glass fiber filters are susceptible to damage from conditions such as high temperatures, moisture, and chemicals. Metal and ceramic filters offer protection against some of these conditions but also produce much higher pressure drops [13]. The increased pressure drop reduces the filter quality parameter q_f but may be a welcomed trade off for increased protection under certain conditions.

Development and testing of new media for filtration applications has focused on efficiency, pressure drop, durability, and loading capacity. Filters efficiency is an obvious first priority for nuclear HEPA filtration. The other three areas of media focus are largely due to cost effectiveness of the filters. Low pressure drop filter allows for easier air flow and directly affects the parameter known as the filter energy quality. Durability and

loading capacity help to increase safety and reduce costs by reducing the chance to exposure from having to change out fully loaded or damaged filters as well as reducing the number of filters used.

Challenge aerosols produced by different process have different size distributions. The current version of AG-1 requires qualififaction testing using 0.3 μm aerosols from one of three compounds:, dioctylphthalate (DOP), dioctylsebacate (DOS/DEHS), and 4 centisoke poly-alphaolephin (PAO). Traditionally the test aerosol of choice is DOP [2]. Aerosol from liquid DOP is produced using a thermal aerosol generator or a Laskin nozzle generator. Thermal aerosol generators pass a liquid through a heat exchanger that condenses the liquid then when injected into ambient air. Laskin nozzle generators operate using one or more nozzles and create aerosols with a specific particle size distribution when operated at correct temperature and pressure [14]. Alumina, Carbon Black, Arizona Road Dust, and Potassium Chloride (KCl) are dry powders and have been used in testing of HEPA filters. Dry aerosols are generated using a powder feeder with compressed air and then injected into the test air stream. KCl and other soluble compounds or slurries can be used to produce aerosols via a spray dry process. Aerosols of varying particle diameters have been used to show the effects of particle size on surface and depth loading and loading capacity. Figure 1 shows the particle size distributions for three aerosols produced from dry powders during testing at ICET [15]. Equations in the aerosol statistics section on page 22 are used to describe the log normal distributions as shown in Figure 1.

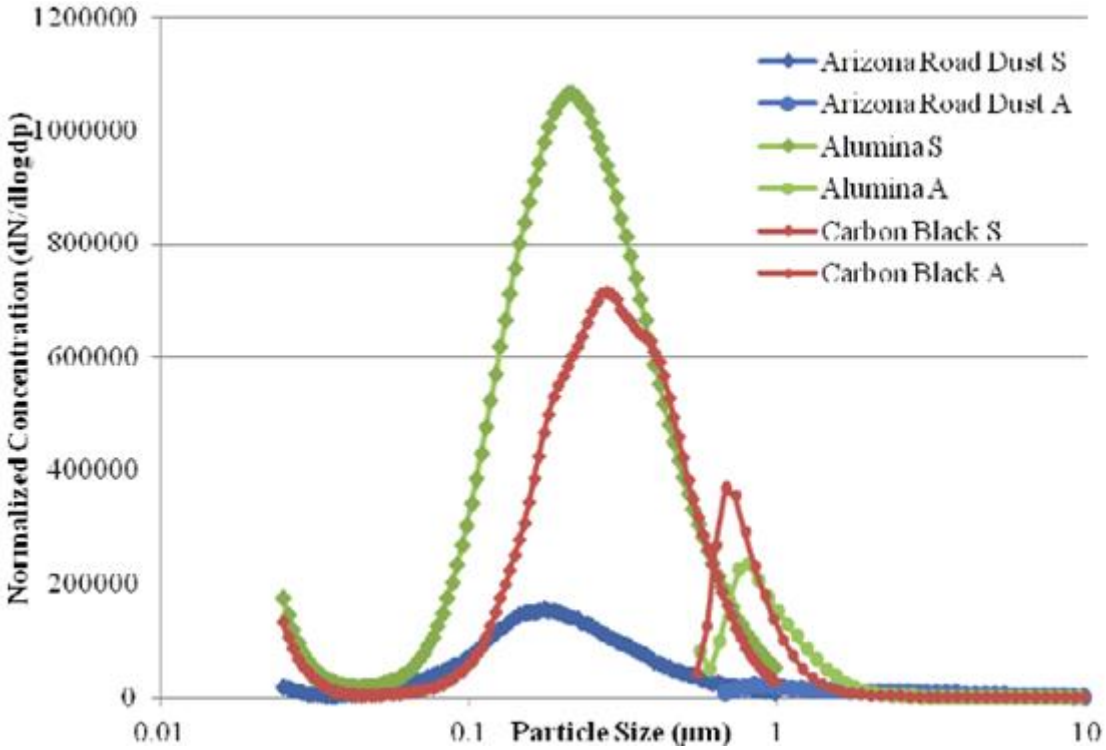

Figure 1 Dry powder aerosol particle size distribution from previous ICET testing

Table 1 gives the aerosol statistics for this set of data [15].

Table 1 Dry Powder Aerosol Particle Statistics from Previous ICET Testing

Aerosol	**Upstream**			
	Number Concentration	CMD	GSD	MMD
Alumina	650,000 #/cc	0.185 µm	2.17	0.8 µm
AZ Road Dust	100,000 #/cc	0.186 µm	1.86	5 µm
Carbon Black	450,000 #/cc	0.250 µm	2.21	1.2 µm

The lognormal distribution of an aerosol produced by spray drying a saturated solution of potassium chloride (KCl) is provided in Figure 2.

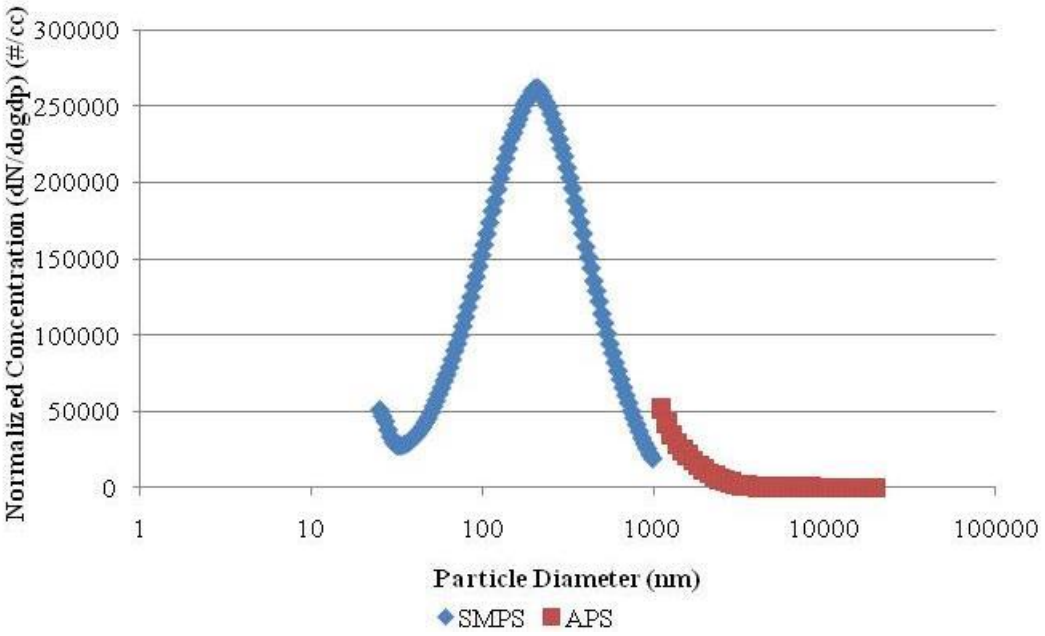

Figure 2 Lognormal particle size distribution of potassium chloride.

The aerosol statistics for the lognormal distribution given in Figure 2 is shown in Table 2. These statistics display the numerical values for the distribution above.

Table 2 Aerosol Statistics for Potassium Chloride

Potassium Chloride Aerosol Statistics	
Median(nm)	205
Mean(nm)	249
Geo. Mean(nm)	197
Mode(nm)	211
Geo. Std. Dev.	1.64
Mass Median Diameter	431
Mass Mean Diameter	487

Aerosol measurement instrumentation

The measurement of aerosol particles for HEPA filter qualification has been changed over the years due to advancements in methods and instrumentation. Instruments can be categorized into two groups. (1) Collection devices such as cascade impactors, Aitken-type condensation nuclei counters, or filter samplers and (2) real-time, direct-reading instruments, such as an optical particle counters, photoelectric condensation nuclei counters or photometers [10].

The origin of aerosol measurement dates back to before 1900. This is referred to as the preclassical period of aerosol measurement [10]. John Aitken's preclassical research on condensation in 1875 led to the development of the first portable instruments for counting dust particles [10]. In 1941 the first observations of what later became known as condensation nuclei methodology was observed. It was recognized that condensation occurred on unfiltered air quicker than it formed in filtered air. Thirty years later the experiments of P.J. Coulier demonstrated that condensation was enhanced due to the existence of fine particles in the air.

The classical period of aerosol measurement is identified by the use of measurements and experimental techniques after the preclassical period and prior to the use of lasers, computers, and spectroscopic analytical tools. Aerosol measurement instrumentation during the classical period described aerosol populations by number concentration. Number concentration methods during this period required a volume of sample to be collected followed by counting and sizing the particles. The detection of particles by scattering of light led to the invention of the tyndallometer, nephelometer, ultramicroscope, and John Tyndall's optical particle counter by the 1960s [10]

Examples of classical measurement instruments include: Konimeters, Cascading impactors, Impingers, and Precipitators. Konimeters are single stage impactors. Particles are collected on a glass plate by impaction and their physical size/description is examined under a microscope. Cascading impactors utilize multiple stages to allow sampling and sizing of aerosol particles. Cascade impactors of up to 6 stages were built before 1960 during the classical period of aerosol measurement. For cascading impactors stages are designed to capture a faction of the aerosol with smaller average diameters collected on succeeding impactor stages. Impingers use the same technique as Konimeters except the dust particles are first collided with a liquid. Classical measurement instrumentation utilizing impaction methods are time consuming, have poor size resolution, no real-time analysis of particle size distribution, and errors originating from particle bounce [10]. Precipitators utilize thermal and electric fields to separate aerosol particles [10]. Precipitators of the classical period were shown to have a lack of homogeneity in particle deposition obtained during dust sampling. In samples obtained in thermal precipitator, the average particle size increases continuously from the front edge to the back edge of the collection plate as a result of thermophoresis [10]. Precipitators have also been found to have decreased collection efficiency as particle size increases above 2 μm [10].

Classical measurement methods are limited due to errors associated with each measurement technique. Differences in different instrument measurements were found to be in the range of ±100%, therefore, it is impossible to compare measurements from different instruments of this era [10].

The impactor is the most extensively used aerosol measurement instrument for characterizing particle size distributions. Ken May is responsible the first true cascade

impactor for determining a particle size distribution [16]. Three areas of impactor development have stood out: (1) extending the cut sizes of impactor size ranges, (2) development of impactors to provide near real-time indication of the particle mass collected, and (3) designing impactors that provide precise particle size characterization for medical and aerosol inhalers [16].

The emergence of microelectronics, laser and computer techniques, modern physical methods in analytical chemistry, analytical electron microscopy, and light scattering technology revolutionized aerosol measurement instrumentation. Unlike the instruments used before 1960, newer instruments are able to incorporate computers and automation to collect and analyze data. Commercial development of currently available instrumentation along with their calibration technologies has dramatically increased the consistency of aerosol measurements [10].

Aerosol statistics

Gravitational settling is not commonly view as a filtration mechanism even though it does represent a removal mechanism. However, gravitational settling has a broader impact on air filtration nomenclature than may be apparent. Particle sizes can be classified or described in a variety of physical ways. Irregular sizes make measurements such as physical diameter, aspect ratio or volume difficult to correlate to the behavior of an aerosol particle.

The most popular description is that of aerodynamic diameter. The aerodynamic diameter of a particle is said to be equivalent to the diameter of a spherical droplet of unit density with the same settling velocity [7]. The Stokes diameter is another common way to size aerosol particles. The Stokes diameter is equivalent to the diameter of a spherical

aeroso of the same bulk density and settling velocity as the test particle [7]. Unless otherwise stated, particle sizes will be given in aerodynamic diameters.

Particle size distribution curves provide a functional representation for analyzing aerosol properties. Aerosol populations tend to follow a lognormal distribution of particle sizes as opposed to a true normal distribution [7]. Particle size distributions provide graphical representation of count fraction as a function of particle diameter. The most commonly used quantities for describing statistical locations of a distribution are the arithmetic mean, median, mode and the geometric mean. An aerosol population can generally be described by its geometric mean, geometric standard deviation and number of particle per cubic centimeter. An example of a particle size distribution is shown in Figure 3

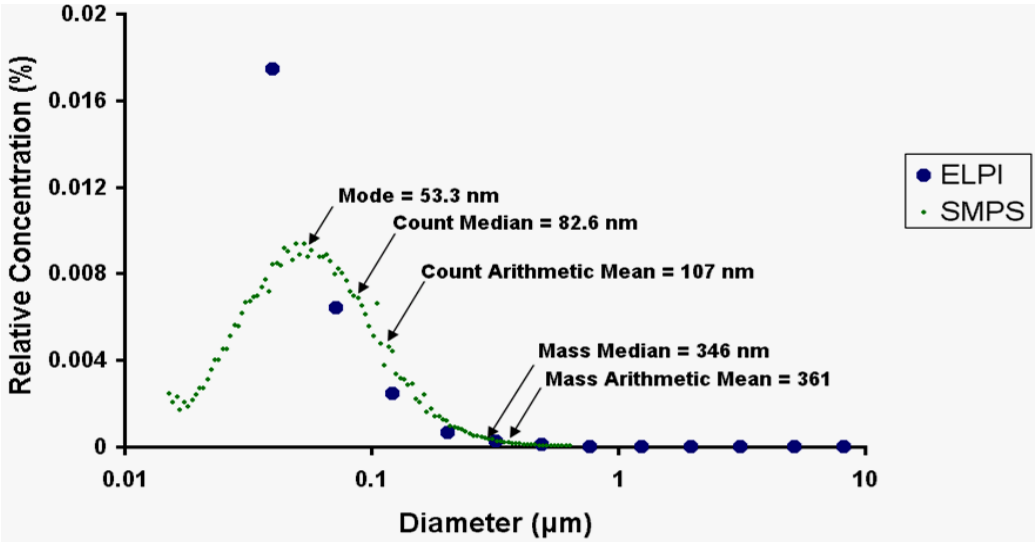

Figure 3 Particle size distribution with mean, median, mode, mass median, mass mean, and geometric mean labeled.

The arithmetic mean is the sum of all the particles sizes divided by the number of particles. The median diameter (CMD) is the size at which half the particles are larger and half are smaller. The mode is the most frequent particle size and geometric mean is the Nth root of the product of N values. The geometric mean diameter is shown in Equation 20.

$$\mathrm{d_g} = (d_1 d_2 d_3 \ldots\ldots d_N)^{1/N} \tag{20}$$

Geometric standard distribution (GSD) describes the spread of the particle sizes. The equation for GSD is shown in Equation 21 below.

$$\ln \sigma_g = \frac{\sum n_i (\ln d_i - \ln d_g)^2}{N-1}^{1/2} \tag{21}$$

Normal distributions of polydisperse aerosols result in a skewed distribution because of the long tail at large particle sizes [7]. This wide range of particle sizes skews the distribution such that it requires a fraction of the particle sizes to have a negative value to result in a true distribution. This is impossible.

Lognormal representation of aerosol data collected during testing has been found to be much more useful than normal distributions. No fundamental theoretical reason has been established as to why particle size data should approximate the lognormal distribution, but it is routinely seen in experimental data [7]. The lognormal distribution is useful for describing aerosol size distributions because it fits the observed size distributions reasonably well and its mathematical form is convenient for aerosol statistic applications. The lognormal distribution is best used where the quantity must have a positive value and the data range is greater than a factor of 10 [7]. A very narrow range of particles causes the population to more closely follow a normal distribution. In a

lognormal distribution the geometric mean diameter of the normal distribution is replaced by the count median diameter. The mean and the median of a lognormal distribution are equal and therefore the lognormal distribution is symmetrical.

The MMD is also displayed in Figure 3 and shows how significantly the larger particle fraction of the PSD is emphasized. The filtration efficiency for HEPA filter allows projection of mass loading to be the mathematical product of the particle number density, MMD, bulk density of the aerosol, volumetric flow rate and time.

Particle size distributions can also be described based on mass as opposed to particle counts. One mass distribution value is of particular usefulness, the mass mean diameter (MMD). This value is often employed in filter loading computations because of its simplicity of applications. The MMD is also displayed in Figure 3 and shows how significantly the larger particle fraction of the PSD is emphasized. The filtration efficiency for HEPA filter allows projection of mass loading to be the mathematical product of the particle number density, MMD, bulk density of the aerosol, volumetric flow rate and time.

CHAPTER III

NUCLEAR CONTAINMENT VENTILATION

Nuclear HEPA filter standards

High Efficiency Particulate Air (HEPA) filters currently play a major role in safety and ventilation systems for nuclear facilities. HEPA filters are required to perform reliably under a multitude of conditions. Many experiments and studies have been conducted over the last 70 years to ensure the performance of these filters. Nuclear grade HEPA filters are required to meet specific standards and use must follow guidance documents established by governing bodies such as the US DOE and NRC. Examples include: the DOE Nuclear Air Cleaning Handbook (NACH) and the Nuclear Quality Assurance standard (NQA-1) maintained by the American Society of Mechanical Engineers (ASME) [1,17]. These documents provide quality control for application of standards. The standard for design, fabrication, and qualification of nuclear grade HEPA filters is ASME AG-1 Code on Nuclear Air and Gas Treatment [2].

Development of guidance and control documents began in the 1950s shortly after the need for nuclear grade HEPA filtration and quality control was realized. The requirement for having to qualify HEPA filters came about because of allegations in the late 1950s that commercial filter manufactures were sending defective filters to facilities [1]. The AEC responded by publishing strict quality assurance (QA) requirements for this categories of filters. Filters manufactured prior to 1960 were found to have a rejection

rate of 49% when tested at the Army Chemical Center in Edgewood, Maryland [1]. The AEC established and used three QA testing facilities for inspection and testing of filters used within the weapons complex, (1) Oak Ridge National Laboratory in Oak Ridge, Tennessee, and (2) Rocky Flats plant in Golden, Colorado and the (3) Hanford facility at Richland, Washington [1]. Establishment of AEC QA filter test stations functionally enforced the requirement for quality control on filter manufactures to implement their own quality assurance practices [1]. Filter rejection rates dropped to 5% during the period of 1960-1968 as a result of filter quality assurance testing [1]

Efforts in the United States during the 1960s focused on standardizing manufacturing and test criteria for filter media (called paper) and fabricated filters, with a special emphasis on fire and water resistance [1]. Filters are required to meet standard qualification requirements in order to demonstrate that filter designs have been produced using allowed high-quality components and carefully assembled to meet performance requirements. Discussion sessions held during the 1960s included issues ranging from aging of fibrous glass media in filters to the integrity of shipping containers [1]. The aging of glass filters became an important topic because of the quantity of filters that had been sitting in storage or remaining in service for an extended period of time [18]. This issue is still being discussed as the service life of a fibrous glass HEPA filter. Aging of filters had not been discussed in length before the discussion sessions during the 1960s [1]. The inclusion of a non-mandatory appendix for Section FC of AG-1 is currently in the balloting process.

Substandard filtration system performance led to an additional phase of testing, in place testing of all filter installations, this has resulted in improved designs for filter housings and installation guidelines [1].

The next step in providing guidance and standardizing development of overall system design and performance was taken when the Oak Ridge National Lab published 1966 ORNL/NSIC-13, *Filters Sorbets and Air Cleaning Systems as Engineered Safeguards in Nuclear Installations* in 1966 [1]. ORNL/NSIC-13 would later become known as the 1st edition of the Nuclear Air Cleaning Handbook. The first edition of the NACH presented the latest developments in the trapping of airborne radioactive materials encountered in reactor operations, fuel fabrication and processing plants and radiochemical plants of all types [1]. The purpose of presenting this information was to increase containment reliability under adverse conditions, as well as lowering costs and increasing capture efficiencies for radioactive aerosols and gases [1]. The AEC was replaced by the Energy Research and Development Administration (ERDA) in 1975 to focus the federal government's energy research development activities under a single agency, this action included AEC's nuclear energy defense activities. [DOE.gov]

The American National Standards Institute (ANSI) assigned the overall responsibility for coordination among technical societies and development and the maintenance of nuclear power quality assurance standards to ASME in 1975 [17]. ASME established an organizational structure to accomplish this that is currently housed under the ASME Board on Nuclear Codes and Standards (BNCS). ASME BNCS currently maintains the following committees responsible for codes:

1. Committee on Nuclear Quality Assurance (NQA)
2. Committee on Cranes for Nuclear Facilites (CNF)
3. Committee on Operation and Maintenance (O&M)
4. Committee on Nuclear Air and Gas Treatment (CONGAT)
5. Committee on Qualification of Mechanical Equipment Used in Nuclear Power Plants
6. Committee on Nuclear Risk Management (CNRM)
7. Boiler and Pressure Vessels Committees (Nuclear)

ASME established the Committee on Nuclear Quality Assurance and began operation under the ASME Procedures for Nuclear Projects on October 3, 1975 [17]. The Committee on Nuclear Quality Assurance established a series of documents for quality assurance at nuclear power facilities [1]. The purpose of these standards was to reflect industry experience and current understanding of the quality assurance requirements necessary to achieve safe, reliable and efficient utilization of nuclear energy and management and processing of radioactive materials [17] Difficulties experienced during application of this set of standards resulted in their combination into the single, multipart document labeled as NQA-1-1994. The latest edition of NQA-1 was published in 2012 [17]. The NQA standard provides requirements that prescribe the extent of controls needed in specific areas of a nuclear quality program [17]. The 18 requirements outlined in NQA-1 are shown below [17].

- Organization
- Quality Assurance Program
- Design Control

- Procurement document control
- Instructions, procedures and drawings
- Document control
- Control of purchased material, equipment and services
- Identification and control of materials parts and services
- Control of special processes
- Inspection
- Test control
- Control of measuring and test equipment
- Handling, storage, and operating status
- Nonconforming items
- Corrective action
- Quality assurance records
- audits

The ASME Committee on Nuclear Air and Gas Treatment (CONGAT) was formed in 1976 to help meet industry needs for nuclear air and gas containment. CONGAT created and maintains four codes and standards that dictate requirements of nuclear air and gas treatment. The four CONGAT codes are: *ASME AG-1 - Code on Nuclear Air and Gas Treatment* [2], *ASME N509 - Nuclear Power Plant Air Cleaning Units and Components* [19], *ASME N510 - Testing of Nuclear Air Treatment Systems* [20], and *ASME N511 - In-service Testing of Nuclear Air Treatment Systems* [21]. DOE Technical Standard *DOE-STD-3020-97 Specification for HEPA Filters Used by DOE Contractors* was issued by the DOE in 1997 [22].

DOE-STD-3020-97 was developed to provide guidance to DOE contractors for procurement and included the required testing of HEPA filters used in DOE nuclear facilities. The purpose of DOE 3020 is to achieve technical coordination among individuals of recognized authority from affected DOE programs, including manufacturers, purchasers, users, and technical experts [22]. DOE 3020 is currently undergoing revision and updating.

The U.S. DOE initiated a program in the early 1990s to more precisely define HEPA filter efficiency [1]. Filter efficiency studies conducted at Los Alamos National Laboratory showed that the most penetrating particle size for all-glass-paper HEPA filters at the design airflow is close to 0.1 μm [1]. Development and acceptance of a new HEPA filter standard that utilized a polydisperse aerosol to determine filtering efficiency resulted from determination of the MPPS [2]. DOE filter test facilities (FTF) at Rocky Flats, Oak Ridge and Hanford improved the characteristics of aerosols for HEPA testing to yield more consistent results [1]. All filters used at DOE facilities were required to be tested at a FTF before installation. Rocky Flats and Hanford were closed by 1992 with operations consolidated at the Oak Ridge National Lab K-25 facility. Closure of the ORNC facility in 2005 included transfer of FTF activities to ATI in Baltimore, Maryland [23].

DOE research on filters existed not only at Los Alamos National Laboratory (LANL) but also at Lawrence Livermore National Laboratory (LLNC). Work by Vern Bergman included development of filters capable of performing under much more aggressive conditions than fibrous glass media can withstand. Dr. Bergman's research in metal media filters is particularly important to section FI development [31].

Overview of AG-1

The DOE NACH dictates that nuclear grade HEPA filters in the U.S. must meet the requirements of ASME AG-1. The AG-1 code contains mandatory requirements, specific prohibitions and non-mandatory guidance for material, design, fabrication, inspection, testing, and certification for nuclear containment systems. [2]. AG-1 also provides unbiased performance criteria to ensure products meet design qualifications regardless of designer or manufacturer [2].ASME is the required code for the United States nuclear industry and has been used internationally.[24]

AG-1 contains two approved sections associated with nuclear grade HEPA filters, sections FC and FK. The following table lists the current and in development sections of AG-1 associated with filtration [2]. Table 3 lists the sections of AG-1 with their name, subject and status [2].

Table 3 Sections of AG-1

AG-1 Section Name	Subject	Status
FA	Moisture Seperators	Final
FB	Medium Efficiency Filters	Final
FC	HEPA Filters	Final
FD	Type II Adsorber Cells	Final
FE	Type III Adsorber Cells	Final
FF	Adsorbent Media	Final
FG	Mounting Frames for Air Cleaning	Final
FH	Other Adsorbers	Final
FI	Metal Media	In-Development
FJ	Low Efficiency Filters	Final
FK	Special HEPA filters	Final
FL	Deep Bed Sand Filters	Final
FM	High Strength HEPA Filters	In-Development
FO	Ceramic Filters	In-Development

Section FC

Section FC serves as the blueprint for development of new sections of AG-1. Section FK was added to AG-1 and there are currently three sections listed in the above table listed as in development. Sections in development contain many similarities to Section FC. Many of the basics have remained the same but many specific parameters have been changed out of necessity from the difference in the filter behavior. Differences include:

- Intial differential pressure
- Maximum media velocity
- Qualification procedures, particularly with respect to differential pressures
- Qualification infrastructure
- Aerosol Challenge

The table below shows what section FC has required for nuclear HEPA filters.

Table 4 Section FC HEPA Filters

Section	Title	Subsection	Title	Description
FC-1000	Introduction	FC-1100	Introduction	Purpose and limitations of section FC
FC-2000	Referenced Documents			
FC-3000	Materials	FC-3100	Allowable Materials	Defines allowable materials for FC HEPA filters
		FC-3200	Special Limitations of Materials	Materials can be used if acceptable by the qualification and design requirements in FC-5000 and FC-4100
FC-4000	Design	FC-4100	General Design	Design requirements including specifications for splices and patches, filter case, filter pack, gaskets, separators, and faceguards.

Table 4. Continued.

		FC-4200	Performance Requirements	Test aerosol penetration and resistance to airflow
		FC-4300	Seismic Qualification	Requirement of seismic qualification
FC-5000	Inspection	FC-5100	Qualification Testing	Resistance to airflow, test aerosol penetration, resistance to rough handling, resistance to pressure, resistance to heated air, and structural requirements.
		FC-5200	Inspection	Visual examination of filters
		FC-5300	Production Testing	Filters manufactured for delivery shall be tested for penetration and resistance to airflow.
FC-6000	Fabrication	FC-6100	General Requirements	States the filters shall be assembled in accordance to FC-3100, FC-4000, FC-5100, and FC-5300
		FC-6200	Manufacture and Assembly	Specific values for tolerances in construction and media installation
		FC-6300	Workmanship	Filters must be free of foreign matter and damage.
FC-7000	Packaging, Shipping, and Storage			Shipping and storage to be in accordance to AG-1 AA-7000
FC-8000	Quality Assurance	FC-8100	Responsibility	
		FC-8200	Certificate of Conformance	
FC-9000	Name Plates	FC-9100	Filter Marking	
		FC-9200	Package Marking	
Mandatory Appendix FC-I	Filter Media: Fire-Resistant High Efficiency			supersedes MIL-F-51079D
Non Mandatory Appendix FC-A	Division of Responsibility			Identifies the roles normally assumed by the organizations responsible for fulfilling Code requirements.

HEPA Filter design qualification testing for nuclear services outlined in the DOE Nuclear Air Cleaning Handbook includes: Penetration (Efficiency) testing, Airflow resistance test, tests aerosol test, resistance to rough handling qualification test, moisture and over pressure resistance qualification test, fire and hot air resistance qualification test, and spot flame resistance [1].

Section FC is the oldest and by far the most mature section related to nuclear grade HEPA filters and has been the primary focus of the filtration subcommittee. Newer sections describing HEPA filters have been greatly influenced by design characteristics of existing filtration systems that employ FC filters. This includes a clean differential pressure of 1.0 or 1.3 inches w.c. for filters. There has also been a maximum media velocity of five feet per minute used to insure that Reynolds numbers retain a laminar flow regime. Project teams responsible for developing new sections also face limitations that exist in qualifying filters of differing geometries or performance capabilities. Development of Section FI for metal media nuclear grade HEPA filters has reached an impasse restricting the progress until infrastructure is available to collect needed data and also provide capacity to qualify filters. The infrastructure located at Edgewood will not accommodate geometries or test conditions exceeding these of section FC filters. Project teams developing code sections that exceed existing qualification infrastructure must also deal with how and where needed infrastructure can be developed.

Defense Nuclear Facilities Safety Board documents

The Defense Nuclear Facilities Safety Board (DNFSB) is an independent organization started in 1989 with the responsibility of providing recommendations and advice to the President and Secretary of Energy regarding public health and safety issues

at DOE defense nuclear facilities [25]. The goal of the DNFSB is protecting general public and worker health, safety and environment at defense nuclear facilities [25].

The DNFSB identified potential significant weaknesses in the maintenance and operation of nuclear containment ventilation systems. Weaknesses in the procurement, testing, application and use of HEPA filters were specifically recognized. These issues were attributed to degrading DOE infrastructure for HEPA filters and from the lack of reliance on FTFs. The DNFSB released Technical Report 23 (Tech 23) entitled *HEPA Filters Used in the Department of Energy's Hazardous Facilities* in May of 1999 to identify actions to restore the necessary infrastructure [26].

Tech 23 focused on five failure issues. The first issue is fire. Fires pose a potential safety issue for containment systems in nuclear applications by production of smoke can rapidly blind filters and cause physical failure. One example is the fire that occurred in building 776-777 at the Rocky Flats Plant in Golden, Colorado in May 1969. This fire was reported to have produced large amounts of contaminated smoke. Some filters were reported to be burned or damaged by heat and air pressure. Although most of the ventilation systems continued to operate, the vulnerability of fibrous glass HEPA filters to fires was apparent [27]. Tech 23 called for development of strategies to prevent destruction of HEPA filters [26]. The DNFSB report addressed heat and elevated conditions that can pose a threat to the proper functioning due to the materials of construction of the HEPA filter installations [26]. A third area addressed is the material of construction.

HEPA filter medium is manufactured in a manner similar to that of making paper. The similarity of manufacturing along with historical use of cellulose in addition to

fibrous glass caused HEPA media to also be referred to as paper. Use of this term included the implicit understanding that media are susceptible to water damage even with water repellent media. Moisture-laden air carried through a HEPA filters can seriously degrade filter performance [26]. The fourth concern a Tech 23 addressed is that the strength of HEPA media under challenging conditions can pose a threat to the integrity of the filter [26]. Determining the extent of the threat to the integrity of the filter is difficulty since nondestructive in-place testing is not available for these HEPA filtration systems [26]. The fifth and final concern addressed in tech 23 is air leaks [26]. Even with careful design, attentive operation and disciplined maintenance the operation of a HEPA installation can be diminished by air leaks in the negative pressure region of the system downstream of the filters and upstream of the fans [26]. Leaking gaskets, fan seals, and damper actuator penetrations are particularly vulnerable. These regions are not regularly checked for leaks and can cause problems if they are not discovered and addressed immediately [26].

The Defense Nuclear Facilities Safety Board issued several recommendations on March 8, 2000 to assist in resolving issues discussed in Tech 23. Recommendations to resolve some issues discussed in Tech 23 were listed in DNFSB Recommendation 2000-2. The first recommendation was to establish a team of experts in confinement ventilation systems to examine the past and present operational condition of all confinement ventilation systems [28]. This included assessing the causes for the less than satisfactory operational history of critical safety systems and an action plan to address the causes and estimating the remaining system lifetime with and without refurbishing [28]. When assessment of the causes is complete the team was called to recommend upgrades or

compensating measures to ensure reliability of the safety systems [28]. Recommendation 2000-2 also included recommending the development and maintenance of documentation that captures key design features, specifications, and operational constraints to facilitate configuration management throughout the life cycle of the facility [28]. This requires designation of a system engineer during each facility life cycle-design, construction, operation, and decommissioning as well as education and training of successor system engineers due to changes in contractor organizational changes, facility life cycle change or other causes for reassignments [28]. This recommendation also tasked the Federal Technical Capability Panel to establish necessary staff and expertise required for operation of confinement systems [28].

In October 2000 the DNFSB issued a implementation plan for Recommendation 2000-2. The implementation plan set the objective of completing a baseline assessment of the operation readiness of vital safety systems. This plan also addressed actions to identify and compensate for degradation to vital safety systems [29].

Section FI development

Development of a new filter standard for metal media HEPA filters began around 1990. Development of a standard for high strength media focused on two high strength mediums with most moisture resistance that can be used for HEPA filters: sintered metal powder and sintered metal fiber media. Development of this section came to almost a stand still until the release of DNFSB document Tech 23. Proposed Section FI addressing metal media filters will be applicable to the full range of filtering efficiencies, including HEPA [30]. Therefore, the major barriers to completing the code section is development of a test stand for collecting data necessary to specify performance requirements for use

and for filter qualification [30]. Differences in metal media filters require section FI to cover a very broad range of performance criteria [30].

Section FI represents a substantive change from the traditions represented by Section FC. Section FC filters tend to be standardized with respect to dimensions and rated flows along with infrastructure required to qualify them. FI allows for user defined parameters including material of construction, initial and maximum differential pressures, operating temperature range, and chemical resistance. Additionally, the geometry of elements and the variably of filtering efficiencies and test conditions require a completely new suite of testing infrastructure to qualify them. Metal media filters addressed in section FI have been shown to exhibit efficiencies as high as 0.9999999 for specific test conditions [31].

Sintered metal fiber and sintered metal powder media are both being evaluated for Section FI qualification. Sintered fiber filters consist of very thin metal filaments uniformly laid to form a three-dimensional non-woven structure sintered at contact points [32]. The sintered metal powder is manufactured by pressing metal powder into porous sheet or tubes, followed by high temperature sintering [32].

Metal media filters can be back pulsed with compressed air to dislodge surface particulate matter, extending the life of the filter [33]. Sintered metal fiber and powder media are viable options for HEPA filtration. Sintered fiber and powder filter elements have strength and durability that exceeds that of fibrous glass, but because of the higher porosity of the sintered fiber the initial pressure drop of a clean sintered fiber filter has a much lower pressure drop than the pressure drop for a clean sintered powder filter [34]. Sintered metal fiber media also typically has a higher holding capacity than the sintered

metal powder and consequently the life expectancy is longer [35]. Both types of metal media filters are more expensive than their glass fiber counterparts, however their enhanced chemical and physical properties or ability to be regenerated (cleaned) in-place make a suitable and cost effective choice in many applications [36].

Development of Section FI for metal media filters of the ASME AG-1 standard has been ongoing since the late 1990s [30]. A multitude of issues has plagued finalizing this standard. The problematic issues have been rooted in the dramatic differences between metal media and fibrous glass media. HEPA filters used in nuclear containment applications have virtually always utilized fibrous glass media. The fibrous glass media limits the conditions in which HEPA filters can be operated: (1) Excessive moisture must be avoided; (2) back pulsing cleaning cannot be used to regenerate conventional FC filters; (3) the tensile strength of fibrous glass media restricts maximum operating differential pressures; (4) fibrous glass media can be degraded by chemical constituents like high pH aerosols or HF; and (5) potting materials for fibrous glass filters have relatively low tolerance for elevated temperatures [2]. Metal media filters have capabilities to with stand conditions that limit classic glass HEPA filters due to materials of construction [30].

The specific performance requirements for fibrous glass media are laid out in detail in AG-1 [2]. Metal media filters have a drastic difference in behavior of FC filters and thus many of the specifications that are applied to glass HEPA filters are not necessary for metal media filters. Many of the performance requirements for section FI filters are user defined, unlike sections FC and FK of AG-1 [2]. Table 5 gives the

parameters that must be supplied by the owner in the operation design criteria for metal media and metal media HEPA filters.

Table 5 Section FI user Defined Design Parameters.

Dimensions	Length, width, depth, maximum mass
Operating Conditions	Temperature and pressure range Initial and max ΔP Relative humidity range Media velocity (min, max) Volumetric flow (min, max) Chemical Composition of Aerosols Particle Size Distribution of Aerosols (GMD and GSD) Mass or Number Concentration of Aerosols Corrosive gases and/or liquids
Materials of Construction	Gasket material Filter media material Adhesive material Filter housing material
Mounting frame/housing	Allowable materials (corrosion resistance, durability) Structural requirements -deflection limits -impact loading -stress limits -equipment design verification
Access	Filter housing, filter element Location of filter
Filter medium	Filtering efficiency Unique challenge conditions (NO_x, HCl, etc)

Differences in the operating envelope and allowing the user defined operational limit requires a completely new suite of qualification and testing infrastructure [37].

A set of standardized qualification tests give reasonable assurance that filters have been produced using good designs, high-quality components, and carefully assembly in accordance with exacting tolerances [1]. Standard qualification test results give an indication of the operating envelope of the filter rather than the actual filter efficiency

under unknown or ill-defined operating conditions. HEPA filters for nuclear service undergo a qualification procedure and two testing regimens [2]. The first regimen consists of a stringent visual examination and penetration tests at the manufacturer [2]. The second regimen is an in-place leak test performed at the facility it is used [2]. DOE requires independent inspection and penetration tests at the designated DOE FTF prior to installation at its final destination [1]. The manufacturer's testing regimen involves two distinct phases: (1) a quality control routine to ensure careful manufacture of the product and (2) a serious of tests to verify filter compliance with standards and performance criteria related to collection efficiency and resistance to airflow [2]. The DOE mandates independent inspection and penetration testing for all filters purchased [1]. Testing is currently required for filters installed in radiological hazard Category 1 and 2 facilities that perform a safety function and a statistical approach for the balance [1]. Filters are tested for compliance with the requirements for physical characteristics, efficiency and airflow resistance [2]. Compliance testing is conducted at the DOE-supported FTF before the filters are released to the customer's facility [1].

Table 6 Current Sub-Sections of Section FI [2]

Section	Title	Subsections	Subsection Title
FI-1000	Introduction	FI-1100	Scope
FI-2000	Referenced Documents	None	
FI-3000	Materials	FI-3100	Allowable Materials
		FI-3200	Special Limitations of Materials
		FI-3300	Alternate Materials
FI-4000	Design	FI-4100	General Design
		FI-4200	Performance Requirements
		FI-4300	Seismic Qualifications
FI-5000	Inspection	FI-5100	Qualification Testing
		FI-5200	Inspection
		FI-5300	Production Testing
FI-6000	Fabrication	FI-6100	General
		FI-6200	Fabrication and Assembly
		FI-6300	Workmanship
FI-7000	Packing, Shipping, Receiving, Storage, and Handling	None	
FI-8000	Quality Assurance	FI-8100	Responsibility
		FI-8200	Certificate of Conformance
FI-9000	Name Plates	FI-9100	Filter Marking
		FI-9200	Package Marking

The current draft of section FI contains subsections of FI-5100 for qualification testing that includes qualification procedures listed below [37]. Qualification requirements have been developed using section FC as a basis and creating unique requirements to section FI because of the uniqueness of the metal media filters.

- Resistance to Air flow. FI-5110 addresses the resistance to air flow at the rated airflow of the clean filter. For metal media HEPA filters intended to

serve as a direct replacement for Section FC filters in existing systems, the resistance to airflow of the clean filter shall meet the requirements of the Tables FI-4121-1 or FI-4131-2 or FI-4131-3 or FI-4132-1 when tested in accordance with FI-5122.

- Test Aerosol Penetration-FI-5120 addresses testing metal media filter elements for penetration of aerosols. Metal media filter elements will be tested for resistance to airflow and aerosol penetration using procedures contained in existing consensus standards and will employ a test stand capable of producing the differential pressures called for by owner/operator specifications
- Resistance to Rough Handling. FI-5130 addresses the durability of filters when exposed to rough handling that could be encountered in shipping and moving the filters in and out of storage.
- Resistance to Pressure-FI-5140 addresses the ability of the filter to withstand extreme pressures that the filter elements could be exposed to during emergency conditions.
- Resistance to Heated Air-FI-5150 addresses the ability of the filter elements to with stand high temperatures
- Spot Flame Resistance-FI-5160 addresses the flammability of the filter media by exposing it to a flame from a Bunsen burner.
- Structural Requirements-FI-5170 specifies that the filters must be evaluated for structural damage.

- Cyclic Testing of Cleanable Filter Designs-FI-5180 address the testing of the cleaning of filters that are intended to be cleaned and reused repeatedly.

The qualification tests outlined above require numerous sets of data to be collected. Some data can be collected simultaneously while other data must be tested separately. Testing with positive pressure air flow for resistance to airflow and test aerosol penetration can be collected simultaneously. Flow rates, up and downstream aerosol concentrations, differential pressure across filter elements, relative humidity, and temperature can all be monitored during resistance to airflow and test aerosol penetration tests. Resistance to elevated pressures will involve using a viscous liquid in a small scale test stand to challenge the filter element to elevated pressures. The differential pressure across the filter must be continuously monitored and recorded. The resistance to heated air involves inserting the filter elements into a specialized small scale test stand and using electric or combustion air heaters to heat the air flow to 750 degrees F [37]. During this testing temperature and differential pressure across the filter is recorded. Cyclic testing of cleanable filter designs requires the filters to be loaded and back pulsed to clear filter cake repeatedly. Aerosol concentrations, loading rates and testing conditions are continuously monitored during this testing. Resistance to rough handling will involve testing the filter on a rough handling machine for 15 min at ¾ inch amplitude and 200 cycles per minute [37]. For testing of spot flame resistance the metal media pack is required to be exposed to a gas flame from a Bunsen burner for a minimum of 5 minutes [37]. Structural requirements for each filter involve examination for structural damage, airflow and penetration resistance, leak testing, and tube sheet leak testing [37]. Each

filter is to be visually inspected to show conformance to size specification and inspection to verify that labels are properly located and indicate they been tested and meet required flow rate, penetration and air flow resistance for metal media filters [37]. The testing sequence should follow that put forth in drafts of section FM as opposed to section FC. Each set of filter elements should undergo a sequence in which the filter set is passed from test stage to test stage that is employed with a final FE determination. This is expected to yield a more accurate representation of how the filter will function when subjected to conditions outside normal operating conditions.

Balloting Section FI

Balloting of a new section to be added to AG-1 is an iterative process that requires the proposed language undergo a series of reviews and panels. Consensus must first be established within the project team. Proposed language is then reviewed and balloted within the filtration subcommittee. Negative votes cast must be resolved before re-balloting. Comments are addressed by the project team and provided to the committee member. The approved draft is then sent to the Main Committee for review and comment. The edited material is then reballoted and negatives resolved. Once the section language has been approved by the main committee it is sent to the BNCS for review. It can either be approved by the board or returned to the project team for modification. This iterative process is commonly long and tedious. The code to be balloted must be based on extensive supporting information to demonstrate that the new standard is sufficient.

CHAPTER IV

TEST STAND DESIGN AND CONSTRUCTION

Test stand performance criteria

Section FI has gone through the balloting process twice and numerous presentations have been made to the Main Committee. Incremental progress has been made over the past ten years; however availability of testing/qualification infrastructure has remained as the most critical issue preventing balloting. The FI project team has been working with DOE-HQ and ICET to design and construct a research grade test stand that can provide data and detailed information necessary for moving forward the process of finalizing section FI. The remaining obstacle is the lack of physical testing capabilities and testing procedures capable of addressing the wide range of user defined needs. The rest of this paper discusses the design and construction of a research grade test stand that is intended to help establish this infrastructure. Performance criteria for the test stand are provided in Table 7.

Table 7 Test stand performance criteria

Performance Criteria	
Capactiy	House up to three 8 foot long Filter Elements
Flow	Produce flow of 50-200 ACFM at pressures up to 15 PSI
Testing conditions	Maintain conditions of 60-80 Degrees F, 40-60% RH, up to 15 psig
Condition Measurement	Continuously measure and record static pressure, differential pressure, temperature, relative humidity, and flow rate
Particle Measurement	Continuously measure and record particle concentration and Size
High Temperature	120 ACFM at 750 degrees F
High Pressure	Differential Pressure o f15 PSI

The Section FI Project team reviewed testing needs and determined the range of test and qualification conditions necessary including dimensions necessary to test an appropriate range of filter elements along with maximum volumetric flow and differential pressure. This catalog of performance criteria were converted into a concept design drawing by ICET personnel as shown in Figure 4.

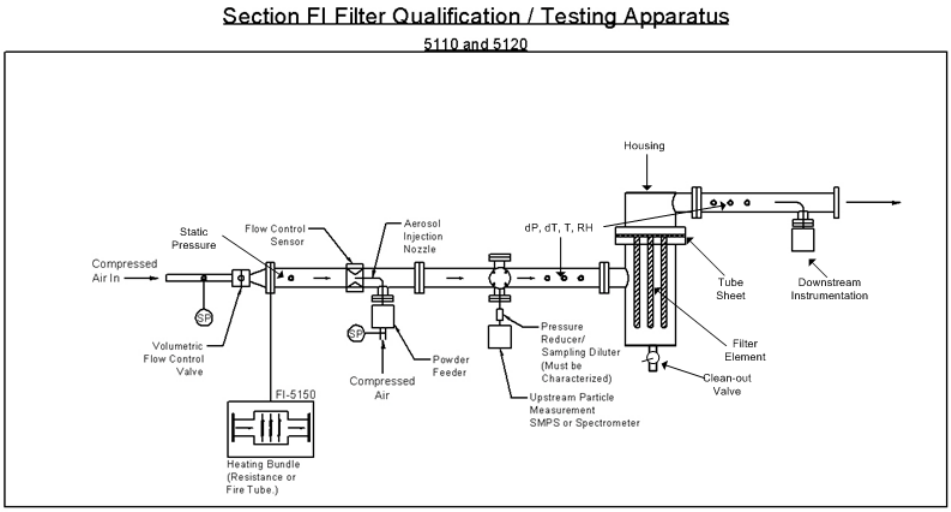

Figure 4 FI project team concept design for FI test stand

These drawings were modified by ICET and during meetings and conference calls with the FI project team.

Traditional HEPA filter test stands utilize a negative pressure air flow. The FI test stand utilizes positive pressure because of the high pressure drop associated with metal media filters. The FI filters have higher initial differential pressure and are capable of performing at differential pressures much higher than fibrous glass filters. To produce differential pressure across the filters to extensively challenge these filters it is necessary to utilize positive pressure. The use of positive pressure air flow in the FI test stand required major design changes. Two major challenges from using positive pressure are complications associated with aerosol generation and aerosol measurement instrumentation.

The test stand design was reviewed and redesigned several times until the design shown in Figure 5 was agreed upon.

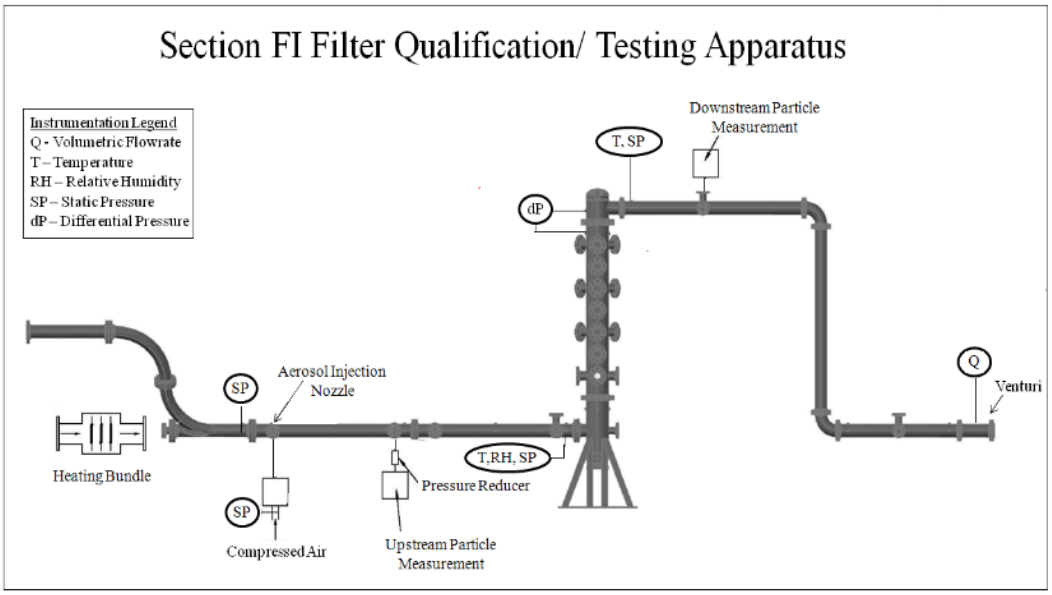

Figure 5 Drawing of test duct and housing with instrument locations marked

This test stand is capable of simultaneously testing up to three radial flow metal media elements four inches in diameter and 2.6 feet (2 m) long. The design is flexible enough to evaluate a wide range of parameters shown in Table 8 to produce data necessary for section FI filter qualification.

Table 8 Capabilities of FI Test Stand

Actual Performance	
Capactiy	Can house up to three 8 foot long Filter Elements
Flow	Can produce flow of 50-160 ACFM at pressures up to 10 PSI
Testing conditions	Can maintain conditions of 60-80 Degrees F, 40-60% RH, up to 10 psig
Condition Measurement	Can continuously measure and record static pressure, differential pressure, temperature, relative humidity, and flow rate
Particle Measurement	Can continuously measure and record particle concentration and Size
High Temperature	Seperate test stand designed
High Pressure	Separate test stand designed

Design calculations

Hoop Stress

Hoop stress is used to calculate the permissible pressure allowed inside the piping. The calculation for hoop stress determines the grade of piping used on the test stand. For the design of the test stand the ICET Pressure Vessel and System Design Standard was used as guidance. Equation 22 was used for this calculation where Sa is the ultimate stress, E is joint efficiency, t is shell thickness, r_i is the inner radius and SF is the safety factor.

$$P = \frac{Sa(E*t)}{2r_i SF} \tag{22}$$

The ultimate stress used for 304L stainless steel is 57,000 PSI, the joint efficiency is 0.7, and SF is 4. The thickness changes with the diameter of piping used. For 12 inch pipe the thickness is 0.375 inches and for 6 inch pipe the thickness is 0.28 inches. Using these values the allowable pressure was found to be 623.5 PSI and 921 PSI for the 12 and 6 inch piping respectably. These values are well above the maximum expected operating pressure for the test stand of 15 PSIG.

Shell Nozzles

ASME Section VII Division 1 UG-37 addresses reinforcements required for openings in shells and formed heads. For openings in pressure vessel, the missing supporting shell area must be replaced by an extension at the shell, nozzle or by a reinforcement pad. Using Equation 19 rearrange and solve for thickness using 18 PSIGfor P with the values from the previous section. This value is the minimum required thickness for the piping wall (t_r). The minimum wall thickness is found to be 0.036

inches. Using this thickness the required area (A_r) can be found using equation 23 where d is the hole diameter, t_r is the required shell thickness, and t_n is the nozzle wall thickness. The required area can be found using the minimum required thickness found using Equation. 19 as t_r. The actual wall thickness is 0.375 inches. Since $t_a > t_r$ then $A_a > A_r$ and no additional thickness is required to be added to the pipe wall.

$$A_r = dt_r + 2t_n t_r \tag{23}$$

Pipe and Flange Selection

Piping for the test stand is required to handle a maximum of 15 PSIG and 750° F. ANSI/ASME B 31.1 for stainless steel piping shows 6 inch schedule 40 stainless steel pipe to be rated to withstand a pressure of 724 PSIGat 750° F. The housing of the test stand is constructed of 12 inch schedule 40 stainless steel piping. These values are well above the required temperature and pressures at which the test stand will be operated. According to ANSI B16.5 flange pressure class of 300 lb will be sufficient for the prescribed conditions in the test stand.

Weight

The large size of the test housing requires that the weight of the housing be determined to ensure that the supports for the test stand will be able to withstand the load without failing. The weight of the housing was calculated to be 1700 lb. Equation 24 was used to determine the weight of the test stand.

$$\text{Weight} = \text{Density}_{\text{steel}} \times \text{Volume}_{\text{steel}} \tag{24}$$

Test Stand Base

The test stand base was design to be able to hold the weight of the test stand as well as provide lateral stability. Calculations were required to assure that the test stand would not collapse once it was assembled. These calculations involved using the material properties as well as geometry of the legs of the test stand to calculate the maximum load capacity. For this calculation only the four vertical support legs were considered. Equation 25 was used to calculate the predicted stress applied to the vertical supports of the test stand.

$$\sigma = \frac{\text{Force}}{\text{Area}} \tag{25}$$

For the legs on the test stand 3 x ¼ inch angle iron was used this resulted in a area of 0.5 ft^2 of total area for the legs. Using the weight and the cross sectional area of the legs the stress in the supporting members was found to be 3400 lb/ft^2. The yield strength of ASTM A36 is $5x10^6$ lb/ft^2. This demonstrates that the legs are designed to with stand much more than the highest expected load.

The horizontal stability of the test stand is provided by the diagonal legs. To determine the horizontal stability of the test stand the equivalent force required to push over the test stand will be calculated. Equation 26 was used to determine the required force.

$$\text{Required Force} = \frac{\text{Weight} \times \text{Width}}{\text{Height}} \tag{26}$$

The width of the diagonal feet from the base is 3 feet. The height of the test stand is 15 ft and the weight of the test stand housing is 1700 lb. using these values the required

force to topple the test stand is approximately 340 lb. This was determined by the ICET safety officer to be sufficient to allow for the test stand to safely be operated.

Piping length

The length of the piping upstream and downstream of the test stand is dictated by Reference Method 1 – Sample and Velocity Traverses for Stationary Sources [38].

Upstream Piping

For the 6 inch (15.24 cm) pipe used in fabrication of the test stand, the aerosol sampling location upstream of the filter housing must be a minimum of 8 pipe diameters or 4 feet (1.22 m) downstream of any flow disturbance such as a bend in the pipe, a venturi, or point of aerosol injection. Likewise, this aerosol sampling location must be a minimum of 10 pipe diameters or 5 feet (1.52 m) upstream of any flow disturbance such as the filter housing [38]. Therefore the upper section of the test stand where sampling will occur must be at minimum of 9 feet (2.75 m) long. Additional length has been added to the upstream section to allow for multiple sampling ports. The test stand upstream of the housing will consist of approximately 10 feet (3 m) of 6 inch (15.24 cm) stainless steel piping, access ports, an air compressor, electric air heating bundle, volumetric flow control valve, DOP Generator, flow control sensor, particle measurement instrumentation, and air property measurement instrumentation.

Downstream Piping

As with the upstream sampling section of the test stand, the aerosol sampling location downstream of the housing must be a minimum 8 pipe diameters downstream of disturbances and 10 pipe diameters upstream of disturbances [38]. Therefore the aerosol

sampling location downstream of the housing must be at least 4 feet (1.22 m) downstream of the filter housing and 5 feet (1.52 m) upstream of any flow disturbance such as a downstream venturi or pipe bend. The downstream measurement section of the test stand must then be at least 9 feet (2.75 m) long. Additional length has been added to the upstream section to allow for multiple sampling ports.

Pressure Drop

The pressure drop down the length of the 6 inch piping immediately before the test stand housing was calculated using Equation 27.

$$P_{loss} = \lambda \frac{L}{D} \frac{\rho * V^2}{2} \quad (27)$$

The pressure loss in the upstream piping was found to be 0.91 PSI. The estimated maximum differential pressure across the filters when loaded is 15 PSIG. These values were used in the selection of the blower.

Flow Rate

The flow rate inside the test stand will be monitored using a venturi downstream of the housing. Because of the expansion of the air through the filters due to the change of pressure, change in flow rate from the upstream to the downstream sections will be accounted for in the calculation of the upstream flow rate by using conservation of mass. The following equations were used to determine the upstream flow rate [39]. The cross sectional area of the downstream section of the pipe is different than the flow area of the filter and thus the flow rate through the filter media must be calculated using the effective

area of the filter. Equations 28-30 are the equations used to calculate the volumetric flow rate.

$$\text{mass}_{\text{in}} = \text{mass}_{\text{out}} \tag{28}$$

$$\text{Mass}_{\text{flow}} = \text{Volumetric}_{\text{flow}} \times \text{Density} \tag{29}$$

$$\text{Volumetric}_{\text{flow}} = \text{Velocity} \times \text{Area} \tag{30}$$

The area is the cross sectional area of the section being calculated. The density is the density of the air at the specified temperature and pressure and the velocity is found using the downstream venturi. The venturi used is manufactured by Primary Flow Signal and has a range of 50 to 375 CFM with an accuracy of ±0.50% of the actual reading.

Media Velocity

An important parameter in filtration is the media velocity through the filter. This velocity is calculated by dividing the calculated media velocity by the effective area of the media that is provided by the manufacturer. Several different media velocities will be tested and these are shown in the results section.

Cooling and Heating for Relative Humidity Control

Conditions of air leaving the blower and entering the test stand will vary during operation due to ambient conditions as well as from the duration of the testing. A cooling then heating process is employed to create consistent conditions during the testing. A water chiller provides a chilled fluid to the cold side of a fluid to air heat exchanger to chill the air stream. An air to air heat exchanger utilizing warm air upstream of the heat chilling heat exchanger is then used to reheat the air stream after the cooling heat exchanger. This allows for testing conditions to be adjusted. To determine the capacity of

the chiller and heat exchanger the heat transfer of a steady state open system with no work for a cooling process was used as shown in Equation 31. The heat transfer of the system must account for the change in temperature of the air stream (sensible heat) as well as the energy required to condense water in the air stream (latent heat). Where m_{dota} is the mass flow rate of the air, h_1 is the enthalpy of the inlet air, h_2 is the enthalpy of the exit air, h_L is the latent heat of condensation, w_1 is the humidity ratio of the inlet air, w_2 is the humidity ratio of the exit air and Q is the heat transfer rate.

$$Q = m_{dot}[(h_2 - h_1) + (w_1 - w_2)h_L] \quad (31)$$

The relative humidity (RH) will need to be maintained between 40% and 60% and the temperature will need to be held between 60° F and 80° F for efficiency and loading testing. The estimated required cooling capacity of the chiller upstream conditions was calculated assuming 70% RH and 100° F. Airstream RH will reach 100% producing condensation when the airstream is cooled to 50°F. The air can then be heated to 70°F at which point the RH will be 50%.

Air temperature and relative humidity values can be used with an ASHRAE psychometric chart to determine the enthalpy of the air. The enthalpy can then be used in equation 31 to determine the cooling capacity required for the chiller. The required cooling capacity was found to be 2.48 tons. The heating capacity of 0.34 tons for the heat exchanger was found using the same equation and the ASHRAE psychometric chart shown in Figure 6.

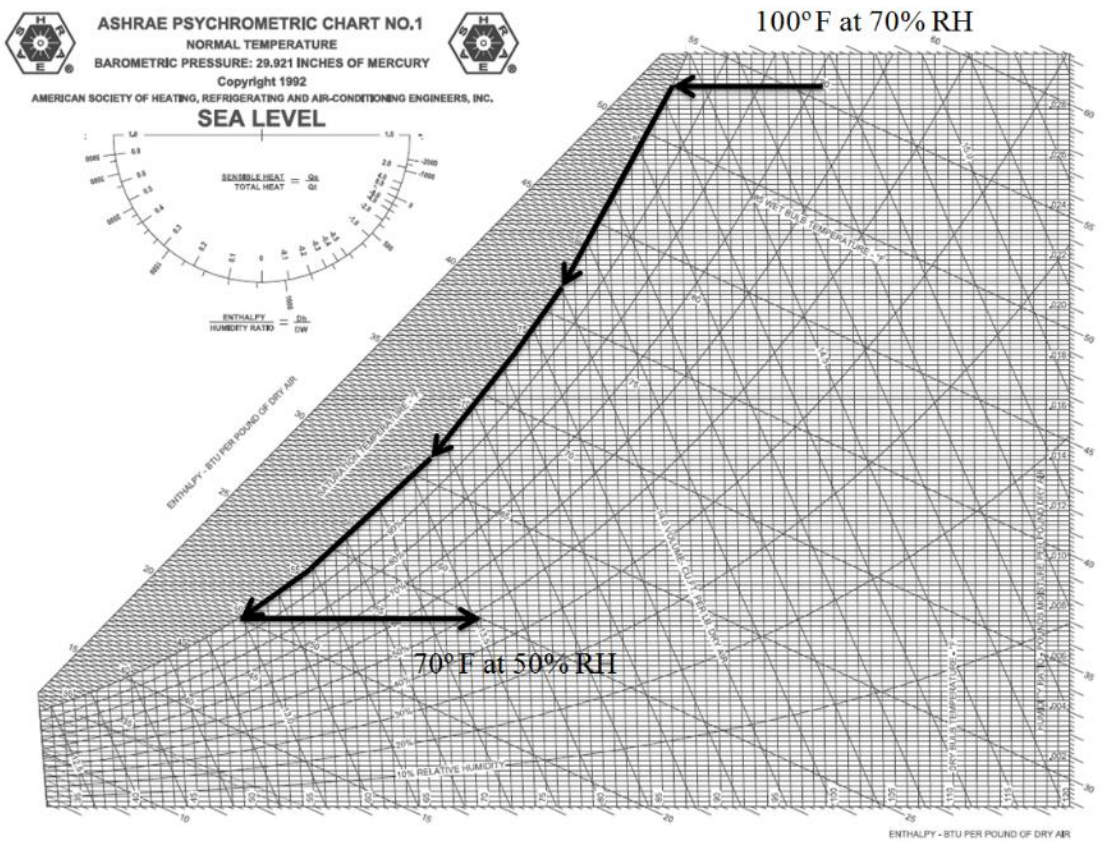

Figure 6 ASHRAE Psychometric Chart No. 1

High Temperature

Resistance to high temperature testing requires filter media be heated to 750° F (400° C) Air will be heated using existing air heaters with a total heating capacity of 63 tons. Using an energy balance the required inlet temperature can be determined. Equations 33-36 were used to determine the temperature requirements of the inlet air[39].

$$E_{in} = E_{out} \tag{33}$$

$$q = mass_{flowrate} \times C_p \times (T_{Entrance} - T_{Exit}) \tag{34}$$

$$q = \frac{T_{inside} - T_{ambient}}{R_{Total}} \times Area \tag{35}$$

$$R_{Total} = R_{inconv} + R_{condpipe} + R_{condinsulation} + R_{outconv} \quad (36)$$

The temperature drop through 23 feet (7 m) of pipe was found to be 6.3° F (3.5°C). Air leaving the air heaters will need to be at least 758.3° (403.5°C) to reach the target operating temperature of 750° F (400°C). The required heating load is 30,359 Watts.

Test stand and components

This section discusses the components of the test stand. Individual design calculations for test stand components are provided in the calculations section. Appendix C provides detailed drawings of the test stand components.

Piping

The upstream and downstream piping are 6 inch stainless steel piping. The upstream and downstream piping contains several ports for sampling. Couplings on the piping allow for readings of pressure, temperature, and relative humidity.

Flanges

300 lb flanges were used on the test stand to withstand design temperatures and pressures of the test stand.

Length

The length of the piping for the downstream and upstream sections of piping was determined using EPA Test Method 1 [ ].This method specifies the length (in pipe diameters) from a flow disturbance to a sampling location.

Housing

The test housing is designed to hold three 4 inch diameter radial flow metal media elements 7 feet in length. It is constructed of 12 inch diameter Schedule 40 stainless steel and capable of withstanding maximum test conditions of 15 PSIGand 750°F. The total height of the test stand base and test section is 15 feet (4.6 m). The test section is comprised of three units; a top section, the middle section with tubesheet to support the filter elements, and a base. The overall mass of the upper two portions of the test section is 1500 lb and a chain hoist/jib crane is used to facilitate assembly/disassembly. A procedure for assembly/disassembly of the test stand is provided in Appendix D.

The top section of the housing is 2 feet (0.61 m) long with an outlet port to the downstream section of the test stand and a dome cap welded on the top. Couplings on the top of the housing will allow for differential pressure and temperature across the filter elements to be measured. The separate sections are connected together using 150 lb class flanges. The top of the housing is shown in Figure 7. The design drawing for this unit can be seen in Appendix B.

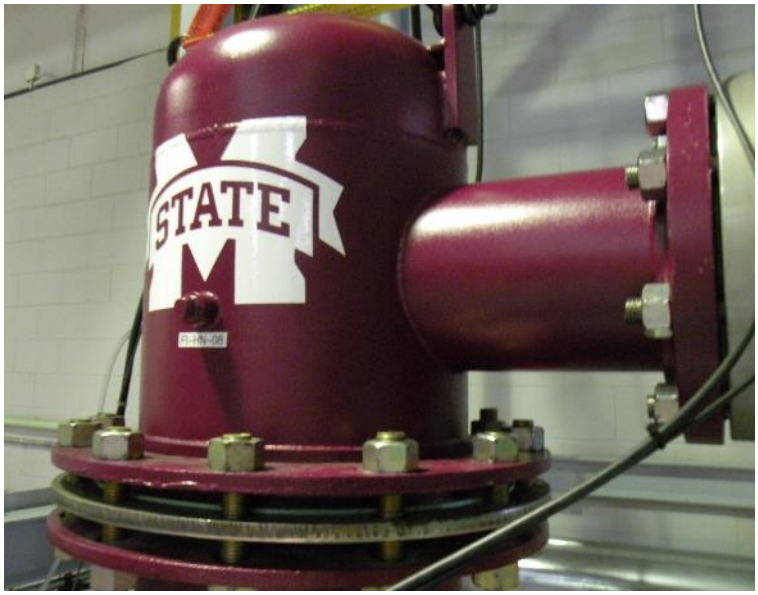

Figure 7 FI test stand Cap shown connected to middle section

The middle section of the housing is 8 feet (2.44 m) long to accept filter elements up to 8 feet (2.44 m) long for testing. The middle section has numerous ports available down the length of the section for sampling and visual examination of filter elements. In the future these ports will be employed to evaluate the process of back pulse cleaning. Couplings on the housing allow for differential pressure and temperature to be measured. The middle section of the housing is shown in Figure 8. The design drawing for this unit can be seen in Appendix B.

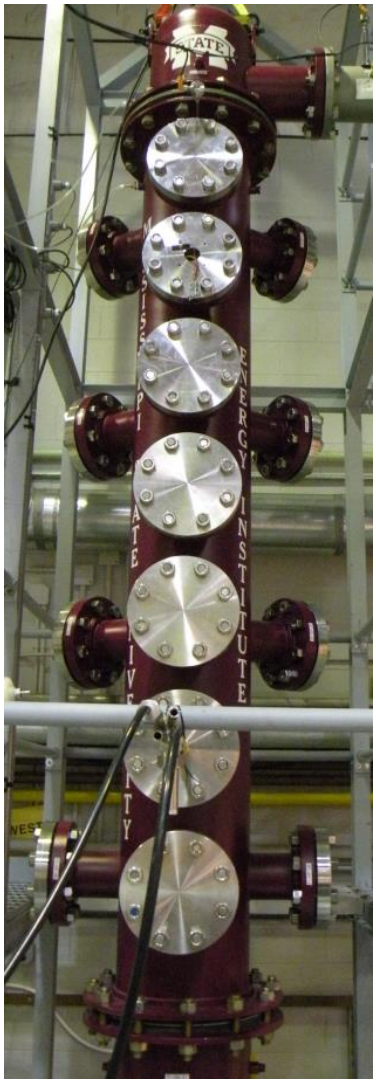

Figure 8 FI test stand housing middle section

The base of the housing consists of a 3 feet (0.9 m) section with an inlet port connected to the upstream piping, an additional port to allow for sampling, and a dome cap and drainage port to capture bulk material cleared during back pulse cleaning of the elements. The access port on the bottom of the housing provides access for cleaning. Couplings on the bottom section allow for temperature and pressure readings. The base of

the test stand is shown in Figure 9. The design drawing for the test stand base can be seen in Appendix B.

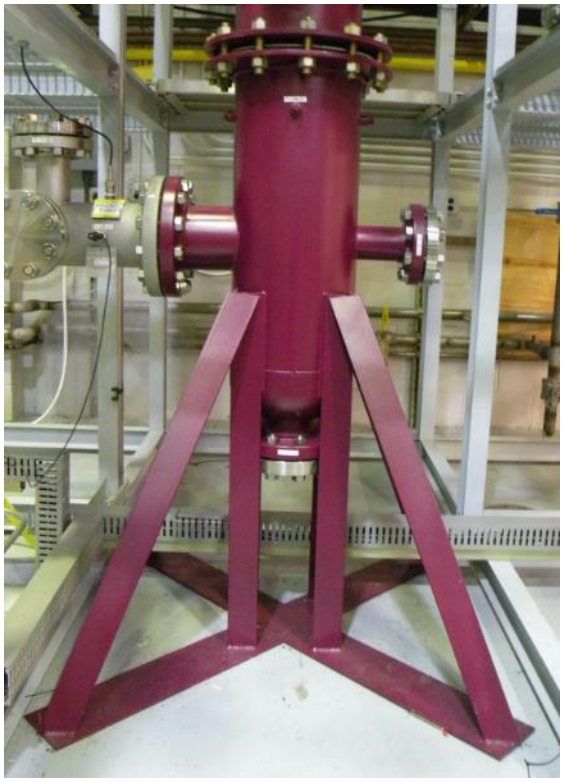

Figure 9 FI test stand housing base section

Tube sheet

A tube sheet is used to support one or more filter elements. The tube sheet can be fitted with a variety of coupling systems for attaching individual elements. An example tube sheet is shown in Figure 10 with three elements attached by threaded fittings. Other attachment options can include threaded nipples, compression fittings or even welding. Tube sheets are also being developed to attach ceramic elements such as are covered by section FO currently under development for evaluation in this test stand.

The tube sheet is positioned between the top and middle section of the housing between slip flanges. This allows the tube sheet to be rotated relative to the body of the middle section for aligning elements with observations ports to view either a single element or the space between elements. The tube sheet designed to hold the filter elements in place inside the test stand housing can be seen in Figure 10. The design drawing for example tube sheets can be seen in Appendix B.

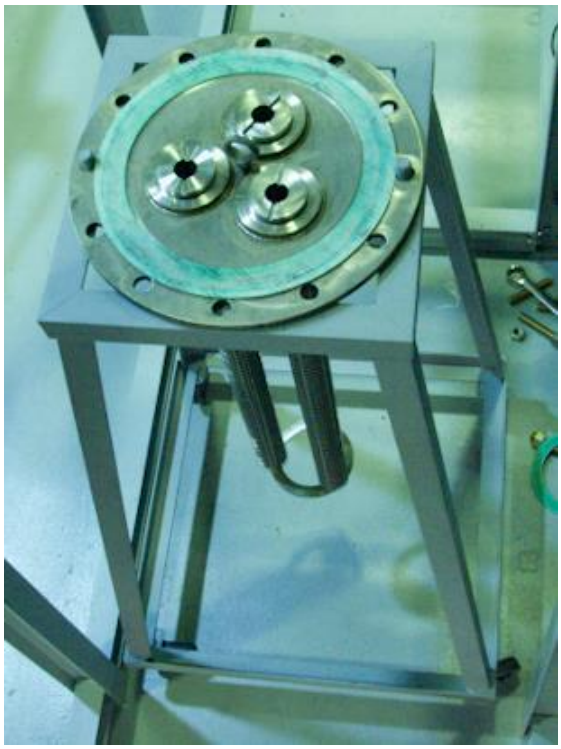

Figure 10 FI test stand tube sheet with filter elements

The filter elements are stabilized on the tube sheet by attaching a spider ring on the end of the filter elements opposite the tube sheet. A set of filter elements attached to

the tube sheet with the spider ring for stabilization are shown ready for insertion into the test stand housing in Figure 11.

Figure 11 Porvair sintered metal media Section FI HEPA filter elements attached to the tubesheet

The tube sheet with the filter elements is secured inside the test stand with slip flanges between the cap and middle section of the housing. Figure 12 shows the slip flanges and location where the tube sheet is secured in the housing.

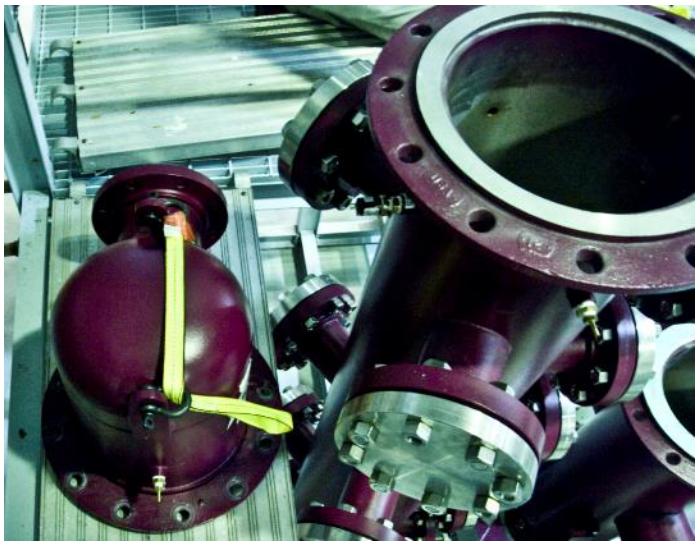

Figure 12 Cap and middle section of FI test stand disassembled showing slip flanges

Support Structure

A structure is needed to support the weight of the housing for assembly and disassembly because of the size of the test stand. The housing is located within the frame of the structure equipped with a chain hoist to lift and move the housing. This structure provides platforms for personnel to stand beside the upper and middle sections of the assembled housing during testing. These platforms allow for access to ports on the sides of the test stand. The support structure is shown in Figure 13 and design drawings are provided in Appendix B.

Figure 13 FI test stand and support structure

Piping

Upstream of Housing

For the 6 inch (15.24 cm) pipe used in fabrication of the test stand, the aerosol sampling location upstream of the filter housing must be a minimum of 8 pipe diameters or 4 feet (1.22 m) downstream of any flow disturbance such as a bend in the pipe, a venturi, or point of aerosol injection. Likewise, this aerosol sampling location must be a minimum of 10 pipe diameters or 5 feet (1.52 m) upstream of any flow disturbance such as the filter housing.[15] Therefore the upper section of the test stand where sampling occurs must be at minimum of 9 feet (2.75 m) long. Additional length has been added to

the upstream section to allow for multiple sampling ports. The test stand upstream of the housing consists of approximately 10 feet (3 m) of 6 inch (15.24 cm) stainless steel piping, access ports, an air compressor, volumetric flow control valve, DOP Generator, flow control sensor, particle measurement instrumentation, and air stream condition instruments. The upstream piping can be seen in Figures 14 and 15. Design drawings for all piping sections and the assembly are given in Appendix D.

Figure 14 FI test stand upstream piping going into housing

Figure 15 FI test stand upstream piping entering building

Downstream of Housing

As with the upstream sampling section of the test stand, the aerosol sampling location downstream of the housing must be a minimum 8 pipe diameters downstream of disturbances and 10 pipe diameters upstream of disturbances [15]. Therefore the aerosol sampling location downstream of the housing must be at least 4 feet (1.22 m) downstream of the filter housing and 5 feet (1.52 m) upstream of any flow disturbance such as a downstream venturi or pipe bend. The downstream measurement section of the test stand must then be at least 9 feet (2.75 m) long. Additional length has been added to the upstream section to allow for multiple sampling ports. The downstream section of piping can be seen in Figures 16. The design drawing can be seen in Appendix B.

Figure 16 FI test stand downstream piping elevated section

The completed test stand housing is shown in Figure 17.

Figure 17 Assembled FI test stand housing

Procedures for the assembly and disassembly of the FI test stand can be found in Appendix D.

High temperature section

An additional component of the test stand is required to accomplish the resistance to heated air test called for in Section FI-5150. FI-5150 calls for testing up to 750^{o} F (400^{O} C). This will include replacing the upstream section of the test stand with a reconfigured one that includes one or more electric heaters. Figure 18 provides a drawing

of the high temperature test configuration. The upstream section of the test stand will be disconnected and replaced with a blind. Insulation, not shown in the following figure, is required as specified by the ICET safety officer for safety of workers during operation.

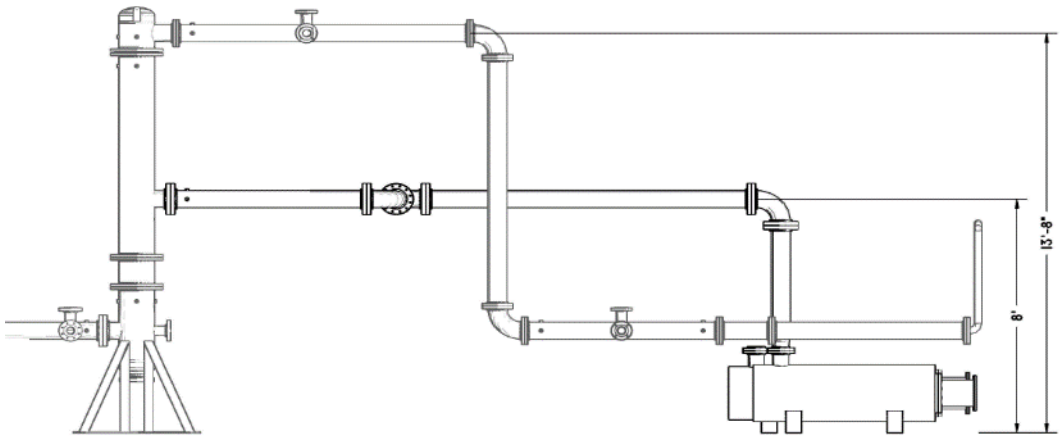

Figure 18 FI test stand high temperature testing section

High pressure test stand

Metal media filter elements using sintered metal fiber in a pleated configuration gain resistance to collapse by an internal cylindrical core. The core material is a heavy gauge lattice work cylinder providing higher lateral strength to the filter element. High differential pressure failure of metal media elements employing either sintered metal fiber or powder normally occurs when the element collapses. Therefore determining the collapse pressure of filter elements is unique to this type of filter. A separate test unit has been designed to determine the core collapse pressure for metal media elements. Figure 19 provides the drawing for high pressure test stand that will employ a viscous liquid to determine collapse pressure.

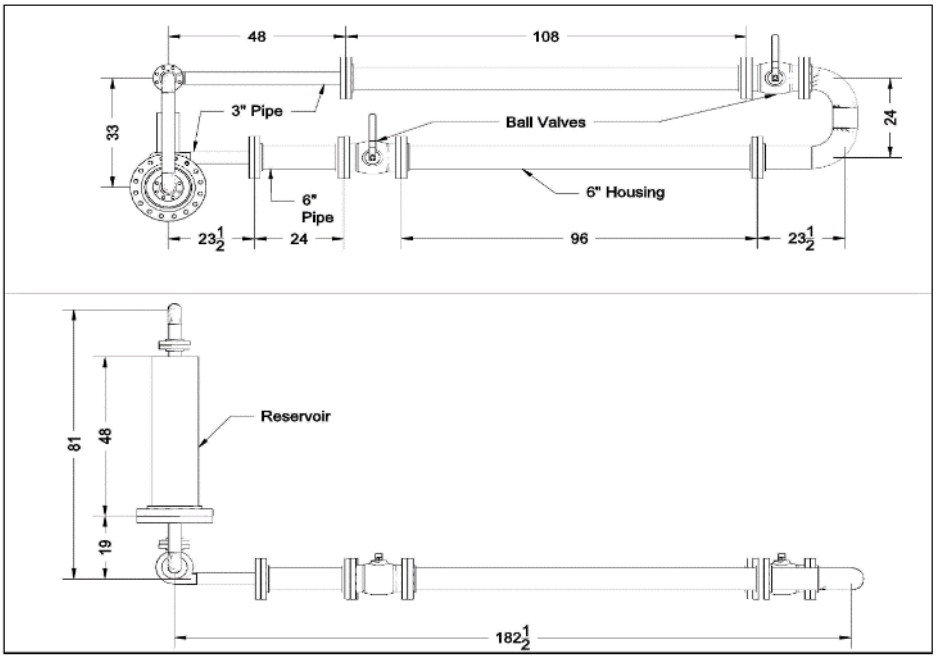

Figure 19 FI high pressure test stand design

Air supply system

Two air supply systems can be used on the test stand. The first consist of two Spencer Vortex blowers connected in series capable of generating a volumetric flow of 133 CFM. The Spencer Vortex blowers are shown in Figure 20.

Figure 20 Spencer vortex blowers for FI test stand

A claw compressor with a variable speed drive is used for flow rates from 50 to 160 ACFM (1.42 to 4.53 m^3/min). This claw compressor was selected because of its ability to reach the desired flow rates as well as be able to overcome the maximum estimated pressure drop. The claw compressor used is shown in Figure 21.

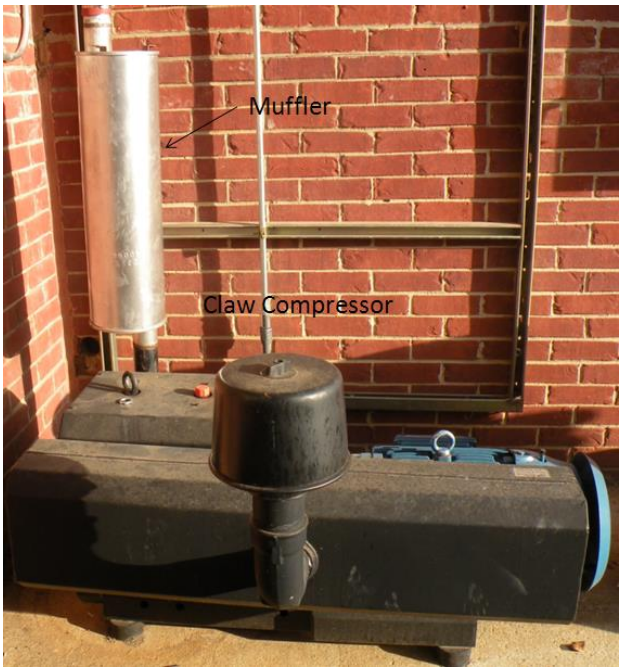

Figure 21 FI test stand claw compressor and muffler

The design of this claw compressor causes it to produce oscillations in flow and pressure. This unsteadiness is undesirable for the filter testing. Pulsation of air flow is damped by connecting a muffler to the claw compressor and providing air flow through a rubber hose going to two air tanks in series.. The rubber hose and air tanks are shown in Figure 22 and Figure 23.

Figure 22 FI test stand rubber hose connecting claw compressor to air tanks

Figure 23 FI test stand buffer air tanks

Flow rates below 55 ACFM (1.6 m^3/min) will be accomplished using an air compressor with an automated flow control valve because of the limited range of the blower,.

The Baldor variable frequency drive shown in Figure 24 is used to control the frequency on the claw compressor or blower. This changes the speed of the blower or claw compressor and increases or decreases the flow rate.

Figure 24 Variable frequency drive for FI test stand

Fine tuning of the flow rate into the test stand is regulated by use of an air bleed off valve. The percent this valve is opened is controlled on the test stand computer. This pneumatic valve is shown in Figure 25.

Figure 25 Pneumatic bleed off valve for FI test stand

For flow rates greater than 50 CFM A venturi flow measuring devise is used to monitor flow rates greater than 50 CFM and for flow rates below 50 ACFM an orifice plate is used. The venture used to measure the flow is shown in Figure 26.

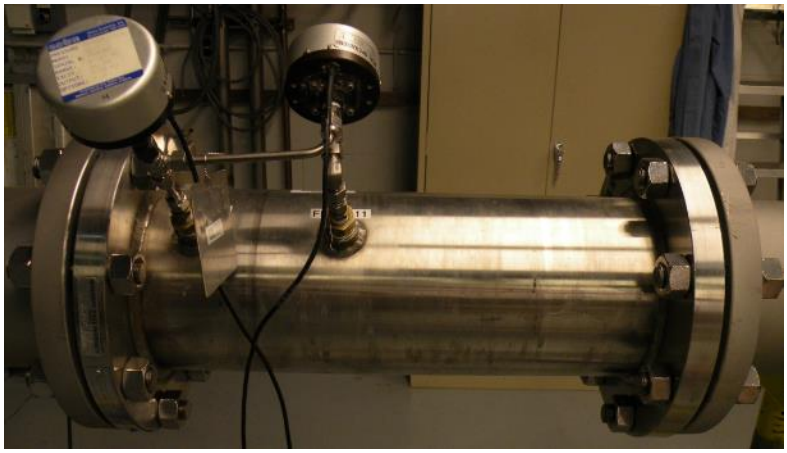

Figure 26 Venturi used to measure flow rate on FI test stand

Chiller and heat exchangers

Conditions inside the test stand are controlled using a water chiller and heat exchanger to adjust the air stream to the desired conditions. Air stream conditioning equipment is located outside due to space limitations. The equipment used to control the relative humidity and temperature in the test stand are a PCW060 Parker Hyperchill water chiller, a 4 foot long Standard Xchange model SX2000 shell and tube heat exchanger for cooling using water from the chiller and a 2 foot long Standard Xchange model SX2000 shell and tube heat exchanger for reheat using waste heat off the air before the chiller heat exchanger. These heat exchangers and water chiller used are shown in Figures 27 and 28.

Figure 27 Hyperchill water chiller for air stream conditioning on FI test stand

Figure 28 Heat exchangers for control of air conditions on FI test stand

Control of temperature and relative humidity is accomplished by changing the percent of air bypassed around the reheat heat exchanger, changing the set point temperature on the water chiller, and changing bypass percent around the chiller heat exchanger. The reheat heat exchanger bypass is controlled using the test stand computer allowing the user to specify how much the bypass valve is opened. Controls on the test stand computer can be seen in Figure 29.

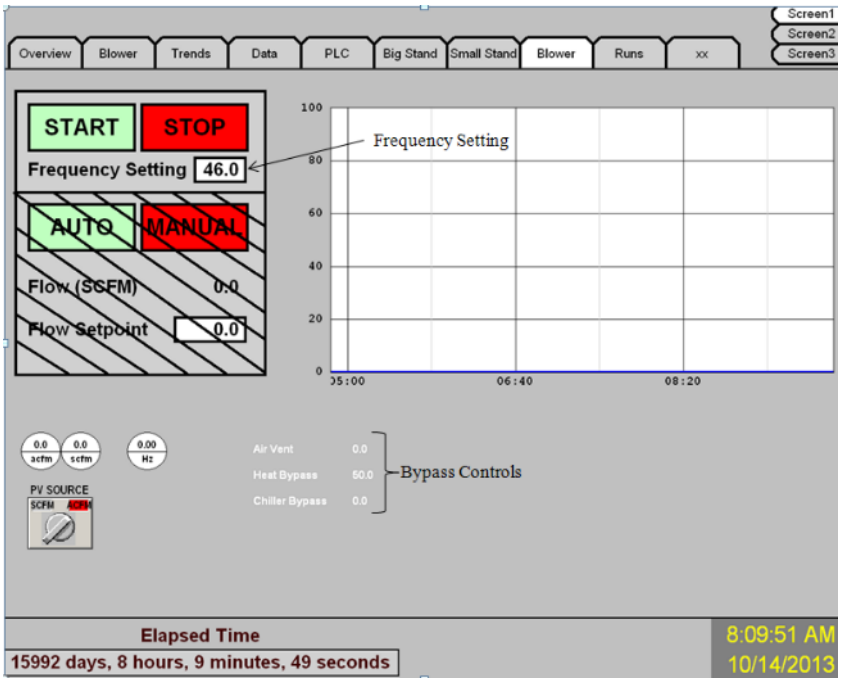

Figure 29 Heat exchanger bypass controls and frequency controller of variable frequency drive shown on test stand computer screen

The chiller temperature is controlled by using the control panel on front of the chiller to set the desired temperature. The chiller temperature control can be seen in Figure 30.

Figure 30 FI test stand chiller control panel

Health and safety

This project presents many possible safety hazards. The test stand to insert and remove filter elements creates several overhead hazards that range from low beams to falling objects. Hard hats are required in the testing area during the phase of operation. Initial problems with loud noise from the claw compressor made it necessary for hearing protection to be worn. This issue has been resolved by using several buffers between the claw compressor and the test stand. Radioactive Sr-90/y-90 beta sources that are used for particle neutralization and Krypton-85 used in the TSI Model 3080 electrostatic classifier requires monitoring of employs exposure by a dosimeter. Dosimeters are read monthly and exposures are added to employee records. Addition of the high temperature section of the test stand will require insulation and safety barriers to be installed during high temperature testing. A health and safety plan was prepared by Donna Rodger, the ICET certified industrial hygienist, and is available at ICET upon request.

Test conditions sensors

The ICET FI test stand is fully instrumented with sensors and controls to continuously monitor and control testing conditions. Installed sensors include temperature, static pressure, relative humidity, flow rate and differential pressure. Table 9 lists these sensors and their respective uncertainties.

Temperature Measurement

Temperature inside the test stand is measured at several locations including immediately before and after the filter elements to ensure they reach the required temperature. Omega mini temperature transmitters with PT100 TRD probes are used to monitor the temperature in the test stand.

Differential Pressure Measurement

Omega differential pressure transducers of various ranges are used to monitor the differential pressure across the filter elements.

Static Pressure Measurement

ProSense pressure transmitters are used to monitor the static pressure at various locations inside the test stand to ensure that the pressure in the test stand does not exceed 15 psig.

Relative Humidity Measurement

The relative humidity of the airstream in the test stand is monitored to ensure consistent humidity levels during testing. Vaisala dew point and temperature transmitter is used to monitor the relative humidity inside the test stand.

Flow Measurement

The flow rate inside the test stand must be monitored. A Primary Flow Signal 6" venturi is used downstream to monitor the flow rate and to assure that the filter elements are being tested at the rated flow for the elements.

Table 9 Accuracy of ICET FI Filter Test Stand Sensors

Sensor	**Manufacturer**	**Model Number**	**Range**	**Accuracy**
Temperature Transmitter	Omega	TX-M12-RTD-C		+/-0.2 + (0.05 %) + output Accuracy
Temperature RTD Probe	Omega	PR-22-3-100-B-1/4--0900-M12	-50 to 500 C	+/-0.15 C of reading
Differential Pressure	Omega	PX409-2.5DDUI	0 to 2.5 psig	0.08% of reading
		PX409-0005DDUI	0 to 5 psig	
		PX409-015DDUI	0 to15 psig	
Static Pressure	ProSense	SPT25-20-0030D	0 to 30 PSIG	+/- 0.50 % full range
Relative Humidity	Vaisala	HMT338	0 to 100%	+/-1.0% (0-90% RH)
				+/-1.7% (90-100% RH)
				+/-0.2 degree C
Venturi	Primary Flow Signal	6" HVT-FV	50 to 375	+/- 0.50% of Actual Reading

The location of test stand components and sensors located inside the building are shown in Figure 31.

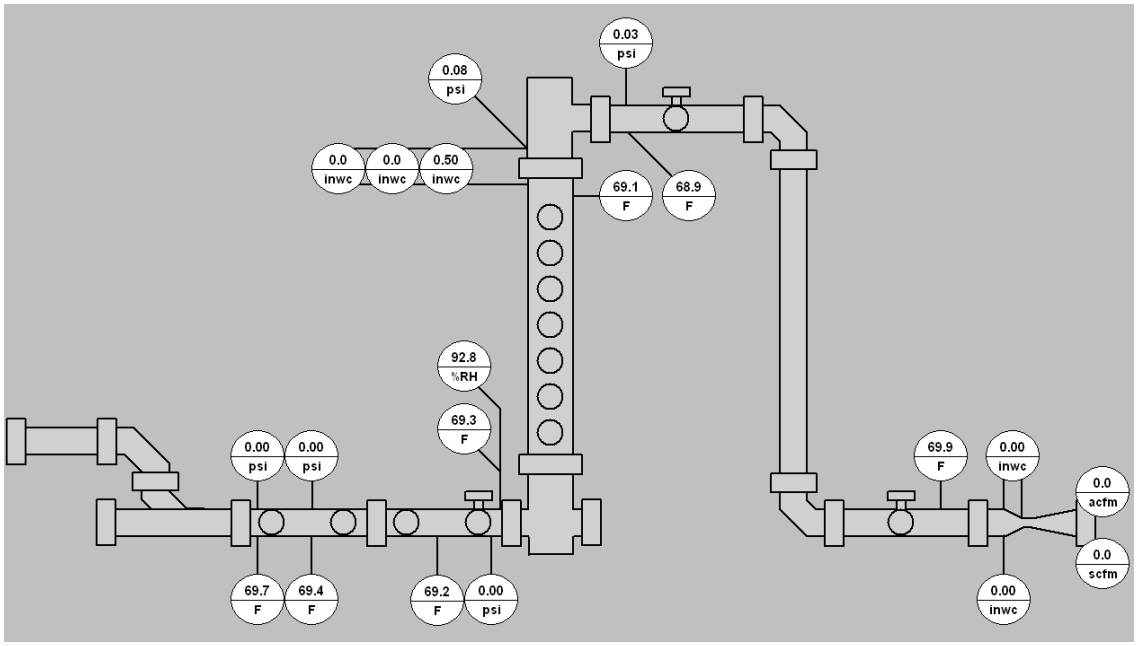

Figure 31 FI test stand sensor locations

Control system

Data from all sensors and controls are continuously logged by the test stand system control and data acquisition (SCADA) computer and software. Wonderware software is used as the interface for input of flow rate parameters, sensor reading display, and data download. The Wonderware software communicates with the Program Logic Controllers (PLC) to send data such as opening and closing valves or receive data such as temperature and differential pressure. Visual monitoring of testing parameters is aided by the presence of a large (42") monitor. This monitor is mounted above filter housing of the test stand and can be easily viewed from most any location within the test facility.

The SCADA unit is equipped with a touch screen display as illustrated in Figure 32 for user input. Flow through the test stand is produced by a forced draft blower with control accomplished by software that uses mass flow data generated as the differential

pressure across a calibrated orifice plate or venturi and a variable frequency drive (VFD) to modulate blower speed. The volumetric flow rate of the test stand is set by input of desired flow rate into the control system computer. This contros the bypass valve and direct the specified flow rate through the test stand.

Figure 32 FI test stand control system computer with touch screen display

Image collection

The ICET FI test stand is equipped with several ports for cameras to be inserted for viewing the entire length of the filters during testing. This also allows for conditions on of the filter elements to be monitored during testing without removing the filters. They

can also be used to observe the effects of the back pulse cleaning down the length of the element. This setup is shown in Figure 33.

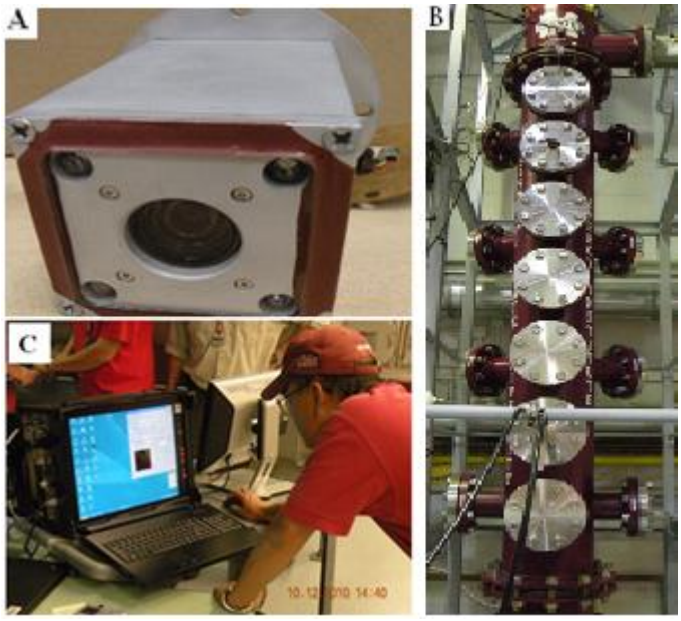

Figure 33 Upstream digital camera used with FI test stand.

A.) Digital camera for insertion into test stand. B.) Camera ports on the housing. C.) Computer and display for image collection software

Aerosol generation

Aerosols used in characterization testing were generated using a system designed and constructed at ICET. The design for this apparatus is discussed in the master's thesis titled "*Design of a Large Scale Aerosol Generator*" prepared by Kristina Hogancamp at the Diagnostic Instrumentation and Analysis Laboratory (DIAL) at Mississippi State University. This aerosol generator is composed of a nozzle for spraying a liquid aerosol and a large heated stainless steel vessel that is used to dry the liquid aerosol. The nozzle used in this apparatus can be seen in Figure 34. The heated body of the aerosol generator is shown in Figure 35. This unit has historically been used with an induced draft test

stand due to the forced draft test stand the traditional Plexiglas top on the unit has been replaced by a steel plate and secured with heavy duty clamps to ensure a tight seal. The aerosol generation segment and all of the test stand must be grounded otherwise static buildup will influence aerosol measurement and filter loading.

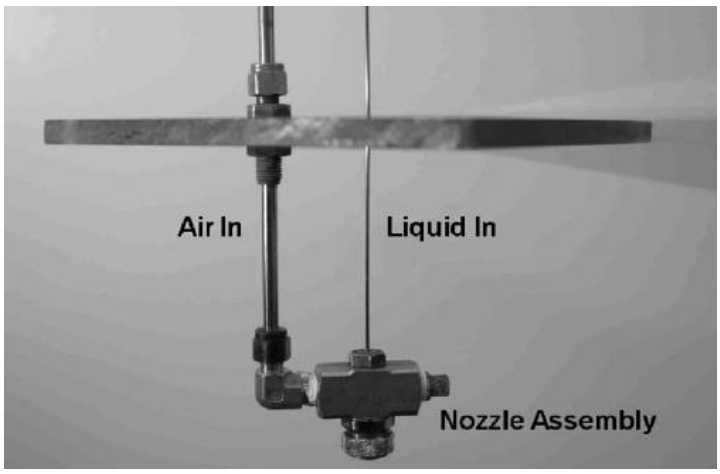

Figure 34 Aerosol nozzle for large scale aerosol generator used on FI test stand

Figure 35 Stainless steel spray vessel and heater system for generating spray dried aerosols used in characterization testing

Aerosol measurement instruments

Three aerosol measurement instruments are used to continually collect and record particle size and concentration values. The TSI Model 3340 Laser Aerosol Spectrometer (LAS) operates on the principle that the light scattered by a particle within an active laser cavity is a direct function of its size. Particles produce pulses of light during transit thought the laser beam. The light pulses are sensed by a pair of detectors that in turn are analyzed by four cascading amplifier stages coupled with analog-to-digital converters for sizing. Particles are aerodynamically focused to a sample stream diameter smaller than the laser beam diameter to avoid edge effects. The use of the LAS is limited to downstream measurements due to the concentration limits of the instrument. TSI model 3340 LAS is shown in Figure 36.

Figure 36 TSI Model 3340 LAS used on FI test stand

The TSI Scanning Mobility Particle Sizer Spectrometer (SMPS) is used for particle concentration measurements upstream of the filter elements. The SMPS measures size distributions from 2.5 nm to 1000 nm using a combination of an electrostatic classifier and a condensate particle counter. Particles are classified with the TSI model 3080 Electrostatic Classifier (EC) and their concentration is measured with a TSI model 3775 Condensation Particle Counter (CPC). The EC measures the size distribution of particle using an electrical mobility detection technique. The a bipolar charger in the EC charges the particles to a known charge distribution. A custom 37.4 in (95 cm) differential mobility analyzer (DMA) is used to measure particles across a wider size range than the standard DMA. The differences in particle size ranges measurement ability can be seen in Table 9. The particles are then classified according to their ability to

traverse an electrical field and counted with a CPC. Figure 37 shows the CPC used at ICET and Figure 38 shows the EC with a 37.4 inch (95 cm) custom DMA that is used.

Figure 37 TSI Model 3775 CPC

Figure 38 TSI Model 3080 Electro Static Classifier with Custom 37.4inch (95 cm) DMA used on FI test stand

The TSI Model 3321 Aerosol Particle Sizer Spectrometer (APS) is used for particle concentration measurements upstream of filtration. The model 3321 APS is a high-performance, general purpose particle spectrometer that measures both aerodynamic diameter and light-scattering intensity. The model 3321 provides accurate count size distributions for particles with aerodynamic diameters from 0.5 to 20 micrometers (μm). It detects light-scattering intensity for particles from 0.3 to 20 μm. The aerodynamic diameter is determined by the difference in speed detected by two lasers to determine the

acceleration of the particle. Larger particles will accelerate slower and smaller particles faster, using this the size is determined by the time of flight. This size and aerodynamic diameter is then converted from this flight time using a calibration curve. The APS is used in conjunction with a diluter to reduce the overall concentration of the sample by a set dilution ratio. The maximum particle concentration for the APS (without diluter) is 1000 particles per cubic centimeters. The APS at ICET is equipped with a TSI 3020A diluter to achieve a dilution ratio of 20:1 or 100:1. This allows for a two order of magnitude increase in concentration of particles evaluated. The concentration of particles is measured to within plus or minus ten percent of the reading. TSI model 3321 APS equipped with a TSI 3302 diluter is shown in Figure 40.

Figure 39 TSI Model 3321 APS with diluter used with FI test stand

Instruments utilized at ICET include CPC, SMPS, APS, and LAS. The instruments used at ICET utlize current technology to provide quality data. Table 10 shows the instruments used at ICET and their performance capabilities.

Table 10 Aerosol Measurement Instrumentation

Instrument	#/cc (min)	#/cc (max)	Particle Size Distribution (µm)
Scanning Mobility Particle Sizer (SMPS) • TSI Model 3080 Electrostatic Classifier • 37.4 inch (95 cm) Custom Differential Mobility Analyzer (DMA) • TSI Model 3775 Condensation Particle Counter (CPC)	2	$1x10^8$	0.008 - 1
Scanning Mobility Particle Sizer (SMPS) • TSI Model 3080 Electrostatic Classifier • TSI Model 3081 Differential Mobility Analyzer (DMA) • TSI Model 3772 Condensation Particle Counter (CPC)	2	$1x10^8$	0.008 – 0.6
TSI Model 3321 APS (with TSI Model 3302A Diluter)	1	$1x10^3$ ($1x10^5$)	0.3 – 20
TSI Model 3340 LAS	<0.02	$1.8x10^3$	0.09 – 7.5

The aerosol instrumentation utilized at ICET represents some of the most up to date and highest performance aerosol measurement instrumentation commercially available.

Pressure reducer

The higher pressure in the upstream section of the test stand will exceed the capabilities of the aerosol measuring instruments. A pressure reduction device is

therefore required at pressures greater than one PSIG in the upstream airflow for aerosol sampling. The pressure reduction device is used to reduce the pressure in sampling lines to those suitable for instruments used for sampling of the aerosol. This device was designed according to the dimensions from "Design and Performance Evaluation of a Pressure-Reducing Device for Aerosol Sampling from High-Purity Gases" [40]. The apparatus combines an orifice plate with an expansion chamber to reduce the pressure of the sample airstream. The completed pressure reducer is shown in Figure 40.

Figure 40 Pressure reducer fabricated for use on FI test stand

Data reduction

Data collected during testing is saved onto non-network computer systems to provide security of data collected. ICET procedures for saving, transferring and handling data collected during testing are utilized for data reduction. Data recorded during testing is reduced using excel spreadsheets that have been prepared for this application and undergone validation and verification. These spreadsheets convert the raw data into a numerical graphical form for ease of interpretation. Some of the data from the instrumentation may be directly used without having to do any calculations manipulation

while other data must be calculated inside the spreadsheet. The SMPS and APS provide normalized concentrations while the LAS provides raw counts and therefore must be normalized. Appendix A lists general procedures available at ICET for data handling.

Particle Concentration

Particle concentration is the measurement of the number of particles in a sample divided by the volumetric flow rate and given as #/cc. The APS and SMPS use on-board software to report the concentration while the LAS must be calculated using an external spread sheet. Concentration measurements used for testing purposes are normalized in order to provide an appropriate comparison between the up and downstream instruments. Data are normalized based on the volumetric flow rate and the number of channels per century of resolution of the measurement instrumentation. The number of channels per century of resolution is the number of channels that are used between an order of magnitude of particle sizes. Data produced using the LAS is normalized using Equation 33 where N_{count} is the raw count of particles, $Q_{sampele}$ is the flow rate of the sample in cubic centimeters per minute, T_{sample} the time required for sampling and Channels is the number of channels per century of resolution.

$$\text{Normalized Concentration} = \frac{N_{Count}}{T_{sample} \times {Q_{sample}}/{60}} \times \text{Channels} \qquad (33)$$

Particle Size Distribution

The particle size distribution for up or downstream measurements are best represented graphically represented as concentration versus particle diameter. Data from the APS and SMPS must be merged to generate the upstream PSD curve. The SMPS

collects sample collection time is 150 seconds while the collection time for the LAS and APS is 75 seconds. The average of every two samples for the APS and LAS is compared to the SMPS sample at the corresponding time to merge the data. The downstream PSD curve must be generated from the LAS. The comparison of concentration of a particle size of upstream and downstream measurements is used to produce a penetration curve. An example of a particle size distribution created from data collected using the TSI APS and TSI SMPS is shown in Figure 41.

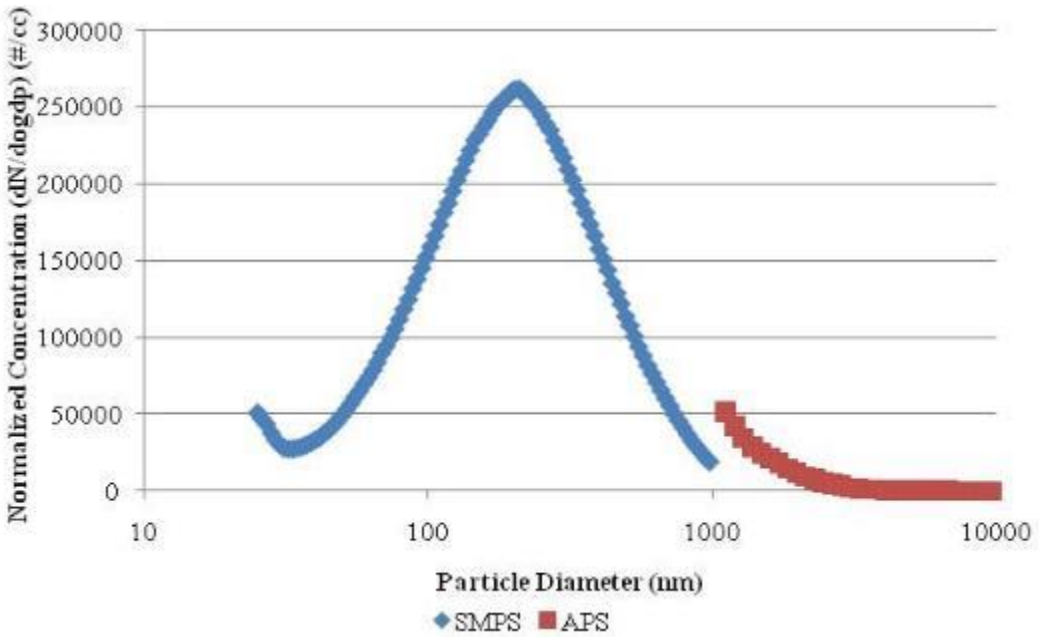

Figure 41 Particle size distribution for potassium chloride during testing of metal media filter elements

Filtering Efficiency

The filtering efficiency for the filters tested was calculated using two different methods to give a comprehensive evaluation of the filtration capabilities of the filter

elements. Equation 34 is used to calculate the efficiency for filter testing. Conc is the normalized concentration and can represent either the mass or number concentration.

$$E = \frac{(Conc_{APS}+Conc_{SMPS})-Conc_{LAS}}{(Conc_{APS}+Conc_{SMPS})} \quad (34)$$

The first method used gives the total filtering efficiency over the whole spectrum of particle diameters. This method for total efficiency is used to determine if the filter meets the HEPA efficiency standard of 99.97% efficient for particle diameters of 0.3 μm and greater. An example of the filtering efficiency and differential pressure versus time is shown in Figure 42.The spikes in filtering efficiency showing a decrease are due to the upstream instrumentation being disconnected for a period to be cleaned.

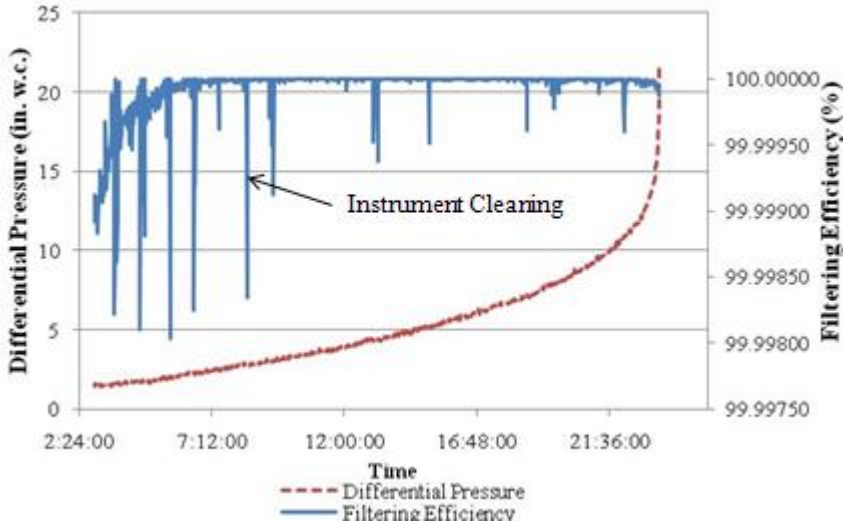

Figure 42 Example of total filtering efficiency and differential pressure versus time

The second method of showing efficiency is to determine the efficiency of the filter as a fraction of particle size. This simply compares the concentration up and down

stream of a particular particle diameter. This uses Equation 34 shown above but for Conc the normalized concentration of one particle size is used. This is generally presented in graphical format. The filtering efficiency curve can be used to identify the most penetrating particle size. The efficiency versus particle size plot can be seen in Figure 43.

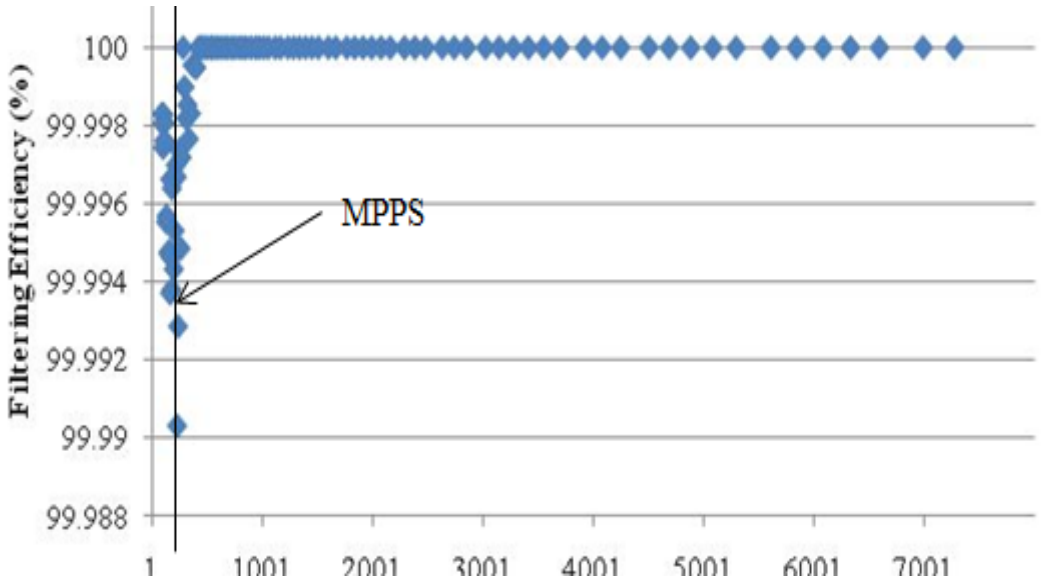

Figure 43 Example of filtering efficiency vs particle diameter curve

Most Penetrating Particle Size (MPPS)

The MPPS is the particle size for which the filtering efficiency is at a minimum [7]. The most penetrating particle size can be affected by a variety of factors such as filter media thickness, filter media packing tightness, flow rate, and filter cake thickness. The most penetrating particle size is found by comparing the upstream and downstream PSDs. The MPPS is identified in Figure 45 above on the penetration curve.

The mass loading curve of a filter gives a representation of the amount of mass that can be loaded onto a filter before it either ruptures or reaches the end of its service

life. Using the PSD, volumetric flow rate, aerosol concentrations, and mass loading curve the life of a filter can be predicted. An example of a mass loading curve is shown in Figure 44.

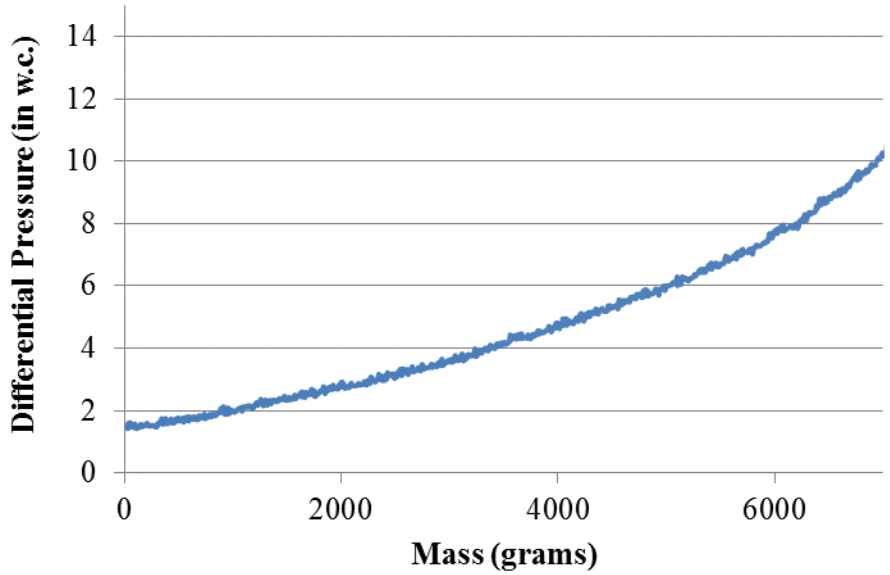

Figure 44 Example of mass loading curve

CHAPTER V

RESULTS AND DISCUSSION

Test stand characterization

Systems used to provide air flow through the test stand need to be matched to the filter elements being evaluated. Section FI will provide for qualification of a broad range of filter volumetric flow rates and maximum differential pressure combinations. It is likely that a range of compressors/blowers will be needed to service the complete range of testing needs.

Two compressor systems have been included in this characterization study. Neither of these systems completely satisfies the performance requirements for the FI test stand. However, one or both may see service for some segment of the filter element size range.

The compressor systems evaluated for providing air flow through the test stand are identified in Table 11 along with their basic information. Flow rates during characterization and filter elment testing is recorded in actual cubic feet per minute (ACFM)

Table 11 Two air supply systems used on FI test stand

Air Supply System					
Manufacturer	**Model Number**	**Type**	**Horse Power**	**RPM**	**Max ACFM**
Spencer	07H660W436	Vortex Blower	10	3450	133
Spencer	36H711X100G1	Vortex Blower	4.2	2850	
Elmo Rietschle	DLR-300	Claw Compressor	20	3450	160

A set of three Porvair Filtration sintered metal fiber filter elements 3.3 feet (1 m) in length and 3 inches (8 cm) in diameter have been used during these characterization studies.

The first series of tests utilized a combination of the two Spence Vortex blowers arranged in series. This set of blower was capable of providing a flow rate of up to 133 ACFM at 6 in. w.c. but are limited in their capability to overcome differential pressure that will occur when filters are loaded.

The second series of tests used the Elmo-Rietschle claw compressor. It was demonstrated to have the capability of producing flow rates from 20 to 160 ACFM and pressures up to 10 PSIG. Characterization of the test stand was performed using each air supply system at multiple flow rates to map performance capabilities.

Figure 45 shows the performance of the dual blower system installed in series tested at various flow rates. The flow and differential pressure began to increasly fluctuate as the flow rate was reached the upper range of the blowers the flow and differential pressure began to increasingly fluctuate.

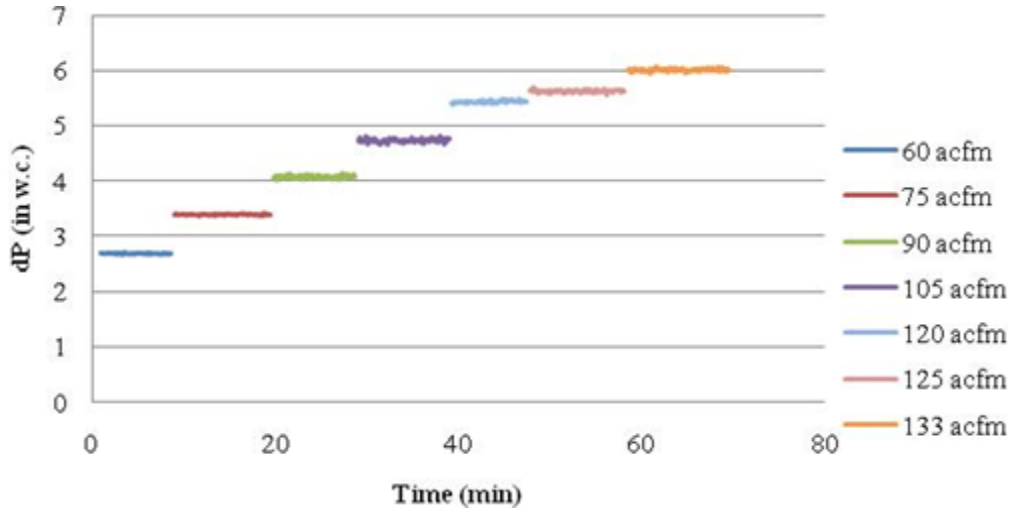

Figure 45 Media velocity for Porvair metal media filter elements using Spencer vortex blowers

Data represented in Figure 45 have been compiled into tabular from in Table 12. These include flow rate, differential pressure across the filter, filter media velocity and the standard deviation of each. Statistical variability of key parameters has also been compiled in Table 12.

The flow rate and the differential pressure are direct readings from the test stand and the media velocity is calculated from the flow rate. Section FC limits media velocity to five ft/min for fibrous glass media filters. FI provides for user specified media velocity that can be in excess of five ft/min. However, it is good to include the five ft/min media velocity in the test matrix to use as a bench mark for comparison with FC filters. Therefore data for less than 5 ft/min is collected as well as data up to the maximum limit of the blowers. Data in Table 12 shows that filter differential pressure increases as flow rate through the filter increases. Data for blower performance in Table 12 shows the blowers best performance under 90 CFM. Once 90 ACFM is reached the standard

deviation in the flow and differential pressure increases. This can be attributed to the increased fan speed and increase in differential pressure.

Standard deviation for all the parameters reached a maximum at 105 ACFM. This is the least desirable point for this blower to operate. The smallest standard deviation occurs at 60 CFM. This is most likely the optimal operating speed for the blowers.

Table 12 Volumetric flow, differential pressure, media velocity and standard deviation for Spencer Vortex Blowers

	Actual Flow Rate (acfm)		**Filter dP (in w.c.)**		**Filter Media Velocity (ft/min)**	
Target Flow Rate (acfm)	**Average**	**Standard Deviation**	**Average**	**Standard Deviation**	**Averages**	**Standard Deviation**
60	60.0647	0.2124	2.2256	0.0249	2.6997	0.0095
75	75.5058	0.3109	2.8205	0.0392	3.3937	0.0140
90	90.7446	0.5127	3.5583	0.0494	4.0786	0.0230
105	105.2932	0.7170	4.3296	0.1302	4.7325	0.0322
120	120.8363	0.5416	5.2668	0.0890	5.4311	0.0243
125	125.1957	0.5839	5.5463	0.0975	5.6270	0.0262
133	133.7373	0.5979	6.0784	0.0728	6.0110	0.0269

Maintaining laminar flow through filter media is an important performance parameter for filtration. A plot of the media velocity versus differential pressure is one method for determining of the flow through the filter media is laminar. If the media velocity and differential pressure have a linear relationship the flow can be considered laminar through the filter. Figure 47 shows the curve to have an increase in slope when the media velocity reaches 4 ft/min. This appears to be the result of the fan performance at 105 ACFM. The data above shows the standard deviation flow parameter to have a noticeable increase at 105 ACFM but remains nearly steady for the rest of testing. Because the curve continues a linear trend after this point it is assumed the flow is still

laminar and the change in slope is not due to increase in velocity but due to the performance of the fan. Values from Table 12 are plotted in Figure 46 to demonstrate the linear flow through the filter elements.

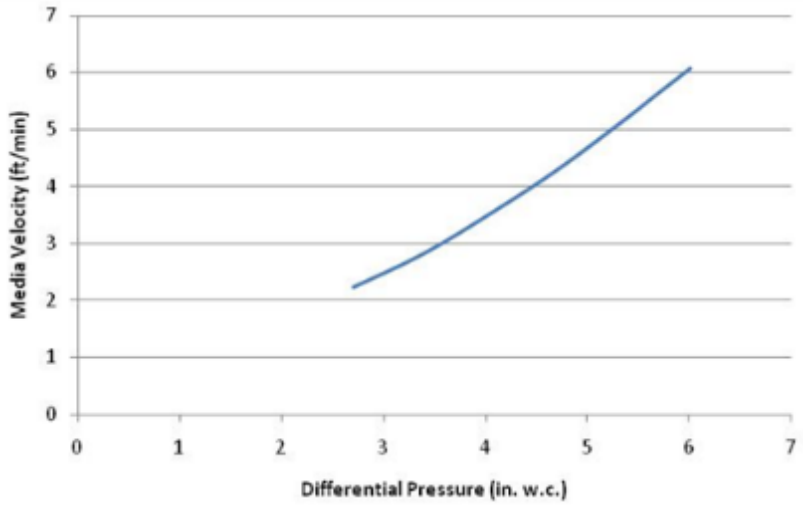

Figure 46 Differential Differential pressure versus media velocity for Porvair metal media filter elements using Spencer vortex blowers

The sintered metal fiber filter elements were tested for resistance to air flow and pressure at flow rates of 60, 80 , 100, 120 , 140 , and 160 ACFM with media velocity of 2.7, 3.6, 4.5, 5.4, and 7.2 feet per minute respectively utilizing the Elmo-Rietschle claw compressor. Figure 47 shows the flow rates for testing conducted with the claw compressor at the specified flow rates. Broadening of line segments show that fluctuations in flow increase as the flow rate increases.

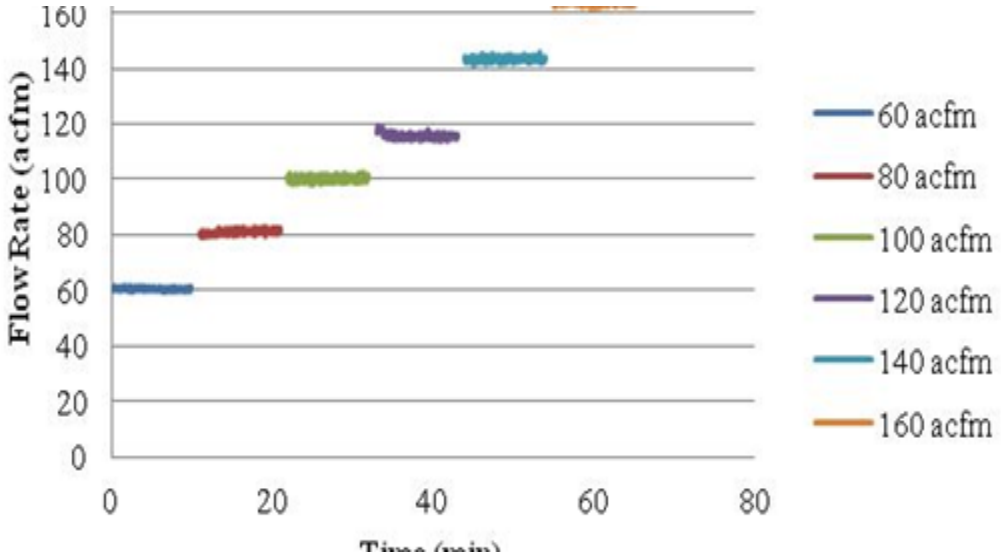

Figure 47 Test flow for Porvair metal media filter elements rate at multiple set points using claw compressor

Figure 48 shows the differential pressure across filter elements for flow rates using the claw compressor. This plot demonstrates the direct correlation between differential pressure and flow rate for the metal media elements. The differential pressure increases incrementally as the flow is increased.

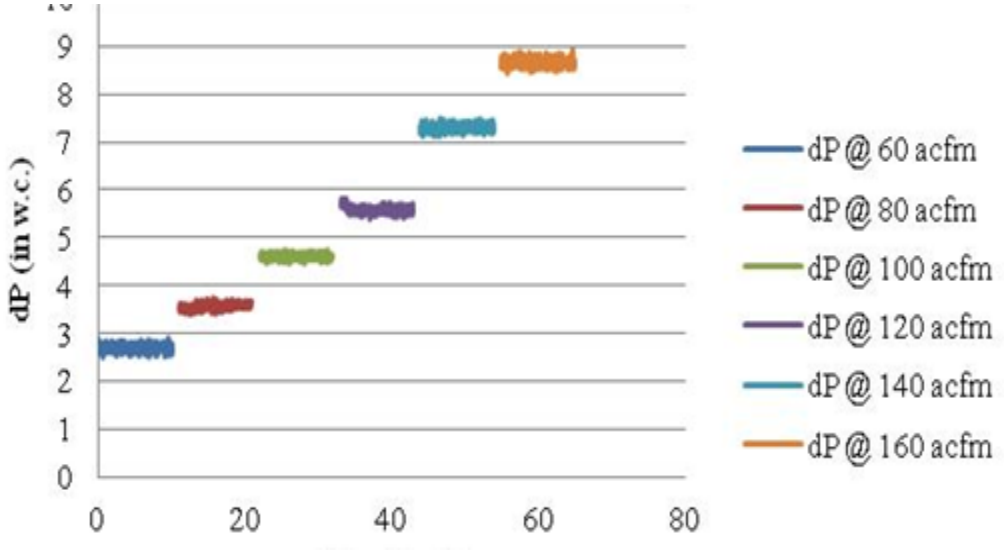

Figure 48 Differential pressure across for Porvair metal media filter elements at multiple flow rates using claw compressor

Media velocities for the Porvair sintered fiber metal media filter elements are provided in Figure 49. Media velocity is routinely used as a reflection of laminar flow through the filter medium. Media velocity corresponding to 60 ACFM is 2.7 ft/min and 160 ACFM is 7.2 ft/min with each step between being the next increase in flow. The higher media velocity (7.2 ft/min) is expected to be at the upper limit of laminar flow.

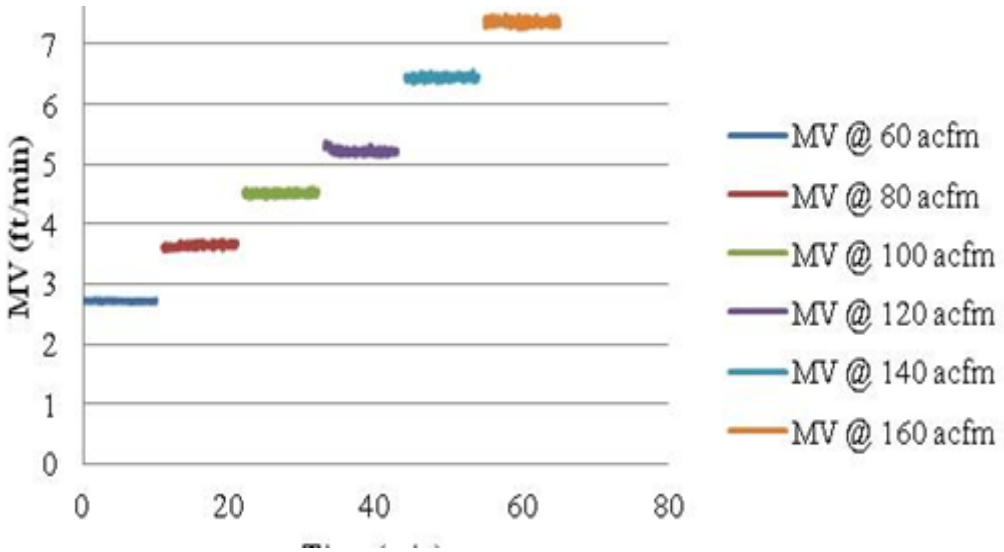

Figure 49 Media velocity for Porvair metal media filter elements at multiple flow rates using claw compressor

Data from Figures 47, 48 and 49 are summarized in Table 13. This includes flow rate, differential pressure across the filter, filter media velocity and the standard deviation of each to display statistical data for the blowers. Flow rate and the differential pressure are direct readings from the test stand and the media velocity is calculated from the flow rate and filter element surface area. Data for less than 5 ft/min were collected as well as data up to the maximum limit of the blowers. The data for the blower performance in the table shows the blowers to have optimum performance under 120 ACFM. The standard deviation in the flow and differential pressure increases at flows greater than 120 ACFM.

The maximum standard deviation for the flow rate and media velocity occurs at 120 ACFM. This was an unexpected finding because it would logically occur at the maximum flow range. The maximum standard deviation for the differential pressure occurs at 160 ACFM. This is the expected point of the maximum standard deviation

because it is at the top of the range of the claw compressor. The smallest standard deviation occurs at 60 ACFM where the compressor speed and differential pressure are the lowest.

Table 13 Differential pressure across filter, flow rate, and standard deviation statistics for the claw compressor testing.

	Actual Flow Rate (acfm)		**Filter dP (in w.c.)**		**Filter Media Velocity (ft/min)**	
Target Flow Rate (acfm)	**Average**	**Std Dev**	**Average**	**Std Dev**	**Average**	**Std Dev**
60	60.4842	0.3361	2.6868	0.0651	2.7185	0.0151
80	81.0568	0.6039	3.5512	0.0461	3.6432	0.0271
100	100.3454	0.6792	4.619	0.0574	4.5101	0.0305
120	115.9792	0.884	5.592	0.0641	5.2128	0.0397
140	143.2432	0.6657	7.2939	0.0611	6.4382	0.0299
160	163.9039	0.8374	8.6486	0.0814	7.3668	0.0376

The values for media velocity and differential pressure from Table 13 are plotted in Figure 50 to demonstrate the nearly linear relationship between differential pressure and media velocity for the claw compressor. The slope decreases at 80 ACFM but overall maintains a linear relationship and thus the flow can be assumed to be laminar through the filter.

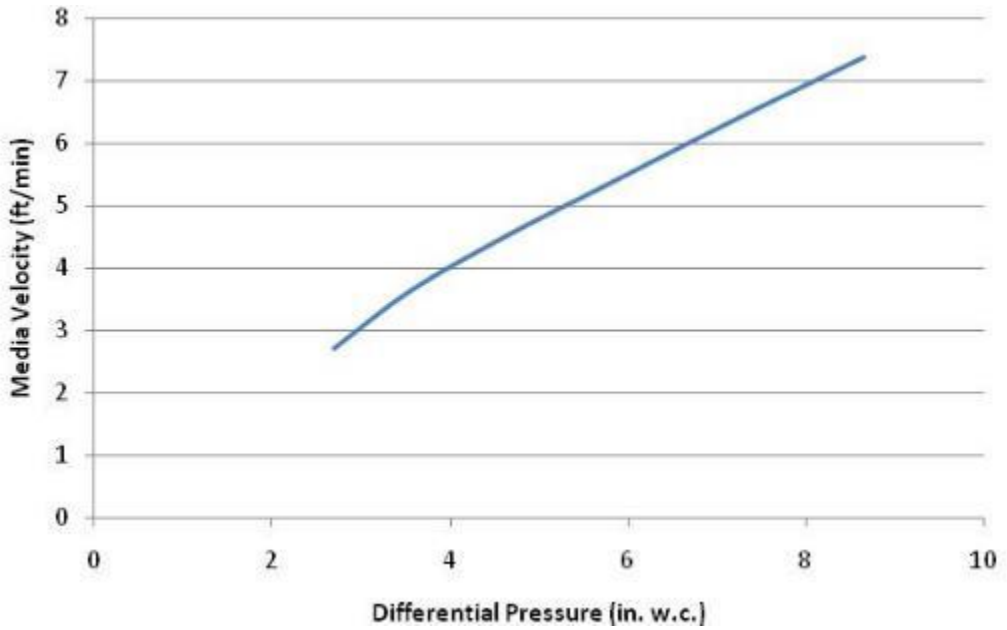

Figure 50 Differential pressure versus media velocity for Porvair metal media filter elements using the claw compressor

The maximum static pressure as a function of flow rate is a demonstration of the performance capabilities of the claw compressor. Figure 51 shows the maximum flow rate for pressures up to 11 psig. To test the maximum pressure at specified flow rates a valve was gradually closed on the downstream section of the test stand to increase the static pressure inside the upstream section of the test stand. The flow was taken to maximum while attempting to achieve 10 PSIG. The maximum pressure of 11 PSIG occurred at 80 ACFM as the flow was increased beyond 80 ACFM up to 160 ACFM the maximum pressure continually decreased. For the flow rate of 160 ACFM the maximum achievable pressure was 1.3 PSIG.

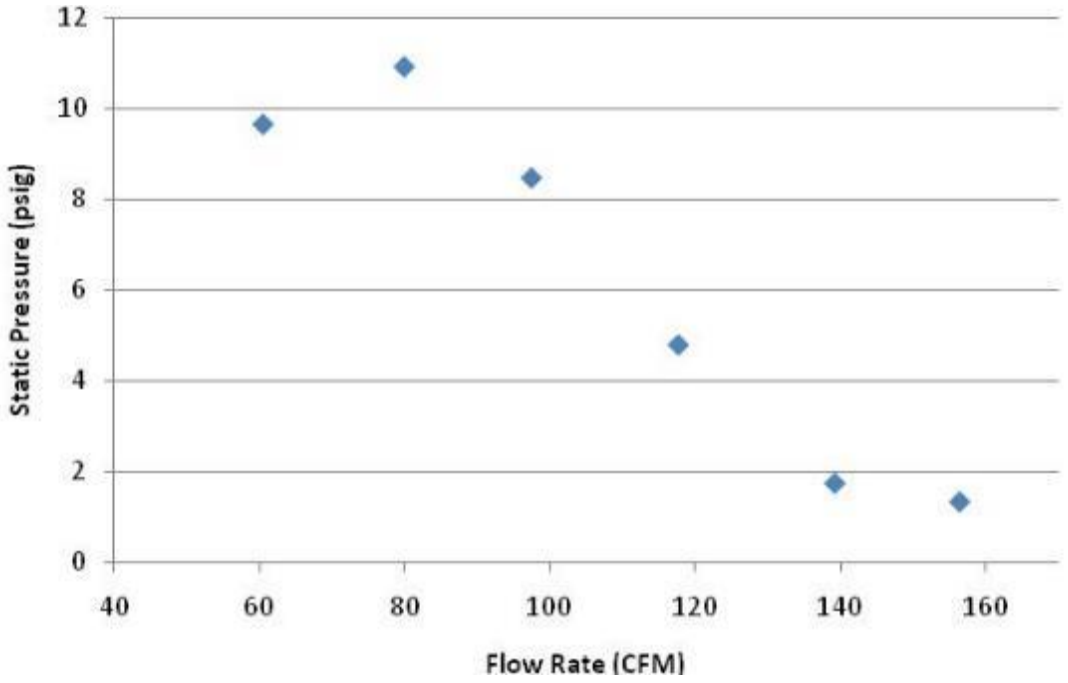

Figure 51 Maximum static pressure at flow rates from 60 ACFM to 160 ACFM for Porvair metal media filter elements

Neither air supply system (Spencer or Elmo-Rietschle) was able to achieve the performance criteria target of 200 CFM for three one meter elements tested. Filter elements varying in size from one inch in diameter and twelve inches in length to four inches in diameter and almost seven feet in length will be evaluated using this test stand. Sintered metal fiber filter elements can be expected to have a clean differential pressure of three to five in. w. c. at rated flow. Sintered metal powder filter elements can be expected to have an initial differential pressure of 20 to 30 in. w. c. This test stand was designed to with stand static pressure much greater than the maximum expected pressure of 15 psig. Therefore the compressor is the only component needing to be changed to achieve flow rates at the higher static/differential pressure. Both systems evaluated can be successfully employed within their range of capability. The ability of this test stand to

test filter elements individually or up to three at once allows for testing fewer filter elements to increase media velocity.

A comparison of the standard deviation of the flow rate through the test stand for the vortex blowers and the claw compressor show that the vortex blowers maintain a smoother flow. The vortex blowers were not designed for producing elevated differential pressures therefore no data were collected for elevated differential pressure using the Spencer vortex blowers. These are ideal for testing small filter elements that require low flow rates and low differential pressures.

The claw compressor was tested at up to 10 psig. These data show that filter testing at low flow rates and low differential pressures may be accomplished with more steady flow using the vortex blowers but as flow rate and differential pressure increase it is necessary for the claw compressor to be used. The vortex blowers may be used in some applications that do not require loading such as initial efficiency test for small filters. Larger filters or loading tests will require the use of the claw compressor to achieve higher flow rates and differential pressures. To achieve the desired criteria for this test stand a larger compressor must be sized and acquired for use.

Temperature and relative humidity control

Compressors used to produce air flow through the test stand use outside air that requires temperature and humidity conditioning. Temperature and relative humidity can vary during testing due to changing environmental conditions. A series of evaluations were completed to determine the operating envelope for current equipment including the compressors, chiller, and heat exchangers.

The ASHRAE psychrometric chart no. 1 shown in Figure 52 gives the expected path of air stream conditions for the expected upper limit worst case scenario for ambient conditions.

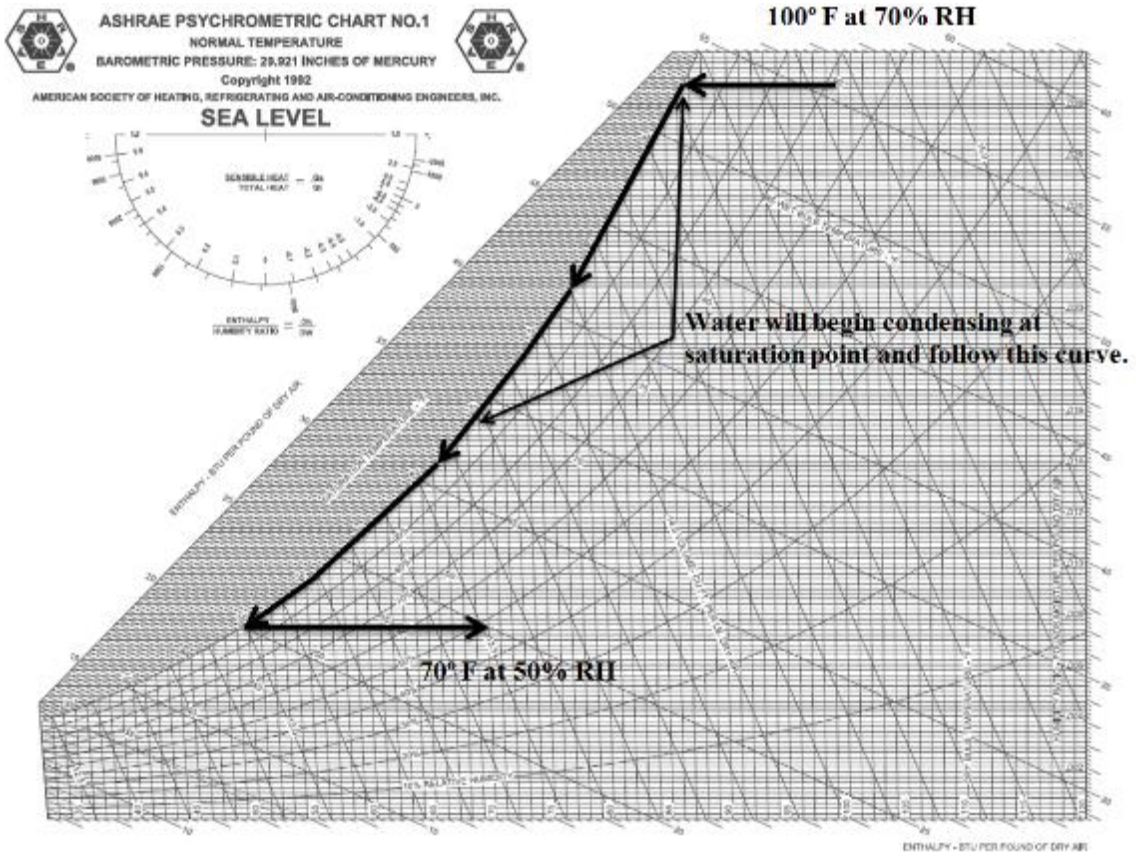

Figure 52 ASHRAE psychrometric chart no 1

Manipulation of the water chiller and heat exchanger parameters is required for adjusting the relative humidity and temperature inside the test stand. Decreasing water temperature in the chiller will cause water to condensate and therefore reduce the relative humidity of the reheated air stream. Allowing more air to flow through the reheat heat exchanger from the chiller will increase temperature of the air thus decrease relative

humidity. These adjustments will not be consistent because environmental conditions vary throughout the day and over the course of the year. The conditions of the air stream dictate changes that must be made to the air conditioning system using the bypass controls on the test stand computer and chiller control panel located on the front of the chiller unit.

Employing a proper balance of the chiller and reheater allows the test stand to operate within required limits. The plot of relative humidity and temperature versus time shown in Figure 53 demonstrates the effect of the chiller temperature on the relative humidity and temperature. The chiller water temperature setting is shown incrementally being stepped up over the course of the testing from 45° F to 65° F. The temperature of the air stream is shown to slightly decrease then increase over the course of the testing. The relative humidity is shown to increase steadily over the course of the testing. The line representing the chiller temperature is the setting on the chiller and not the actually temperature of the water in the chiller. The chiller is set for a differential temperature setting of 2° F so that it will cycle and continue chilling once the water gets outside of the ±2° F range. Appendix C gives the procedures for adjusting the temperature and relative humidity.

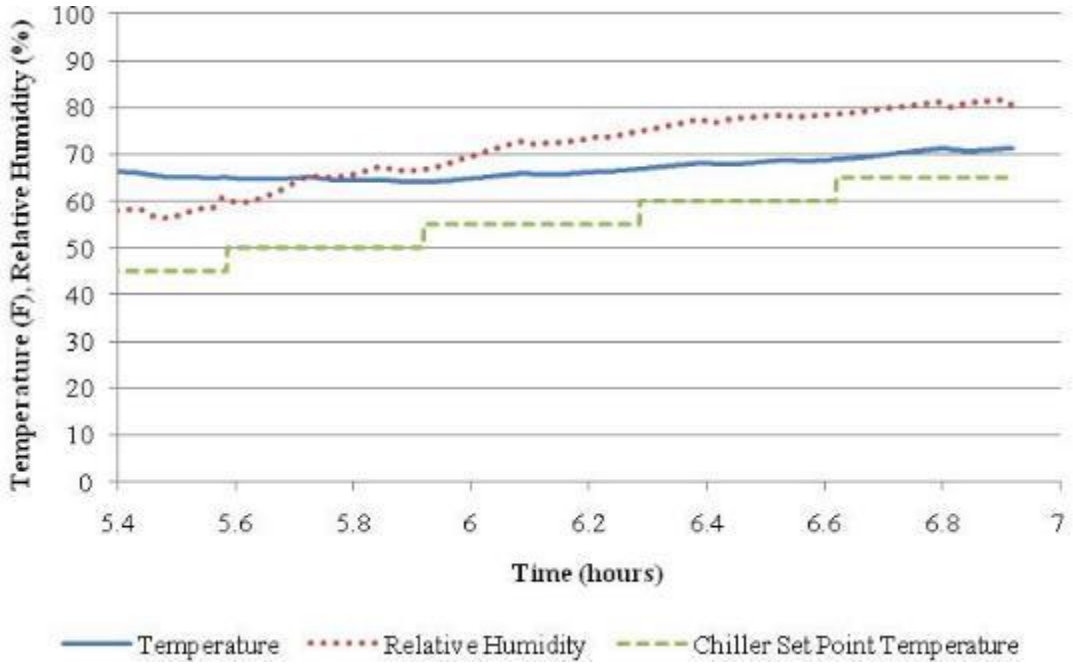

Figure 53 Plot of the effects of the chiller water temperature setting on the temperature and relative humidity of the air stream

Figure 54 shows that as the reheat heat exchanger bypass is increased the temperature decreases while relative humidity oscillates slightly about the desired set point. During this testing the reheat heat exchanger bypass was incrementally increased by 25% from 0 to 100%. This increase is shown as the step function on the plot. This can be seen on the plot as the line that is stepped up from 0 to 100%. The temperature during this testing is shown to decrease slowly and steadily and the bypass percent for the reheat heat exchanger is increased. The relative humidity in this plot has a large dip at the beginning and varies throughout the testing possibly due to the system during warm up. This plot also shows that there is no noticeable trend on the relative humidity as the bypass percent on the reheat heat exchanger is increased. This demonstrates that the chiller has greater control on the operating parameters.

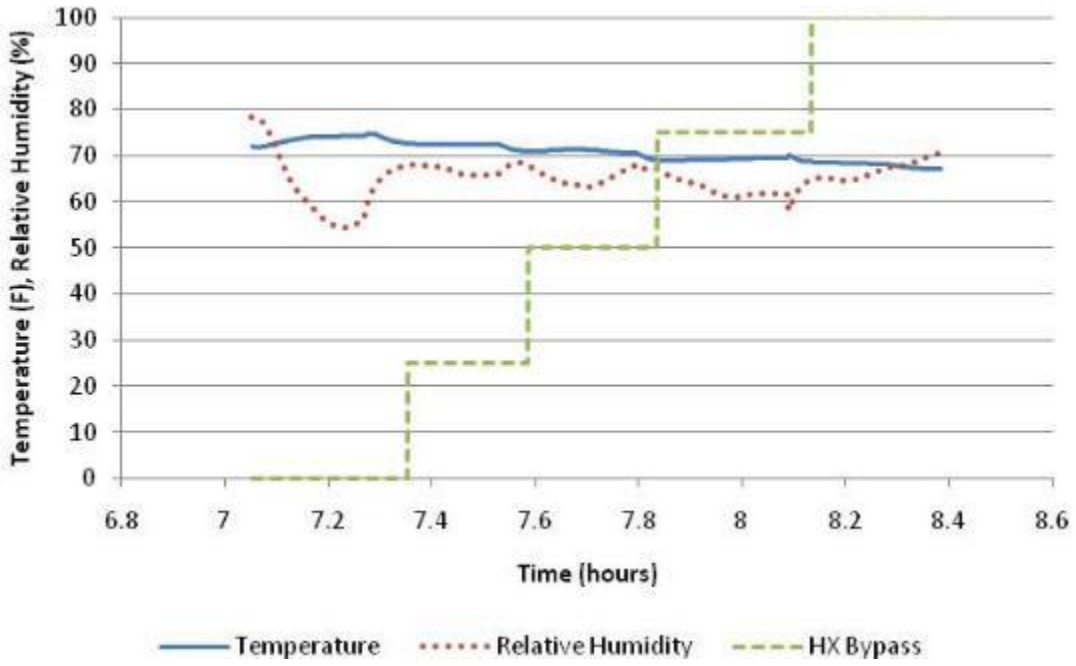

Figure 54 Plot of the effects of the reheat heat exchanger on temperature and relative humidity of air stream

The following figures show the controllability of test parameters while achieving a combination of the maximum and minimum of each parameter at 50 ACFM. This demonstrates the ability to control multiple parameters during operation to keep the test conditions at 50 ACFM within the required range of 60° F to80° F and 40% to 60% relative humidity.

Testing data given in Figure 55 were calculated using the target point of 60° F and 40% RH at 50 ACFM. Throughout this test the temperature was maintained near 72° F and the relative humidity near 38%. There are noticeable oscillations in the relative humidity that occur with a frequency of about 11 minutes and amplitude of about 2% RH. The aerosol generator has an high exit air flow and very low moisture content. Input from the aerosol drying process exceeds the capability of the chiller to properly control the

temperature under very low flows. This will need to be resolved by using a heat exchanger to cool the heated aerosol air flow before it is injected into the test Stand. The flow could not be brought below 70° F during this testing due to the effects of the heat from the aerosol generator.

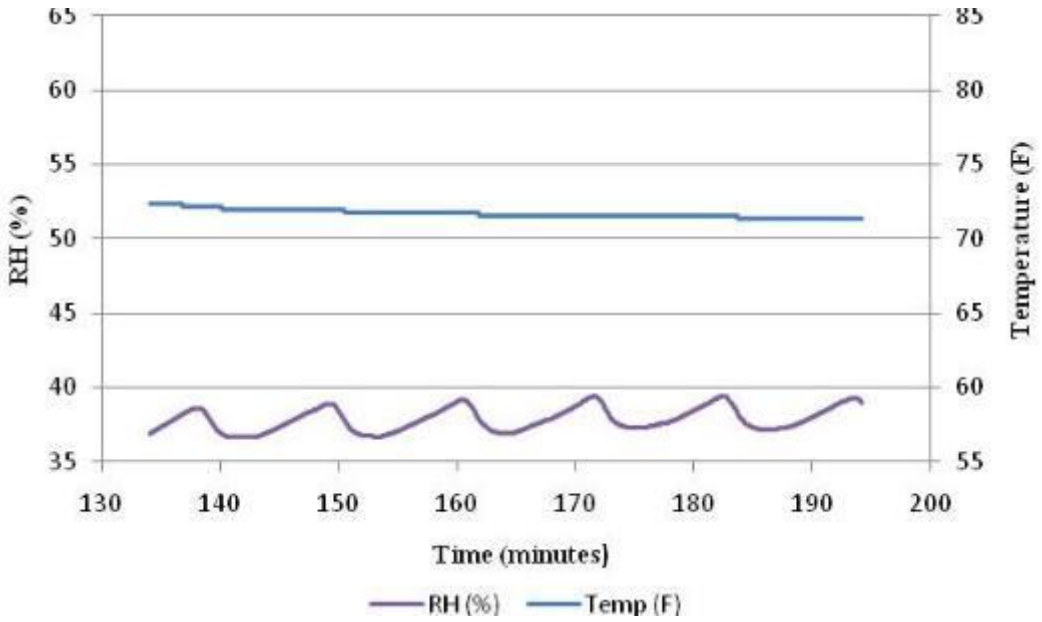

Figure 55 Demonstration of control of temperature and relative humidity for 50 ACFM and target point of 60° F and 40% RH

The target control conditions for testing shown in Figure 56 was 60° F and 60% RH and 50 CFM. Through this test the temperature was maintained near 75° F and the relative humidity average starting near 50% and decreasing to about 48% . Once again there are noticeable oscillations in the relative humidity that occur with a frequency of about 11 minutes and amplitude of about 2% RH. The flow stayed near 75° F during this testing due to the effects of the heat from the aerosol generator. Modification of the aerosol generator and the reheat heat exchanger are required to reach the desired 40%

relative humidity at low flow rates. Results from this test and all of the testing done to evaluate performance of the chiller/reheater combinations have been compiled into Table 15 on page 123.

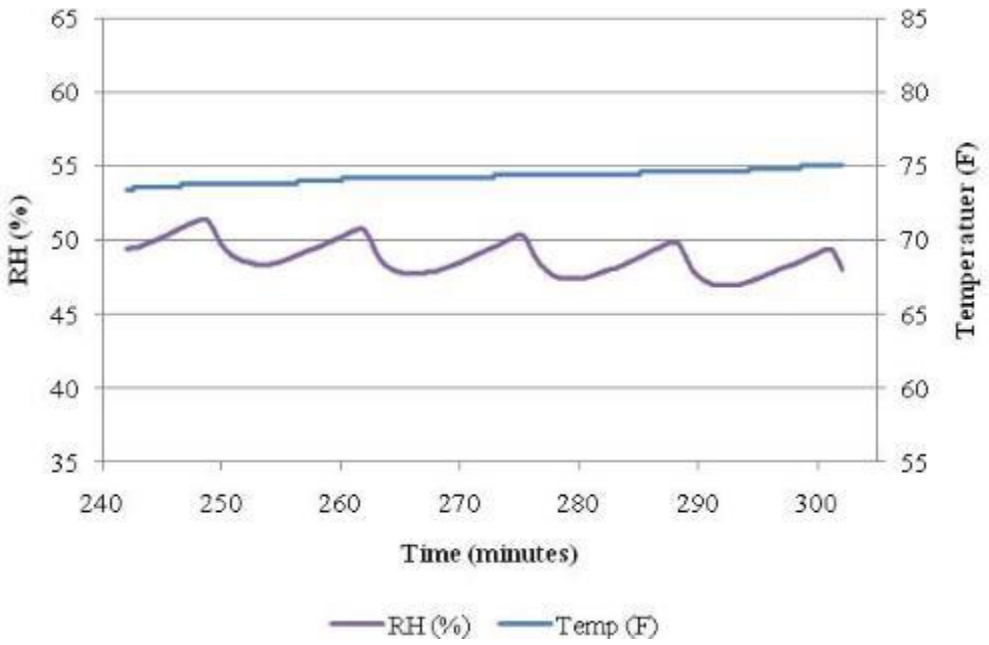

Figure 56 Demonstration of control of temperature and relative humidity for 50 ACFM and target point of 60° F and 60% RH

The target point for testing shown in Figure 57 was 80° F and 40% RH and 50 CFM. Through this test the temperature increased from 80° F to 82° F. The relative humidity started near 43% and decreased rapidly to 33% before the temperature on the water chiller was increased and the relative humidity returned to oscillating as it had been in the above figures and ended near 36%.

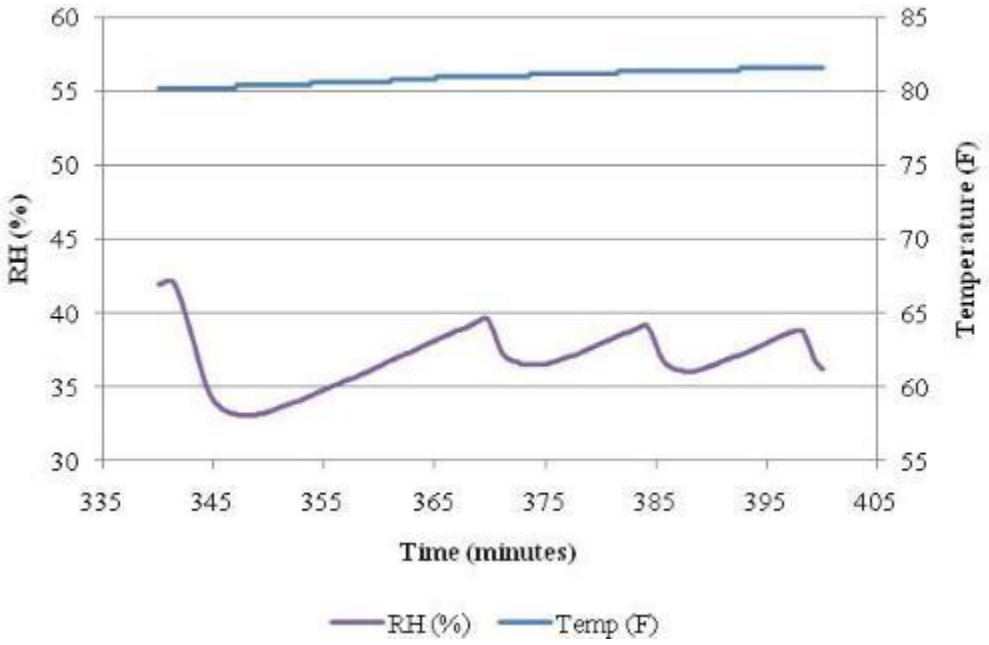

Figure 57 Demonstration of control of temperature and relative humidity for 50 ACFM and target point of 80° F and 40% RH

The target point for testing shown in Figure 58 was 80° F and 40% RH and 50 CFM. Through this test the temperature was maintained at approximately 80° F. The relative humidity started near 56% and ended near 54% . The irregular waves in the relative humidity are due to adjusting the temperature of the chiller water.

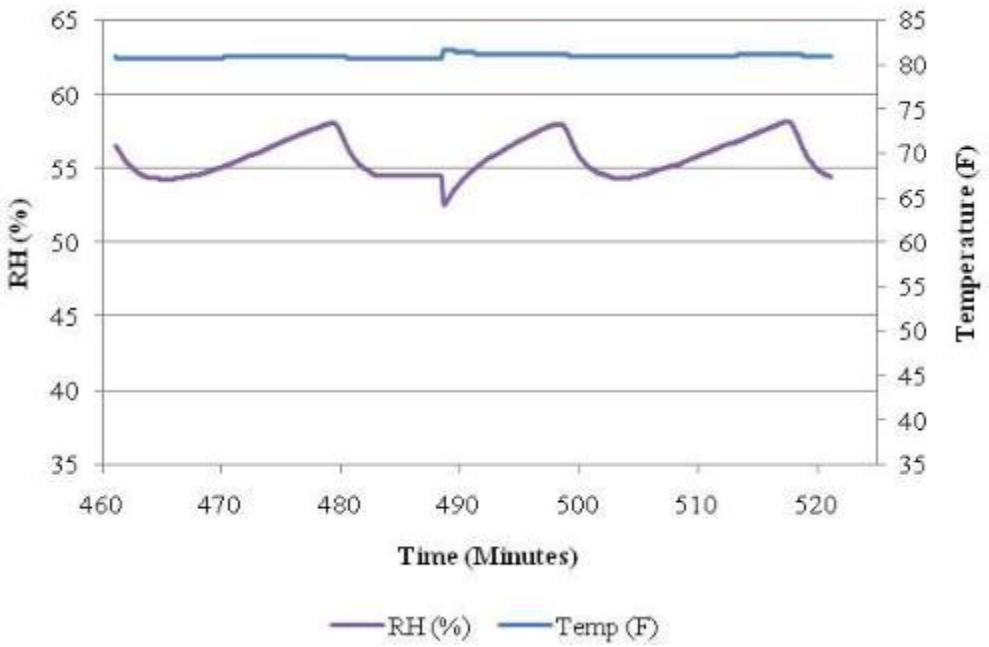

Figure 58 Demonstration of control of temperature and relative humidity for 50 ACFM and target point of 80° F for 60% RH

Flow rate and differential pressure over the entire period of testing at 50 ACFM are shown in Figure 59. The target rate for flow was 50 ACFM but as can be seen on the figure below the flow was actually maintained near 53 CFM. The dP remained relatively constant throughout the testing at 2.4 in. w.c.

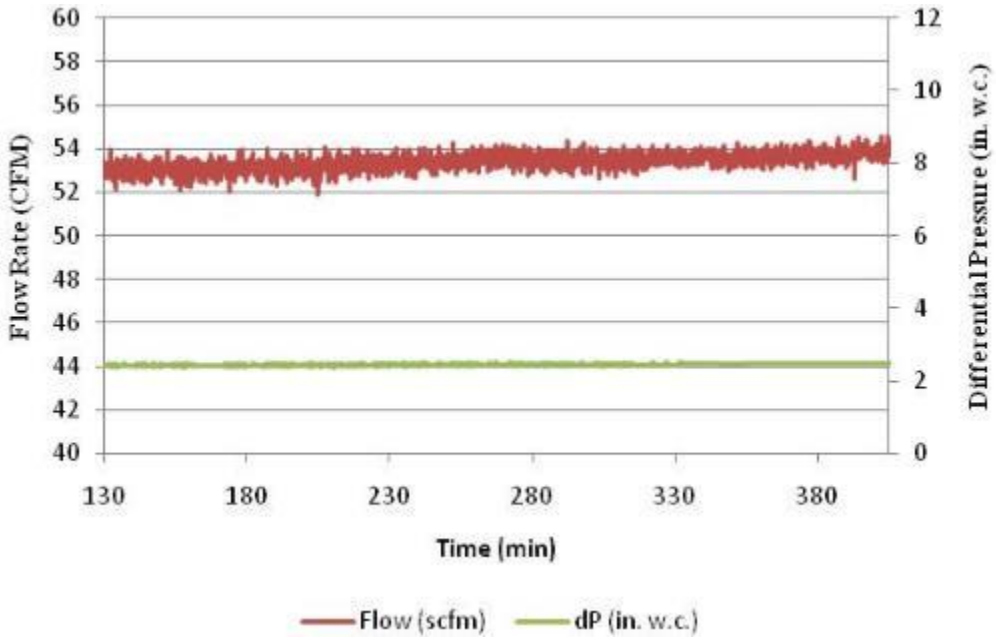

Figure 59 Flow rate and differential pressure for control of temperature and relative humidity testing for 50 ACFM

During testing at 50 ACFM the temperature was difficult to get into the low end of the temperature range because of the heat generated from the aerosol generator. This heat is sufficient to keep the temperature of the air stream above 70° F throughout this testing even when trying to achieve 60° F. This can be remedied by cooling the aerosol delivery temperature before injection into the test stand.

The following figures show the performance of the test stand while achieving the maximum and minimum of each parameter at 160. This series of tests is equivalent to test performed at 50 ACFM demonstrates the ability to control multiple parameters during operation to keep the test conditions within the required range for the upper volumetric flow rate.

Testing for the plot shown in Figure 60 was accomplished using the target point of 60° F and 40% RH for 160 CFM. Throughout this test the temperature was maintained near 68° F and the relative humidity near 41%. There are noticeable oscillations in the relative humidity that occur with a frequency of approximately 7 minutes and amplitude of approximately 2% RH. The temperature was much easier to control for 160 ACFM due to the larger ratio of air from the air conditioning equipment being mixed with the air from the aerosol generator.

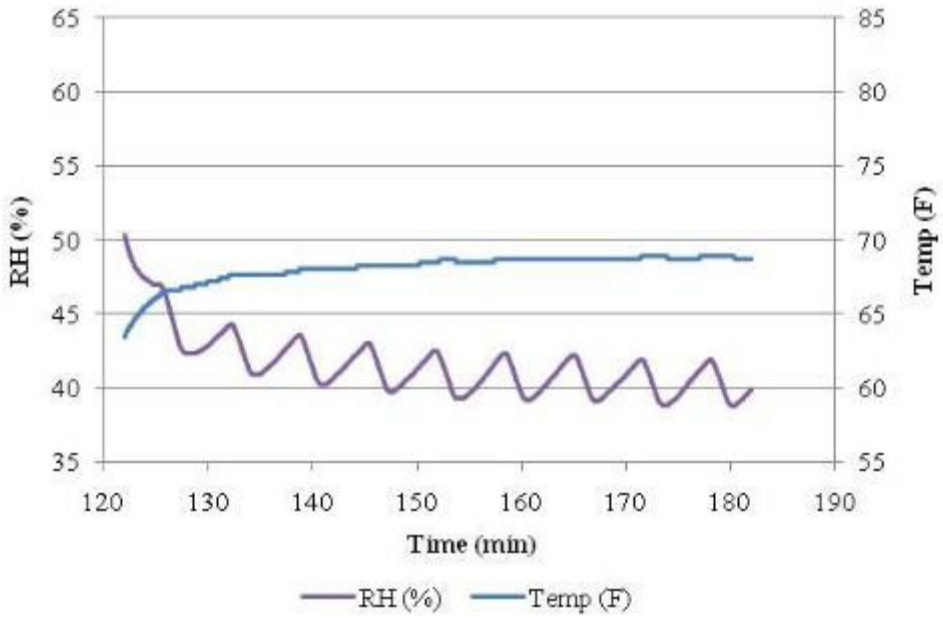

Figure 60 Demonstration of control of temperature and relative humidity for 160 ACFM and target point of 60° F and 40% RH

The target control points for testing shown in Figure 61 were 60° F and 60% RH for 160 CFM. Throughout this test the temperature averaged 63° F but within the acceptable range of 60° F to 80° F. The relative humidity started near 59% and experienced two large oscillations of approximately 10% relative humidity settling into a

regular oscillating curve with a frequency of about 8 minutes and amplitude of about 2% RH.

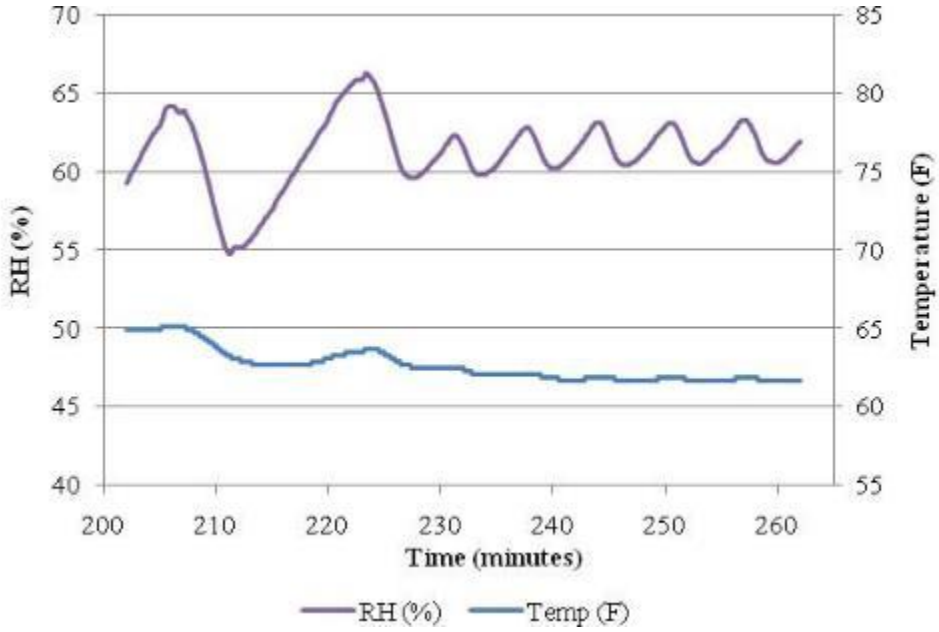

Figure 61 Demonstration of control of temperature and relative humidity for 160 ACFM and target point of 60° F and 60% RH

The target point for testing shown in Figure 62 was 80° F and 40% RH for 160 CFM. During this 60 minute test the temperature increased from 76° F to 81° F. Once again this is due to attempting to maintain conditions at the outer limits of test conditions. Typical testing calls for target points in the middle of temperature and relative humidity ranges and thus a variation of one or two degrees will not move it out of the range. The relative humidity started near 46% and ended near 40%. These conditions are within the specified range and can be held in this range if no drastic change occurs to ambient

conditions. The same oscillations of approximately 8 minutes and 2% RH are seen on this plot.

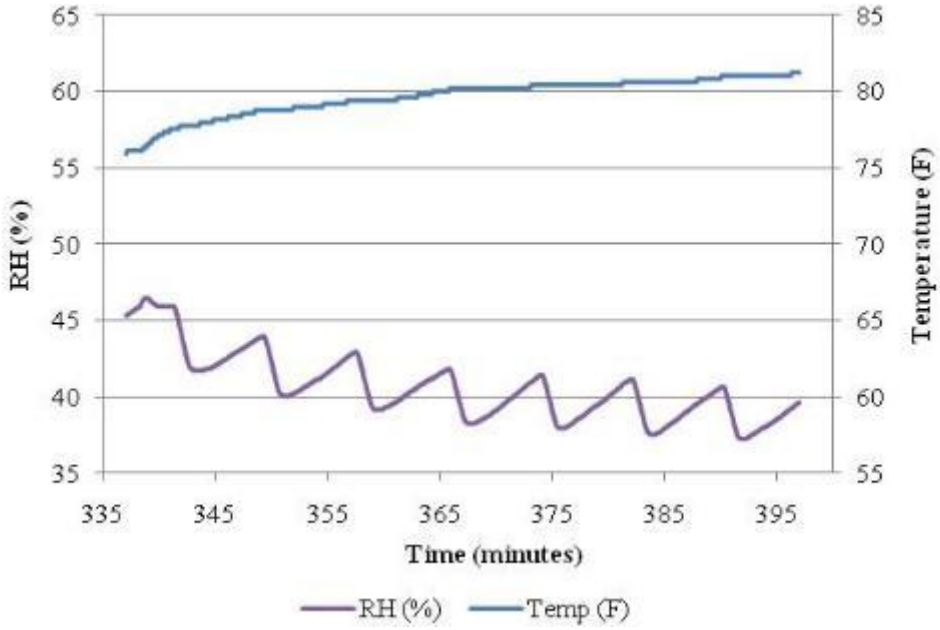

Figure 62 Demonstration of control of temperature and relative humidity for 160 ACFM and target point of 80° F and 40% RH

The target point for testing shown in Figure 63 was 80° F and 60% RH for 160 CFM. Through this 60 minute test the temperature averaged 82° F. The relative humidity started near 54% and ended near 56% with an average of 59%. The temperature for this test was slightly above the prescribed testing range. This was due to maintaining the temperature and relative humidity at the upper limit of their range. Balancing these two resulted in the temperature exceeding 80° F. For typical operating conditions the temperature and relative humidity will not be held at the upper limit and will be easier to

keep within the prescribed conditions. The irregular waves in the relative humidity are due to adjusting the temperature of the chiller water.

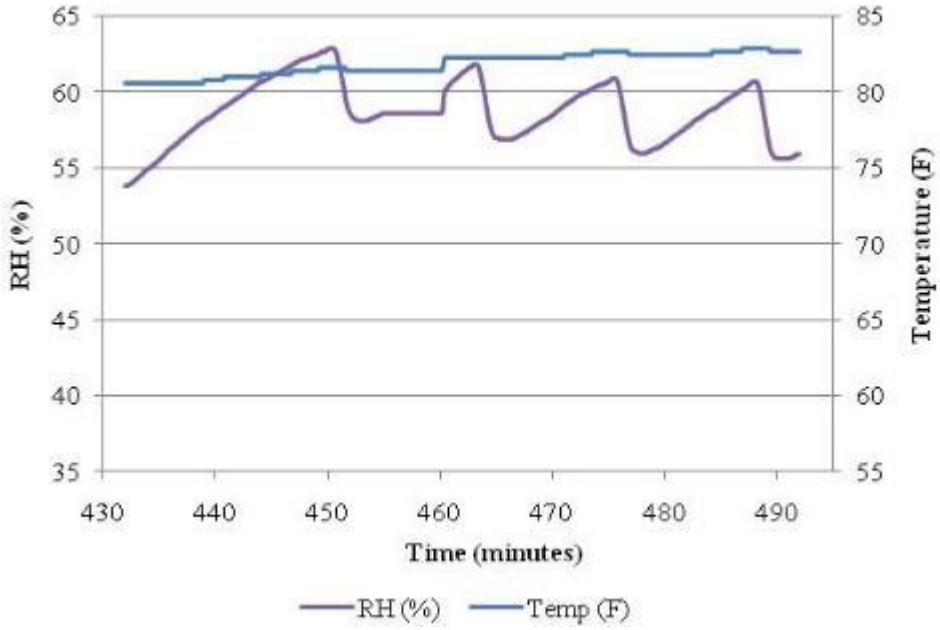

Figure 63 Demonstration of control of temperature and relative humidity for 160 ACFM and target point of 80° F and 60% RH

Flow rate and differential pressure over the entire period of testing for 160 ACFM are shown in Figure 64. The differential pressure during testing for 160 ACFM remained relatively constant at 8.5 in. w.c. The flow rate varied during the testing with an initial average flow rate 158 ACFM and an average of 162 ACFM.

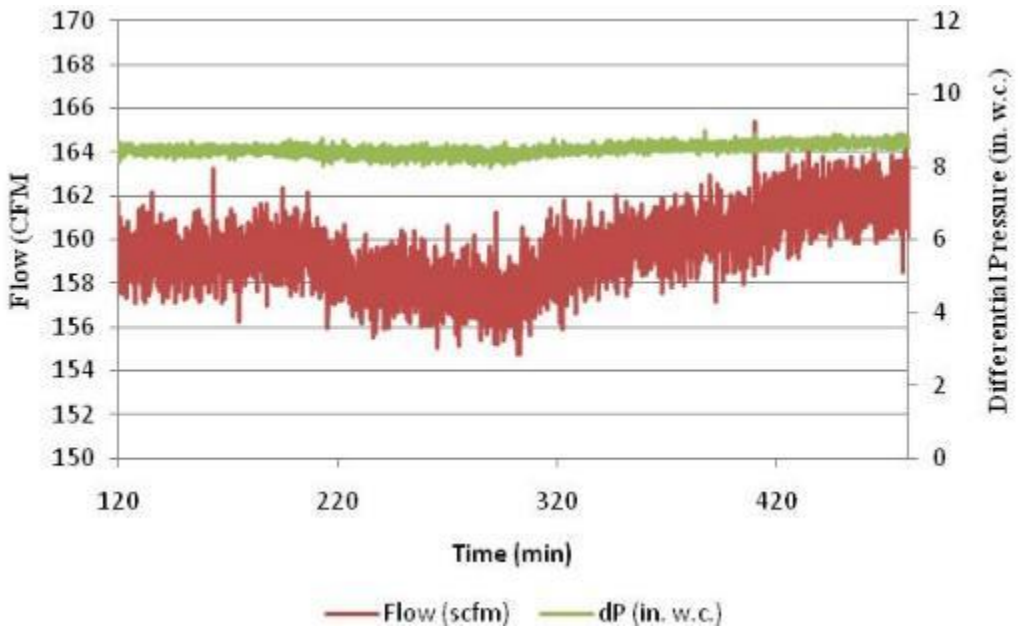

Figure 64 Flow rate and differential pressure for control of temperature and relative humidity testing for 160 ACFM

The FI test stand must be capable of performing testing at consistent conditions to ensure accurate results. The ability of this test stand to maintain consistent conditions can be shown using standard deviation for testing parameters. Average and standard deviation for the flow rate, differential pressure, temperature and relative humidity during characterization testing at 55 ACFM and 160 ACFM are shown in Table 15.

Table 14 Statistics for characterization of air stream conditions control

	Flow Rate (ACFM)		Filter dP (in. w.c.)		Temperature		Relative Humidity	
Target	**Avg.**	**St. Dev.**	**Avg.**	**St. Dev.**	**Avg.**	**St. Dev.**	**Avg.**	**St. Dev.**
Initial	53.2448	N/A	2.4650	N/A	77.4578	N/A	40.6378	N/A
60° F 40% RH	53.0958	0.3010	2.4239	0.0228	71.6688	0.2756	37.8395	0.8012
60° F 60% RH	53.5159	0.2684	2.4505	0.0232	74.2578	0.3986	48.8539	1.1035
80° F 40% RH	53.6915	0.2618	2.4752	0.0026	80.9364	0.4744	36.8615	1.9995
80° F 60% RH	54.4554	0.2583	2.4925	0.0223	80.9994	0.1783	55.7449	1.2747
Initial	158.1962	N/A	8.4320	N/A	68.4697	N/A	81.2966	N/A
60° F 40% RH	159.2201	0.8411	8.4511	0.0761	68.0701	0.9472	41.5855	2.1501
60° F 60% RH	158.3305	1.0047	8.3770	0.1177	62.6072	1.0576	61.2208	2.2967
80° F 40% RH	159.9541	0.8975	8.5469	0.0807	79.6180	1.2427	40.6732	2.2175
80° F 60% RH	161.8867	0.8606	8.6645	0.0767	81.9289	0.6841	58.9492	1.8581

Testing was conducted at the low end (50 CFM) and the top end (160 CMF) of the claw compressor capacity. Testing was conducted during May in Starkville, MS where the approximate ambient conditions were 83° F and 55% RH. This test stand lacks the ability to add moisture to the air and the heat exchangers for reheating are located outdoors. Therefore operation during cold weather testing may require addition of humidifying capability to the current system configuration.

Sinusoidal waves in the relative humidity of air for during testing were caused by cycling of the chiller. Differential temperature settings on chiller allow cycling within the range of the set point. Lowering the cycle temperature range on the chiller reduces the magnitude of these waves but increases the frequency. The lowest differential temperature setting for the chiller is 2° F. In Figure 65 the curve for the relative humidity can be seen. The plot in Figure 65 shows the sinusoidal wave of the relative humidity

from the cycling of the chiller. The small changes in the relative humidity on the plot are due to the resolution of the plot. The differential temperature set point for the testing shown in Figure 65 was 2 degrees Fahrenheit. Relative humidity is shown to slightly increase as the test continues due to changing ambient conditions.

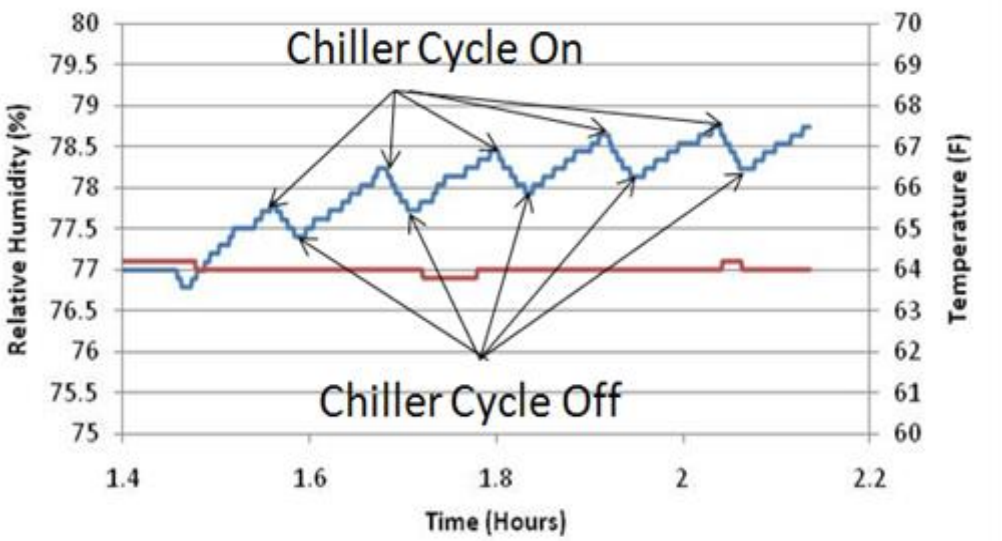

Figure 65 Plot showing the relative humidity with the chiller cycling points notated

Aerosol generation

Continuous aerosol generation is required for loading tests that can last an extended period of time (up to several days). Initial testing demonstrated the difficultly of continually generating aerosol that included clogging of the spraying system. A larger diameter spray nozzle hole allowed the particle generator to operate without frequent cleanings.

Increasing differential pressures as filter testing continues will produce pressures that exceed the one PSIG limitation of the aerosol measurement instrumentation. A

pressure reducer based on the design developed by Rubow is used to accomplish particle size distribution measurements at elevated static pressure in the upstream section of the test stand. Initial characterization of the pressure reducer included comparison of concentration and particle size distributions from conditions that do not require the pressure reducer. Figure 66 shows that there is little to no change in the particle size distribution caused by using the pressure reducer at low pressure (0.40 PSI). As the pressure is increased to 7 PSIG the particle size distribution CMD is shifted slightly to the left from approximately 0.16 µm at 0.40 PSIG to approximately 0.12 µm at seven PSIG. The plot in Figure 76 also shows the number concentration per cubic centimeter reduces as the pressure is increased.

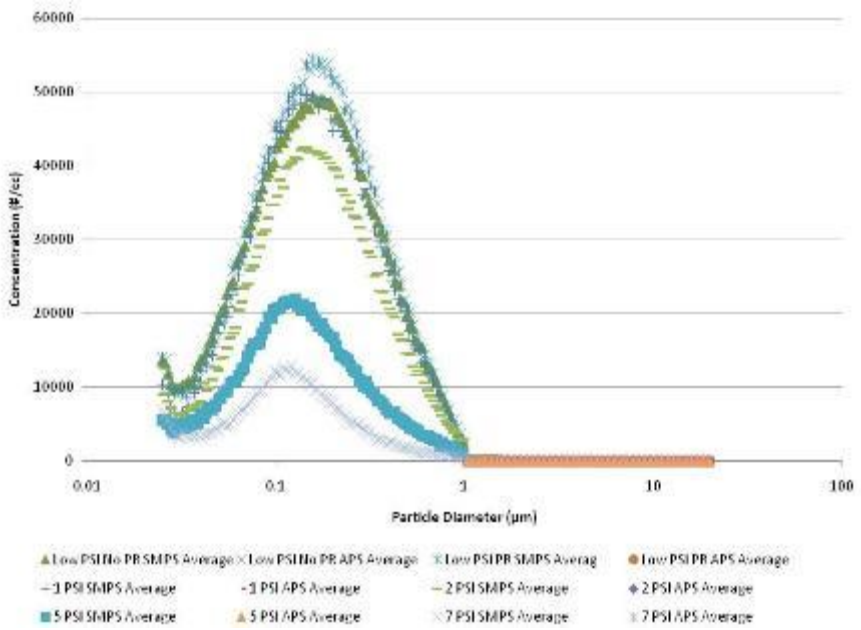

Figure 66 Particle size distribution for initial to 7 PSIG using pressure reducer

Nonlinear reduction in number density values as the static pressure in the upstream section increases may be due to slowed delivery of aerosols from the generator to the test stand. Maintaining constant delivery rates for aerosols requires increasing static pressures within the generator vessel. This will require revising the seals for the vessel and nozzle feed lines. . An alternate method for source sampling of aerosols known as Method 5i is currently being evaluated for use in determining the effectiveness of the pressure reducer.

Filter testing

Filter elements were tested at 120 ACFM under ambient conditions. Table 16 shows the testing conditions.

Table 15 Filter and Testing Parameters

Filter	Filter Type and Testing Parameters and guidelines		Aerosol
POR-F-001	Porvair Sintered Fiber Pleated Filter	120 ACFM 60 to 80º F 40 to 60% RH	
MO-P-001	Mott Sintered Powder Filter	60 to 80º F 40 to 60% RH	Potassium Chloride

Test conditions such as media velocity, relative humidity and temperature will affect the performance of a filter. Test conditions are monitored and displayed graphically to compare changes of performance to changes in test conditions. The blower used during these tests causes oscillations in the flow that can be seen in the width of differential pressure curves in Figure 67. Increasing temperature over the course of the

testing shown in Figure 67 is due to heating from compression as well as heat added from the aerosol generator. A chiller and heat exchanger were connected in line with the blower to bring the temperature within the specified range.

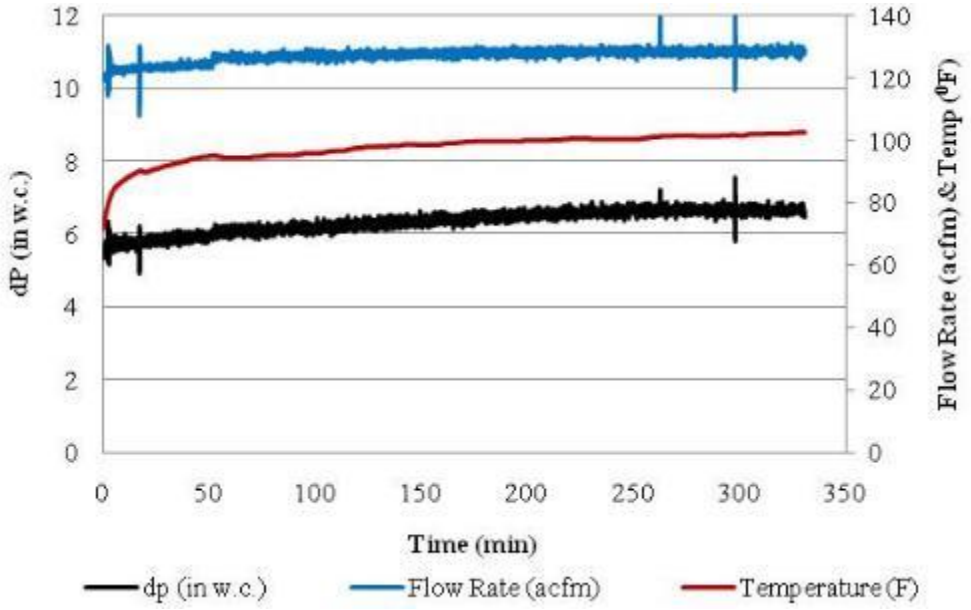

Figure 67 Testing conditions for Porvair metal media filter elements during filtering efficiency testing

A set of three sintered metal fiber filter elements was tested at 120 ACFM to reach an equivalent media velocity of 5.4 ft/min for resistance to pressure, resistance to air flow, and resistance to test aerosol penetration. Raw data collected during these tests was reduced into graphical form to easily display the behavior of these filter elements. Filter elements provided by Porvair Filtration have a length of 3.28 ft (1 m), diameter of 3.1 in. (8 cm), are of pleated geometry and constructed of sintered metal fiber produced by Bekaert of Belgium.

Most penetrating particle size

The upstream particle size distribution (PSD) plot is was produced using data from both the SMPS and APS. It is necessary to combine the particle counts from both to cover the desired particle diameter range due to particle size limitations on each instrument. The graphical representation of the upstream particle size distribution is not lined up perfectly because of the impactor of the SMPS becoming dirty during testing as well as particle size related variable sensitivity of the APS. The PSD plot is created using the average counts of the particle diameter ranges over the length of the test. The upstream PSD can be seen in Figure 68

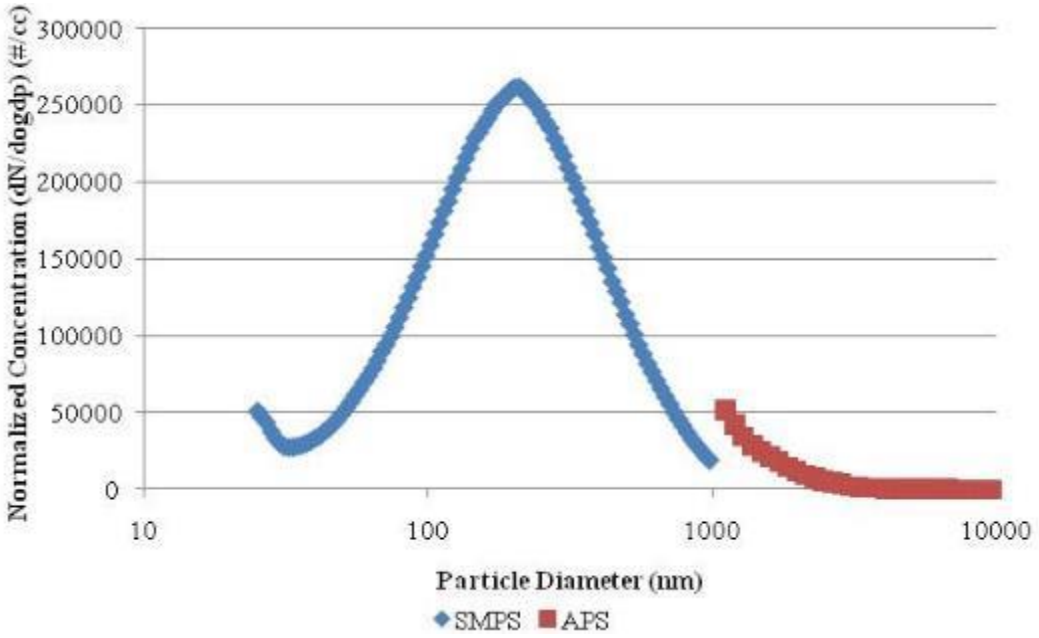

Figure 68 Upstream particle size distribution from combined data from SMPS and APS while testing of Porvair metal media filter elements using KCl

Downstream particle size distribution plots used LAS data that was averaged over the duration of the test. This can be seen in Figure 69. Up and downstream data combined to generate the particle size distribution is used for the penetration curve. The particle size distribution curve is not smooth in some places due to the low particle count in the downstream section. The MPPS can be seen on the downstream particle size distribution in Figure 69.

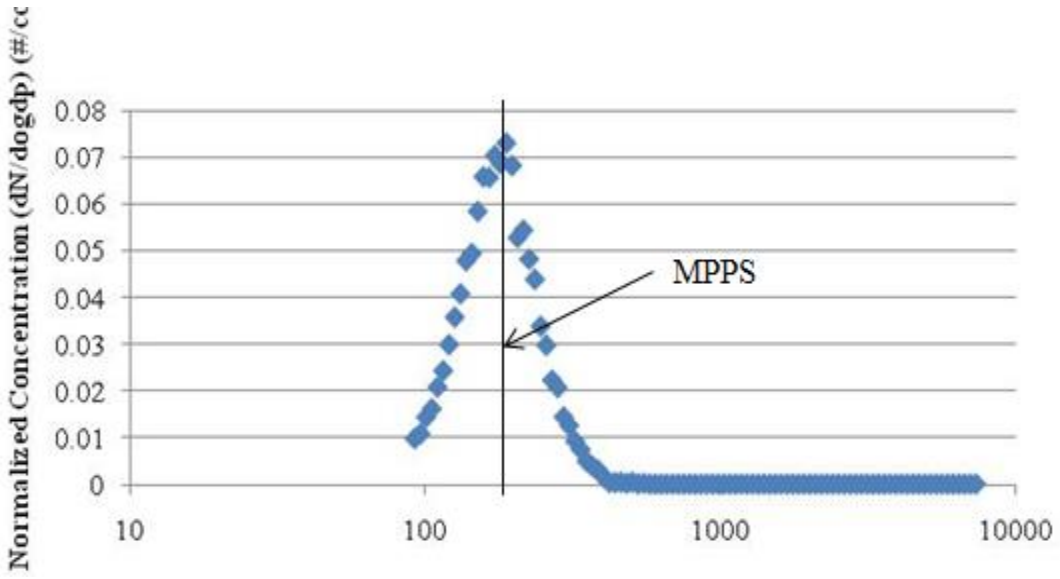

Figure 69 Plot of the filtering efficiency versus particle diameter for testing of Porvair metal media filter elements using KCl aerosol challenge

The filtering efficiency versus particle diameter curve is a direct comparison of the upstream and downstream particle size distributions to see how the filter performs as a function of particle size. This curve helps identify the most penetration particle size. The lowest filtering efficiency for any particle size in these test elements occurs when the filter is clean and is greater than 99.992%. The filtering efficiency curve as a function of

particle size can be seen in Figure 70. These filter elements display HEPA efficiency. As data shown in Figure 70 indicates that filtering efficiency increases as the filter elements become loaded. Therefore, even lower efficiency filters can display HEPA efficiency when partially loaded but they are likely to continue having a MPPS larger than most nuclear grade HEPA filters (0.15 μm)

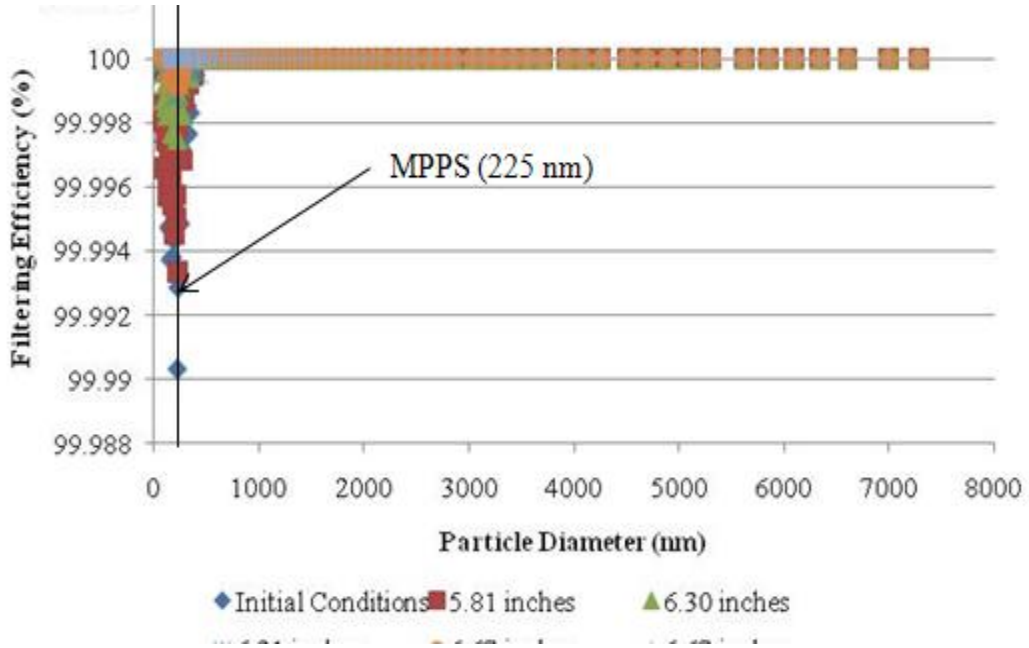

Figure 70 Plot of the filtering efficiency versus particle diameter for testing of Porvair metal media filter elements using KCl aerosol challenge

The most penetrating particle size at several differential pressures is shown in Figure 71. Most penetrating particle size is the size of particle that gives the lowest filtering efficiency. The most common particle size shown on the plot is around 225 nanometers. The efficiency curve shown in Figure 70 also gives a good representation of the most penetrating particle size.

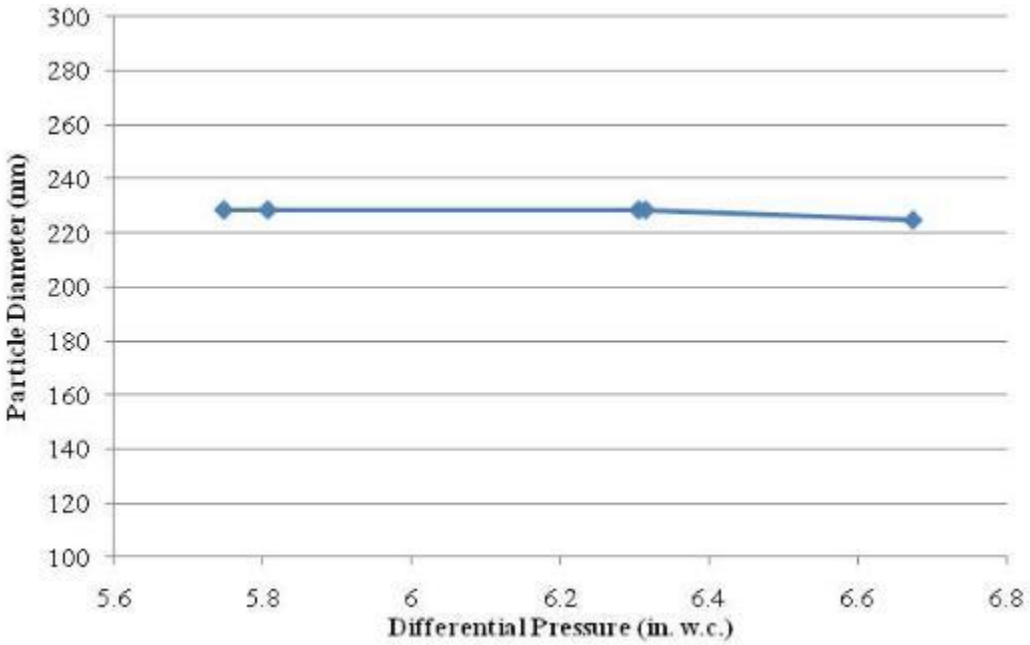

Figure 71 Plot of the most penetrating particle size during testing of Porvair metal media filter elements with KCl as challenge aerosol

Filtering efficiency and differential pressure

Significant results from filter testing includes the overall filtering efficiency of the filter as a function of time. Clean HEPA filters are required to have 99.97% efficiency removing particulate matter of 0.3 μm and larger from the airstream. As the filter loads the differential pressure will increase continuously until the filter either ruptures or becomes plugged. As the filter loads the filtering efficiency will increase until it reaches nearly one hundred percent and remain constant until it physically fails. The plot of filtering efficiency and differential pressure versus time can be seen in Figure 82.

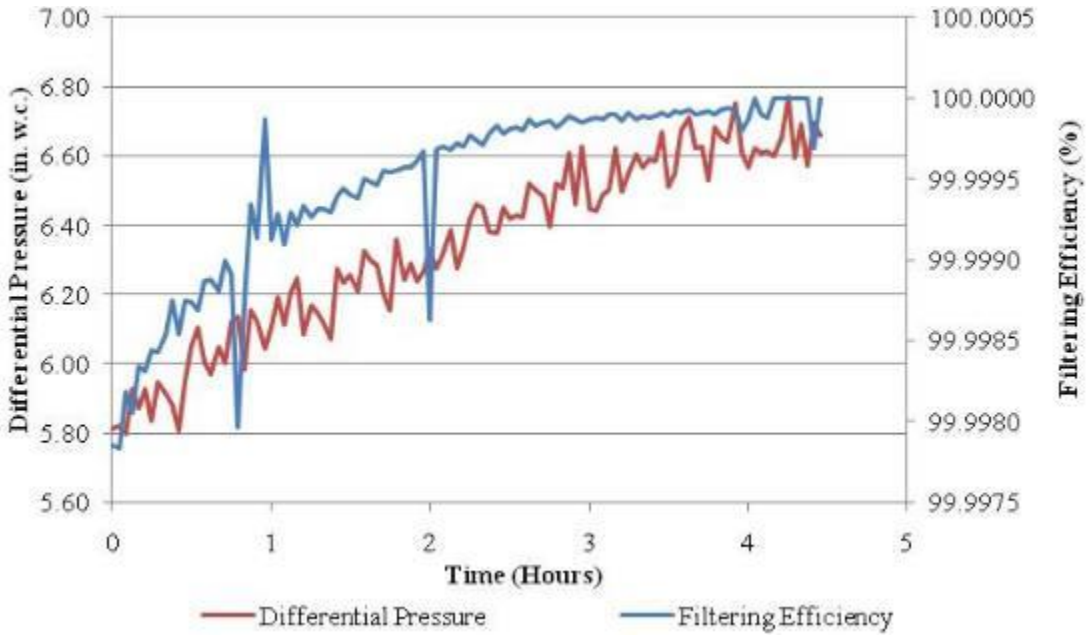

Figure 72 Plot of the total filtering efficiency and differential pressure for testing of Porvair metal media filter elements with KCl challenge aerosol

CHAPTER VI

CONCLUSIONS

Conclusions

The goal of this project has been to provide essential infrastructure for completing Section FI of AG-1. Section FI will cover a broad range of filtering efficiencies. Filter qualified under Section FI will vary from units offered as a direct replacement of Section FC HEPA filters to units designed for a unique application. Section FI provides great flexibility in design and performance to meet specialized needs of the user. Therefore the test stand for qualification testing must offer flexibility of testing.

Performance data characteristics of metal media filter elements, testing procedures, and testing hardware are needed to provide the FI Project team with information to complete the next draft. An essential capability necessary for successful balloting is the demonstrated existence of hardware and procedures to qualify FI filters. A major step forward has been taken with the design, fabrication, assembly, and characterization of the ICET FI test stand.

Section FI covers a broad range of filtering efficiencies and eight qualification testing categories: resistance to airflow (FI-5110), test aerosol penetration (FI-5120), resistance to rough handling (FI-5130), resistance to pressure (FI-5140), resistance to heated air (FI-5150), spot flame resistance, (FI-5160), structural requirements (FI-5170), and cyclic testing of cleanable filter designs (FI-5180). ICET was tasked with designing a

test stand to provide data addressing qualification sections FI-5110, FI-5120, FI-5130, FI-5140, FI-5170.

Subsection FI-5110 requires that resistance to airflow for non HEPA filters at the rated flow is to be specified by the owner. Resistance to airflow for metal media HEPA filters is not to exceed 3 in. w.c. when tested at rated airflow if they are to be used as a replacement for FC filters. Other applications will have initial and final differential pressure value specified by the owner. This requires that the FI test stand have a wide range of operation for volumetric flow at elevated differential pressures. The FI project team concluded that a flow rate of 200 ACFM would be sufficient to cover the range of testing.

The system at ICET has been designed to withstand much higher static pressures. However the air flow systems tested are not capable of achieving the target level of performance. An Elmo-Rietschle claw compressor with specifications capable of achieving operating capabilities was purchased. However, the compressor generated large fluctuations in the flow and high noise levels. These fluctuations were corrected by using a buffering system that includes a muffler, a large rubber hose, and two air tanks. Pressure drop by these additional devices reduced the ability to achieve target operating conditions. A larger air supply component will be required to meet overall objectives.

The air flow conditions for the FI test stand are controlled using a water chiller and heat exchanger utilizing hot air before the chiller. This system is capable of maintaining conditions specified by the FI project team of 40% to 60% relative humidity and 60° F to 80° F for warm ambient conditions with sufficiency relative humidity. For conditions during cold dry weather the test stand will not be able to maintain operating

conditions. To accomplish this it is necessary to increase the relative humidity of the air stream while maintaining the operational temperature. Increasing the reheating capacity of the heat exchanger can be accomplished by using hot water instead of hot air.

The current draft of subsection FI-5120 states that test aerosol penetration for non HEPA filters must meet the user defined efficiency at a user specified flow rate. A variety of aerosols are required for testing of penetration depending on the required efficiency of the filter. Efficiencies less than 95% require KCl particles with aerosol diameters of 0.3 to 10 μm. Efficiencies between 95% and 99.99% require DOP or DOS particles with aerosol diameter of 0.3 μm. Efficiencies between 99.99% and 99.999% require aerosol particles with diameters of 0.1 to 0.2 μm and efficiencies between 99.999% and 99.999999% require aerosol particle diameters' of 0.05 μm, 0.07 μm and 0.1 μm. The testing methods are required to follow existing standards.

For HEPA and ULPA for efficiencies between 99.97% and 99.99% aerosol particle diameter of 0.3 μm is required. Efficiencies greater than 99.999% it are required to use, DOP, dioctyl sebacate (DOS) or equivalent aerosol particles. The test stand designed and constructed at ICET is capable of performing these tests.

Subsection FI-5140: Resistance to Pressure lays out requirements for filter or filter elements to be subjected to a liquid flow sufficient to produce the maximum rated differential pressure at the ambient temperature. Test for resistance to pressure is a design criteria requested by the FI project team for the FI test stand. The FI test stand constructed is not capable of utilizing liquid flow and therefore cannot meet this criteria. A separate test stand has been designed and construction of this test stand can provide capabilities of testing resistance to pressure. A resistance to liquid pressure test stand is

currently under construction for evaluating 2000 ACFM radial flow HEPA filters to differential pressure in excess of seven PSIG. This test stand can serve as a model for finalizing the design of testing protocols for FI filter elements.

Subsection FI-5150 for resistance to heated air criteria requires for the test stand to be capable of rated air flows for filters over a range of temperatures from 250 ±10° F to 750 ±50 ° F. The current test stand has not been equipped with the high temperature testing capabilities. However, electric air heaters at ICET are capable of producing the required temperatures for the flow and an addition to the current test stand has been designed to accomplish this test.

Subsection 5180: Cyclic Testing of Cleanable Filter Designs. Testing of cleanable filter designs is currently not capable using the FI test stand, However modification of this test stand to include back pressure jets will make this possible.

Recommendations

The following modifications are recommended for this test stand to accomplish the full suite of performance criteria.

- Back pulse equipment added to existing test stand to facilitate evaluation of filter performance over a lengthy series of load and clean cycles. It will also comply with requirements of FI-5180.
- Construction of high temperature test section is essential for achieving requirements of FI-5150.
- Install a larger blower or compressor capable of achieving the desired flow rates. This is necessary to accommodate testing at flow rates up to 200 ACFM and at differential pressure values of 10 PSIG.

- Modification of aerosol generator to increase pressure capacity of vessel and modify nozzle to use metal tubing for aerosol generation during elevated pressure.
- Modify the aerosol generation/delivery system to cool air temperatures downstream of the diffusion drier to prevent exceeding air flow temperatures in the test stand.
- Addition of HEPA filters in upstream section to ensure filter elements are being challenged with only the specified aerosol and not particulate matter from outside sources. This will make the system compliant with qualification testing requirements.
- Addition of temperature, pressure, and relative humidity sensors upstream of air conditioning equipment.
- Automation of air conditioning process. This will implement control strategies developed in this study.
- Design and construct a more effective air buffering system. The current system is functional but not permanent.
- Design and construct equipment for adding moisture to air stream for increasing relative humidity when necessary. This will provide capability to achieve elevated relative humidity conditions during winter months.
- Design and construct equipment for providing dry air to decrease relative humidity when necessary. Dual column air driers can be used to accomplish this need.

- Addition of heated air or hot water used as the hot working fluid in the reheat heat exchanger. This will provide additional heating capacity for very cold air intake.

The current FI test stand and its current equipment list fell short in several categories of the performance criteria outlined by the FI-project team. However, this test stand is able to produce useful data for performance and qualification data to assisting in the balloting of section FI. Modification to achieve overall objectives will not be difficult and the estimated cost is on the order of $80,000. Implementation of the modification actions suggested above will equip the FI test stand to accomplish all the required performance criteria. The FI test stand has shown the necessary infrastructure required to accomplish qualification procedures and collect a full suite of qualification data. The design and construction of this test stand is a major step in the process preparing the next draft of Section FI.

REFERENCES

[1] U.S. Department of Energy (DOE): Nuclear Air Cleaning Handbook (DOE-HDBK-1169-2003), DOE Handbook, (2003)

[2] ASME AG-1-2009, Code on Nuclear Air and Gas Treatment, American Society of Mechanical Engineers,

[3] "ASME Committee on Nuclear Air and Gas Treatment (CONGAT) AG-1 Code Development". 32 Nuclear Air Cleaning Conference. (2012)

[4] Pierce, Mary. "HEPA Filter Media Testing: 1950-2000". 25th DOE/NRC Nuclear Air Cleaning and Treatment Conference. (1998).

[5] "HEPA Filters for Nuclear Applications: Dessigns, Qualification, Manufacturing, Inspection and Testing". ATI Test Laboratory. (2008)

[6] Richard D. Porco and Werner Bergman. "Filters and Filtration for Nuclear Applications" 25th DOE/NRC Nuclear Air Cleaning and Treatment Conference (1998)

[7] Hinds, William C. *Aerosol Technology: Properties, Behavior, and Measurement of Airborne Particles.* John Wiley & Sons, Inc. (1999)

[8] K. W. Lee and B.Y.H. Liu (1982). "Theoretical Study of Aerosol Filtartion by Fibrous Filters". Aerosol Science and Technology 1:2, 147-161

[9] Rubow, Kenneth. Louise L. Strange, Billy Huang. Advances in Filtration Technology Using Sintered Metal Filters. 3rd China International Filtration Exhibition and Conference. Shanghai, China, November 2004.

[10] Baron, Paul A., and Klaus Willeke. *Aerosol Measurement: Principles, Techniques, and Applications*, 2nd edition. John C. Wiley and Sons, Inc.,Publication. (2005)

[11] Richard D. Porco and Werner Bergman. "Filters and Filtration for Nuclear Applications" 25th DOE/NRC Nuclear Air Cleaning and Treatment Conference (1998)

[12] Bemer D. and S. Calle. “Evolution of the Efficiency and Pressure Drop of a Filter Media with Loading”. Aerosol Science and Technology 33:427-439 (2000)

[13] L.D. Weber. “Emerging ASME AG-1 Code: Article FI, On Metal Medium Filters.” 25th Nuclear Air Cleaning and Treatment Conference, (1998)

[14] Gilles, D. A. “Emery 3004* as a Challenge Aerosol for HEPA Filter Testing”. Westinghouse Hanford Company. (1994)

[15] Paxton Giffin, Michael S. Parsons, John A. Wilson, Charles A. Waggoner. “Performance Comparison of Dimple Pleat and Ribbon Separated Radial Flow HEPA Filters”. Mississippi State University 32nd Nuclear Air Cleaning Conference International Society for Nuclear Air Treatment Technologies. (2012).

[16] Marple, Virgil (2004). “History of Impactors-The First 110 Years”. Aerosol Science and Technology 39:3, 247-292.

[17] *ASME NQA-1-2012 Quality Assurance Requirements for Nuclear Facility Applications.* The American Society of Mechanical Engineers. (2012).

[18] Gunn, C.A. and D.M. Eaton. “HEPA Filter POerformance Comparative Study”. 14th ERDA Air Cleaning Conference.

[19] ASME. 2002. Nuclear Power Plant Air-Cleaning Unit and Components, ASME N509-2002. American Society of Mechanical Engineers

[20] ASME. 1989. Testing of Nuclear Air Treatment Systems, ASME N510-1989. American Society of Mechanical Engineers

[21] ASME N511 In-Service Testing of Nuclear Air Treatment, Heating, Ventilating, and Air-Conditioning Systems, 2007

[22] “DOE-STD-3020-2005 Specification for HEPA Filters Used by DOE Contractors”. U.S. Department of Energy (2005)

[23] “HEPA Filters for Nuclear Applications: Designs, Qualification, Manufacturing, Inspection and Testing”. ATI Test Laboratory. November 2008.

[24] Porco, Richard D. “Code on Nuclear Air and Gas Treatment”. 8th International Conference on Nuclear Engineering. (2000).

[25] http://www.dnfsb.gov/about/who-we-are. Defense Nuclear Facilities Safety Board.

[26] "HEPA Filters Used in the Department of Energy's Hazardous Facilities"; Defense Nuclear Facilities Safety Board; DNFSB/TECH-23, May (1999).

[27] "Fire Rocky Flats Plant May 11, 1969". *Serious Accidents The united States Atomic Energy Commission*. (1969)

.[28] "Defense Nuclear Facilities Safety Board Recommendation 2000-2 to the Secretary of Energy". Defense Nuclear Facilities Safety Board (2000)

[29] "Recommendation 2000-2 Configuration Management Vital Safety Systems". Defense Nuclear Facilities Safety Board. (2000)

[30] Duane J. Adamson and Charles A. Waggoner. "Development of AG-1 Section FI on Metal Media Filters – 9061." WM2009 Conference, March 1-5, Phoenix, AZ, (2009)

[31] W. Bergman et.al. "Preliminary Field Evaluation of High Efficiency Steel Filters." 23rd DOE/NRC Nuclear Air Cleaning and Treatment Conference, pp. 195-213

[32] Rubow, Kenneth L., Louise L. Stange, and Billy Huang. "Advances in Filtration Technology Using Sintered Metal Filters". 3rd China International filtration Exhibition and Conference. (2004)

[33] Sekellick, Ronald S.and Sunil Jha. "A Washable Porous Metal HEPA Filter". Mott Corporation. National Energy Technology Laboratory (2004).

[34] Rubow, Kenneth "Porous Metal Filters for Gas and Liquid Applications in the Nuclear Industry" Mott Corporation. WM2009 Conference, March 1-5, 2009, Phoenix, AZ

[35] Rubow, Kenneth. Louise L. Strange, Billy Huang. Advances in Filtration Technology Using Sintered Metal Filters. 3rd China International Filtration Exhibition and Conference. Shanghai, China, November 2004

[36] W. Bergman et.al. "Further Development of the Cleanable Steel HEPA Filter, Cost/Benefit Analysis and Comparison with Competing Technologies." 24th Nuclear Air Cleaning and Treatment Conference, (1996).

[37] "Section FI Metal Media Filters" Committee Correspondence Congat Committee Subgroup FI: Metal Media Filters. Draft 2-4-2011.

[38] EPA Reference Method 1 – Sample and Velocity Traverses for Stationary Sources; 40 CFR 60 Appendix A

[39] Incropera, DeWitt, Bergman, and Lavine. (2007) Fundamentals of Heat and Mass Transfer. 6th edition. 2007 John Wiley & Sons, Inc.

[40] Lee, Jae-Keun, Kenneth L. Rubow, David Y. H. Pui, and Benjamin Y. H. Liu. "Design and Performance Evaluation of a Pressure-Reducing Device for Aerosol Sampling from High-Purity Gases" . Aerosol Science and Technology 19: 215-226 (1993).

APPENDIX A

LIST OF INSTITUTE FOR CLEAN ENERGY TECHNOLOGY PROCEDURE,

INSTRUCTIONS, AND TEST CONTROL DOCUMENTS

Procedure documents

1. HEPA-002 Filter as Received Inspection
2. HEPA-003 Data Archiving Procedure
3. HEPA-005 Laboratory Notebooks
4. HEPA-006 Excel Validation Procedure
5. HEPA-007 Version Control Procedure
6. HEPA-009 Receipt Inspection

Instruction documents

1. Aerosol Atomizer Readiness and Operation Instruction
2. APS Operation Instruction
3. LAS Operation Instruction
4. SMPS Operation Instruction
5. LPC Operation Instruction
6. Pilat Mark 5 Cascade Impactor Instruction
7. Powder Feeder Calibration Instruction
8. SMPS Calibration Instruction
9. ATI Photometer Readiness and Operation Instruction
10. ELPI Operation Instruction
11. FI Filter Installation Instruction
12. FI HEPA Filter Removal and Mass Determination Instruction
13. HEPA-LSTS-001 Test Stand Instruction
14. HEPA-LSTS-002 Sensor Repair Replacement Instruction Sheet
15. HEPA-LSTS-002 Test Stand Leak Test Instruction Sheet

16. HEPA-LSTS-003 Sr Insertion Instruction

17. HEPA-LSTS-003 Sr Removal Instruction

Test control documents

1. HEPA-LSTS-001 Test Stand Startup
2. HEPA-LSTS-002 Leak Test of the Test Stand
3. HEPA-LSTS-003 Stromtium Source Chaning Out Procedure
4. HEPA-LSTS-004 Filter Installation
5. HEPA-LSTS-007 Radiation Exposure Control and Monitoring Procedure
6. HEPA-M&TE-002 SMPS Readiness and Operation
7. HEPA-M&TE-003 APS Readiness and Operation
8. HEPA-M&TE-009 LAS Readiness and Operation
9. ICET High Output Aerosol Generator Operating Procedure

APPENDIX B

FI TEST STAND DESIGN DRAWINGS

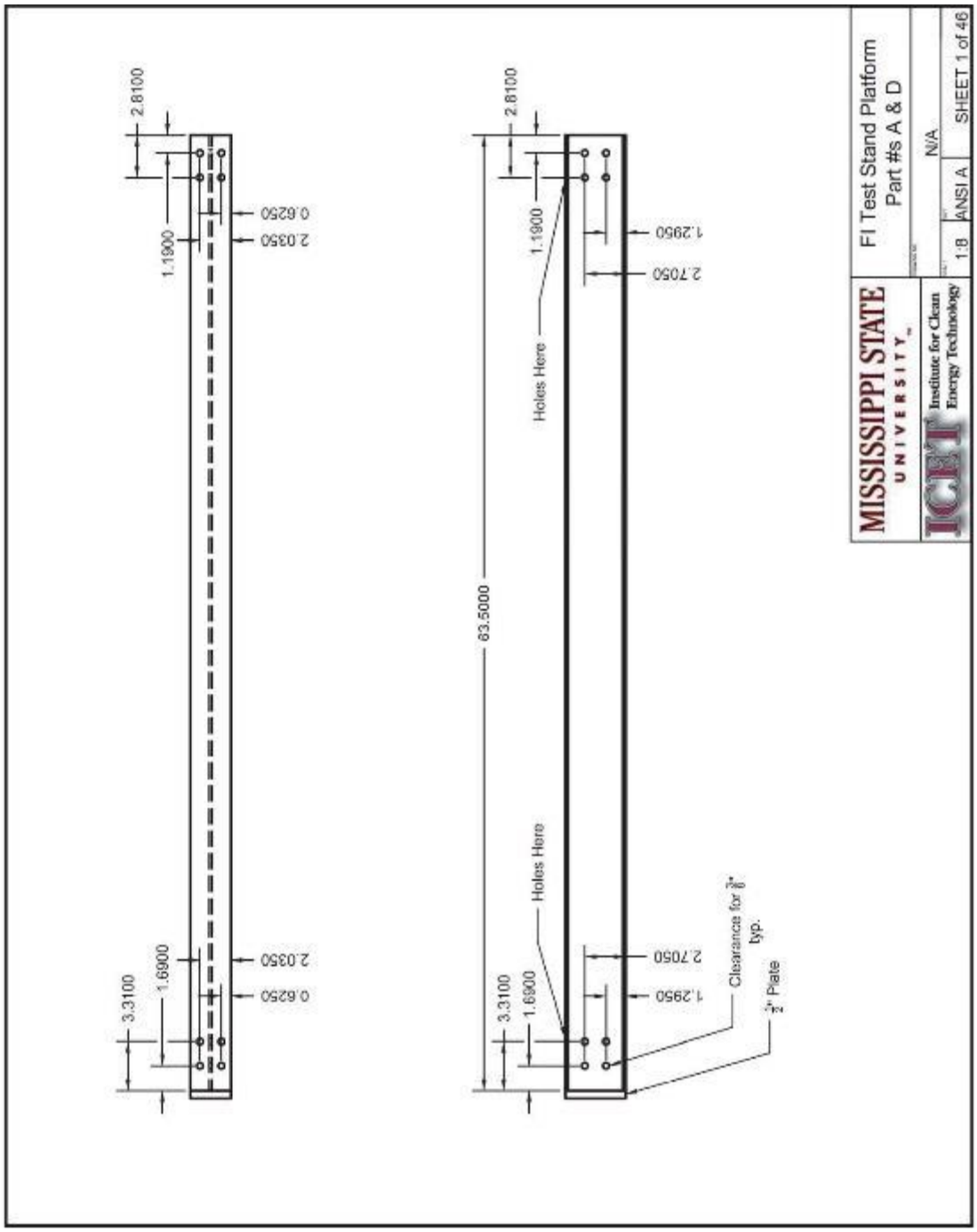

Figure 73 FI test stand platform part #s A & D

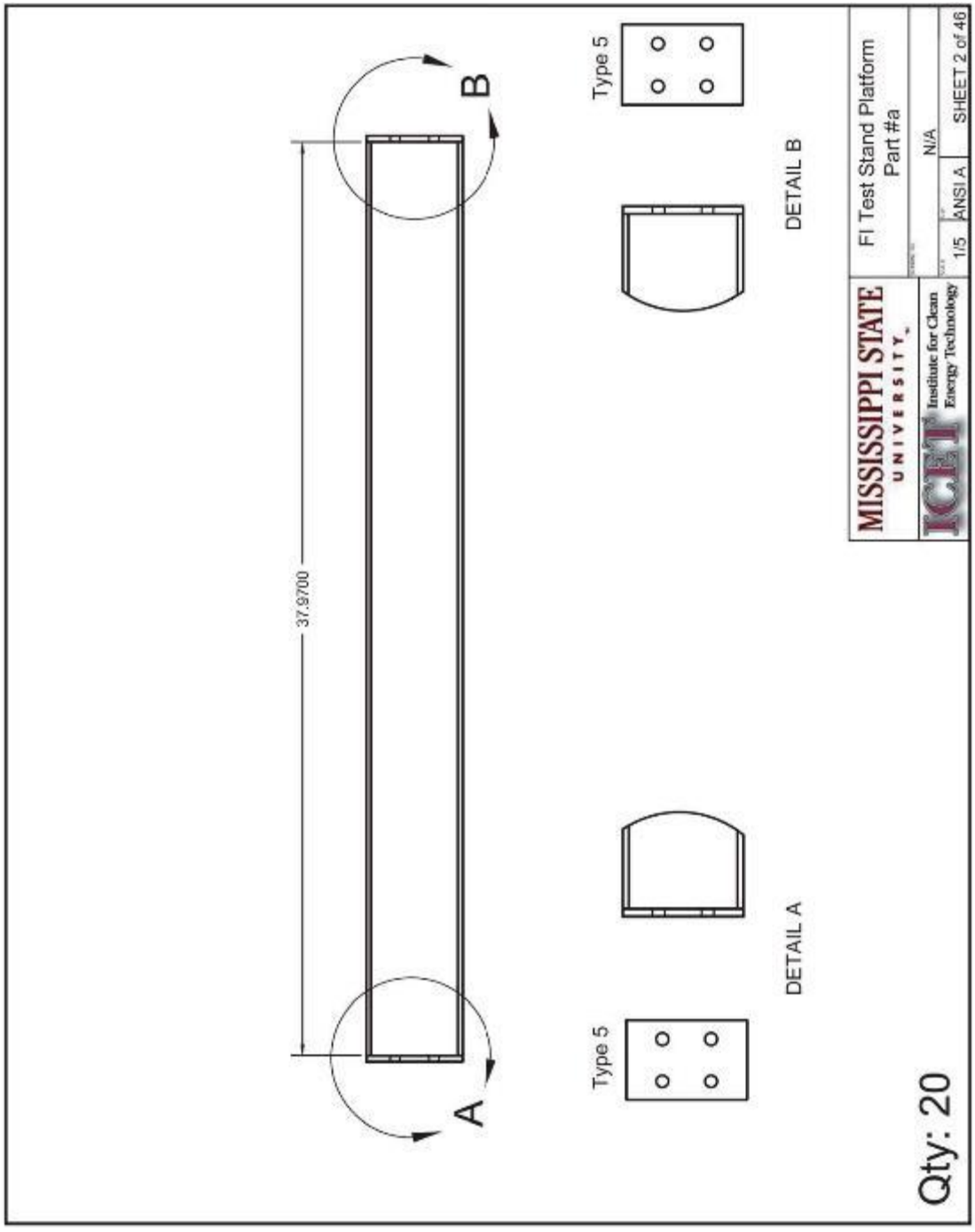

Figure 74 FI test stand platform part # A

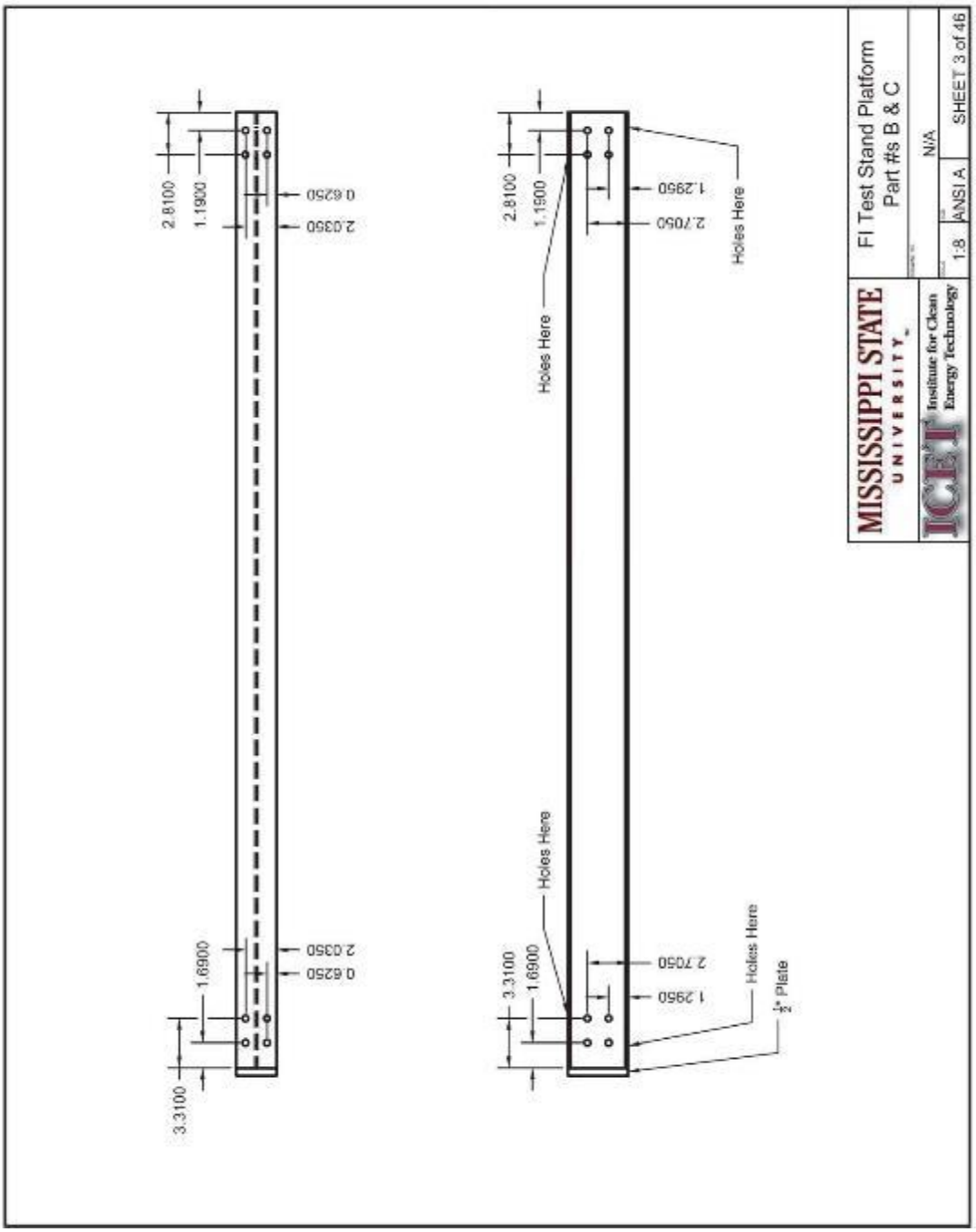

Figure 75 FI test stand platform part #s B & C

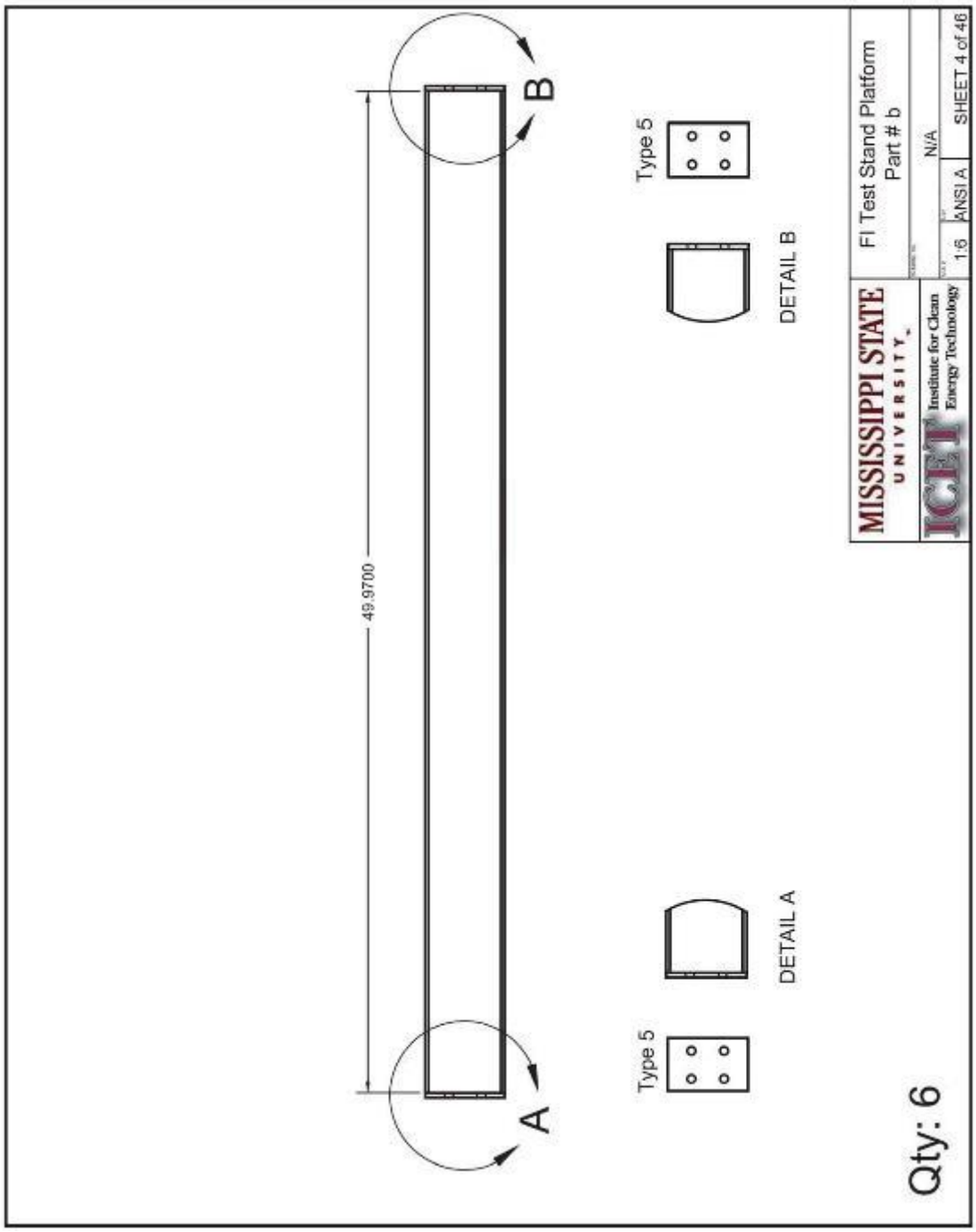

Figure 76 FI test stand platform part # B

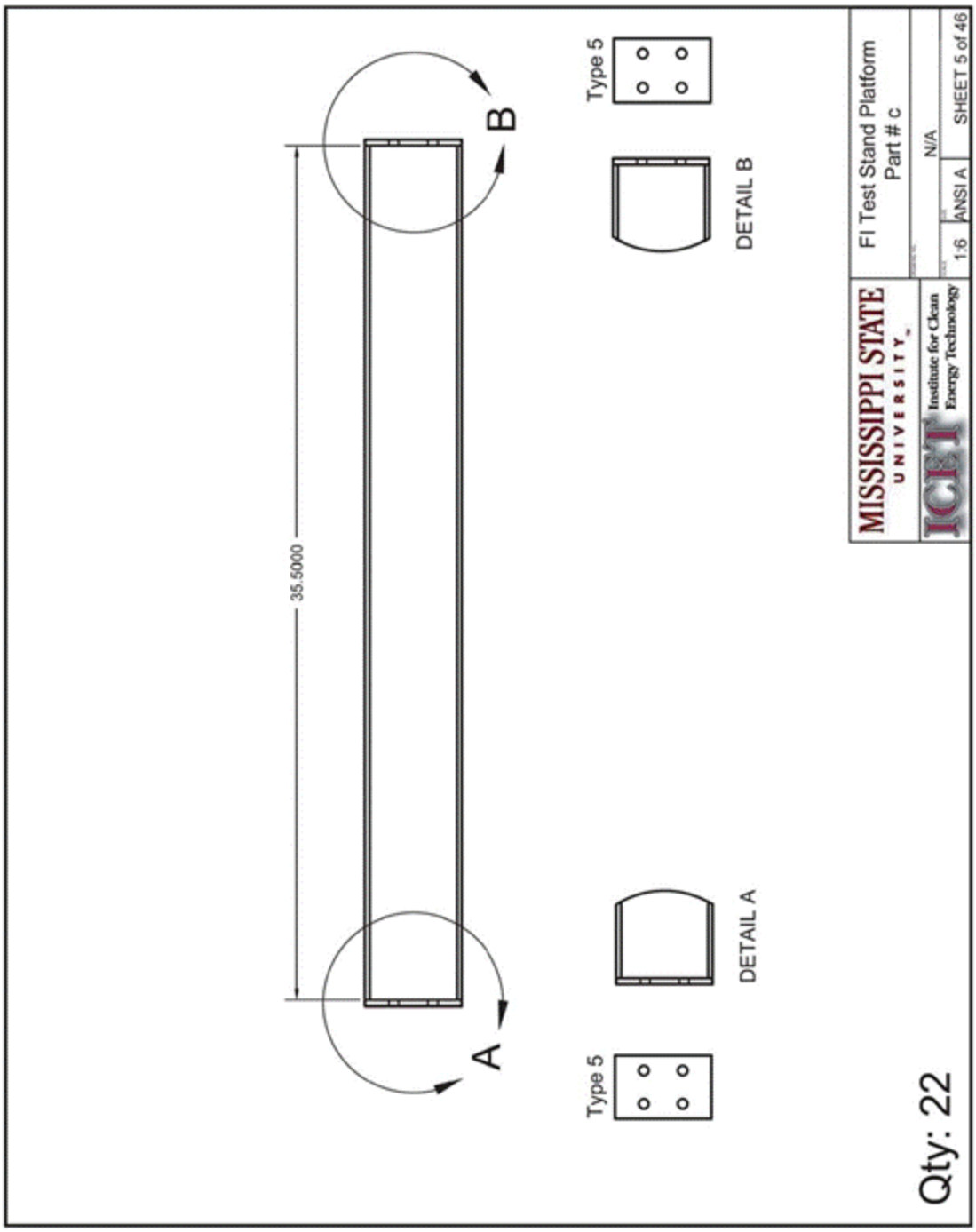

Figure 77 FI test stand platform part # C

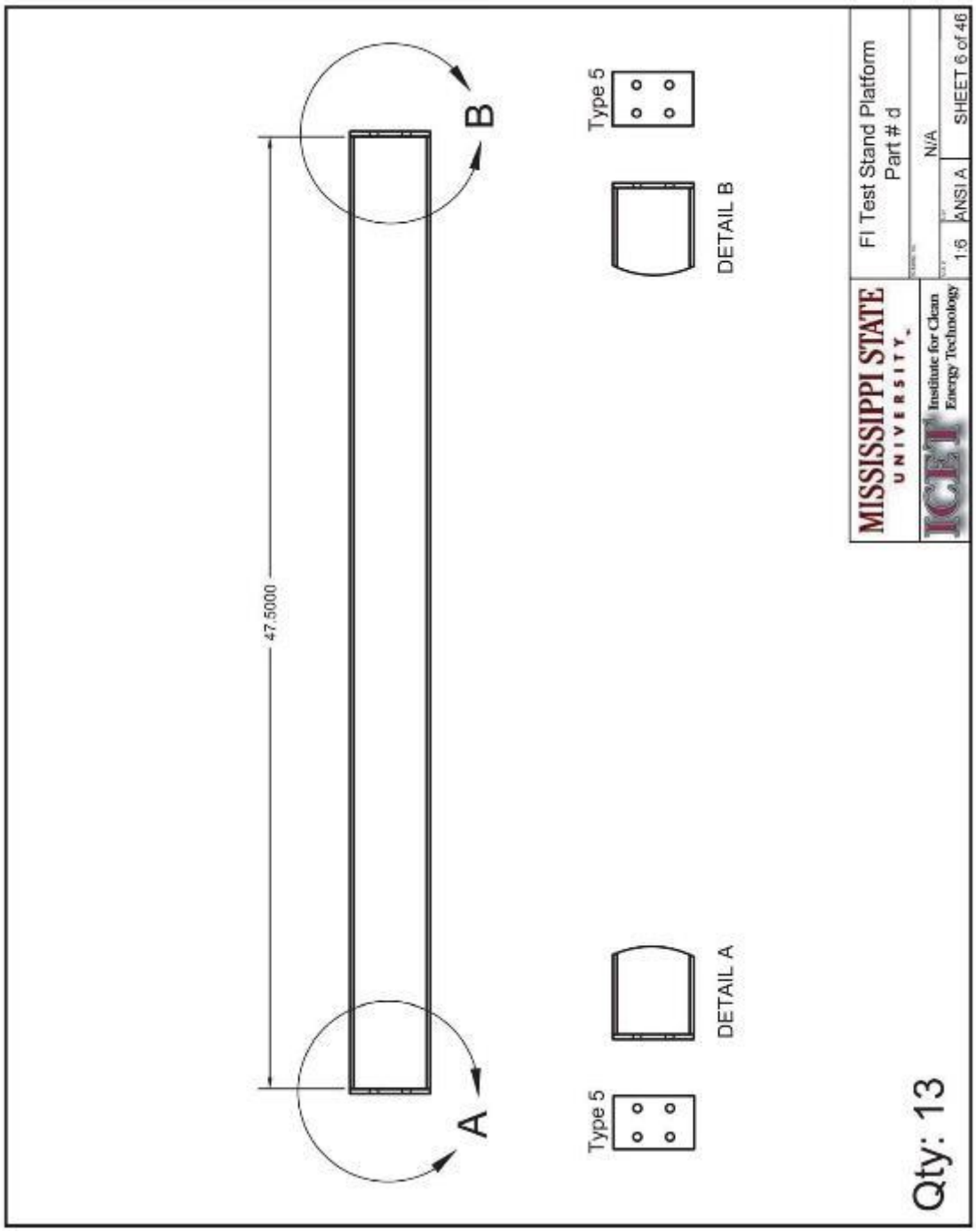

Figure 78 FI test stand platform part # D

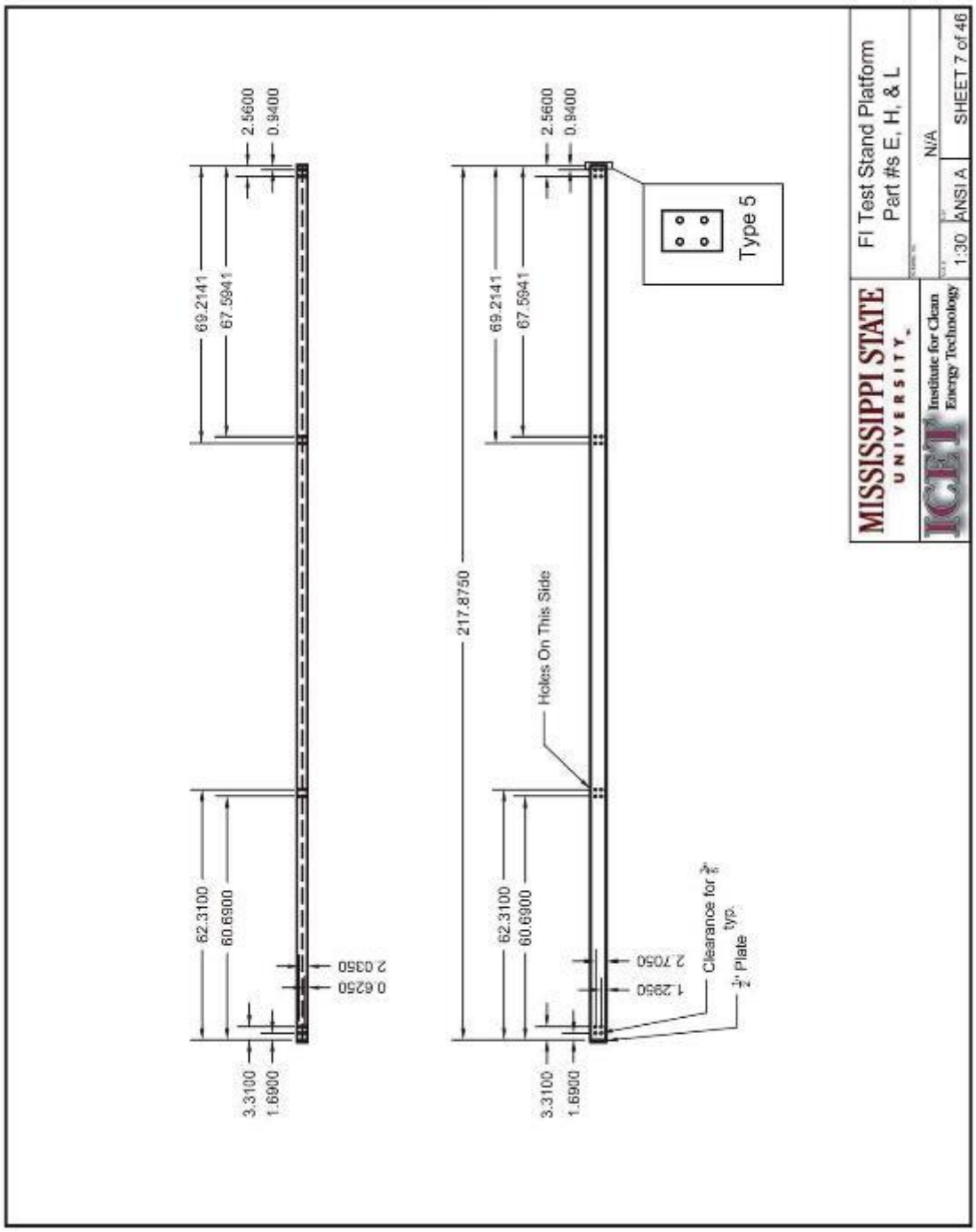

Figure 79 FI test stand platform part #s E, H, & L

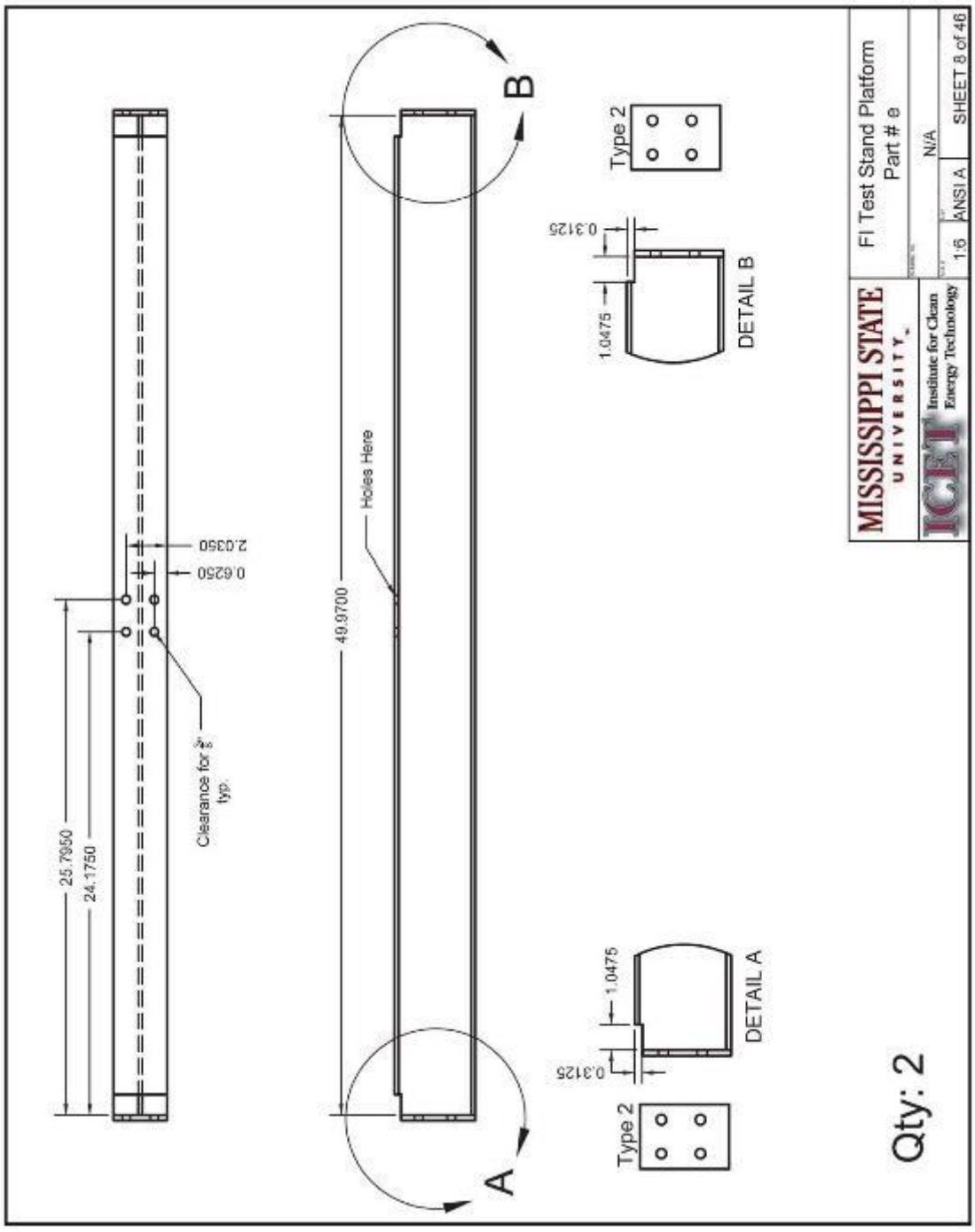

Figure 80 FI test stand platform part # E

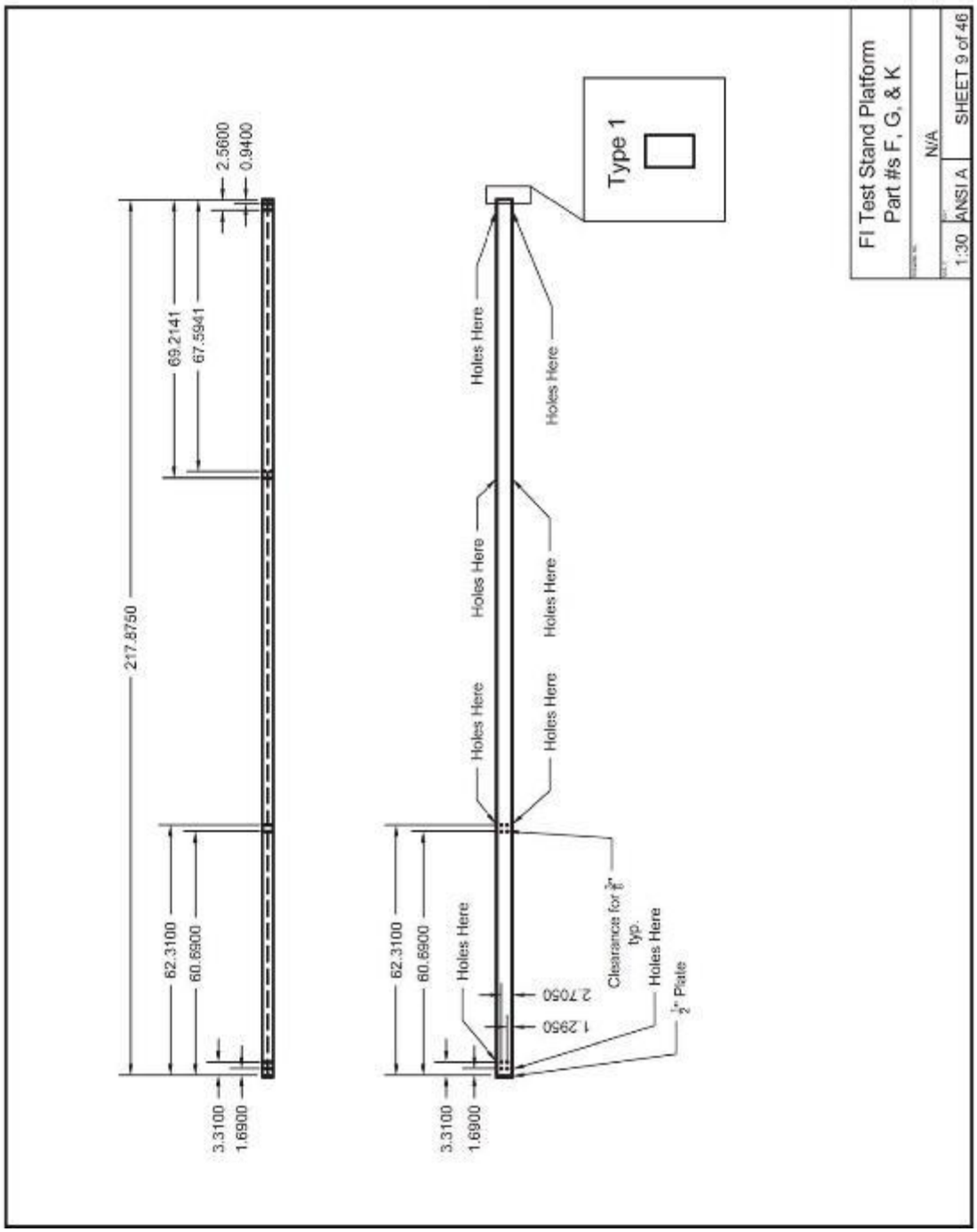

Figure 81 FI test stand platform part #s F, G, & K

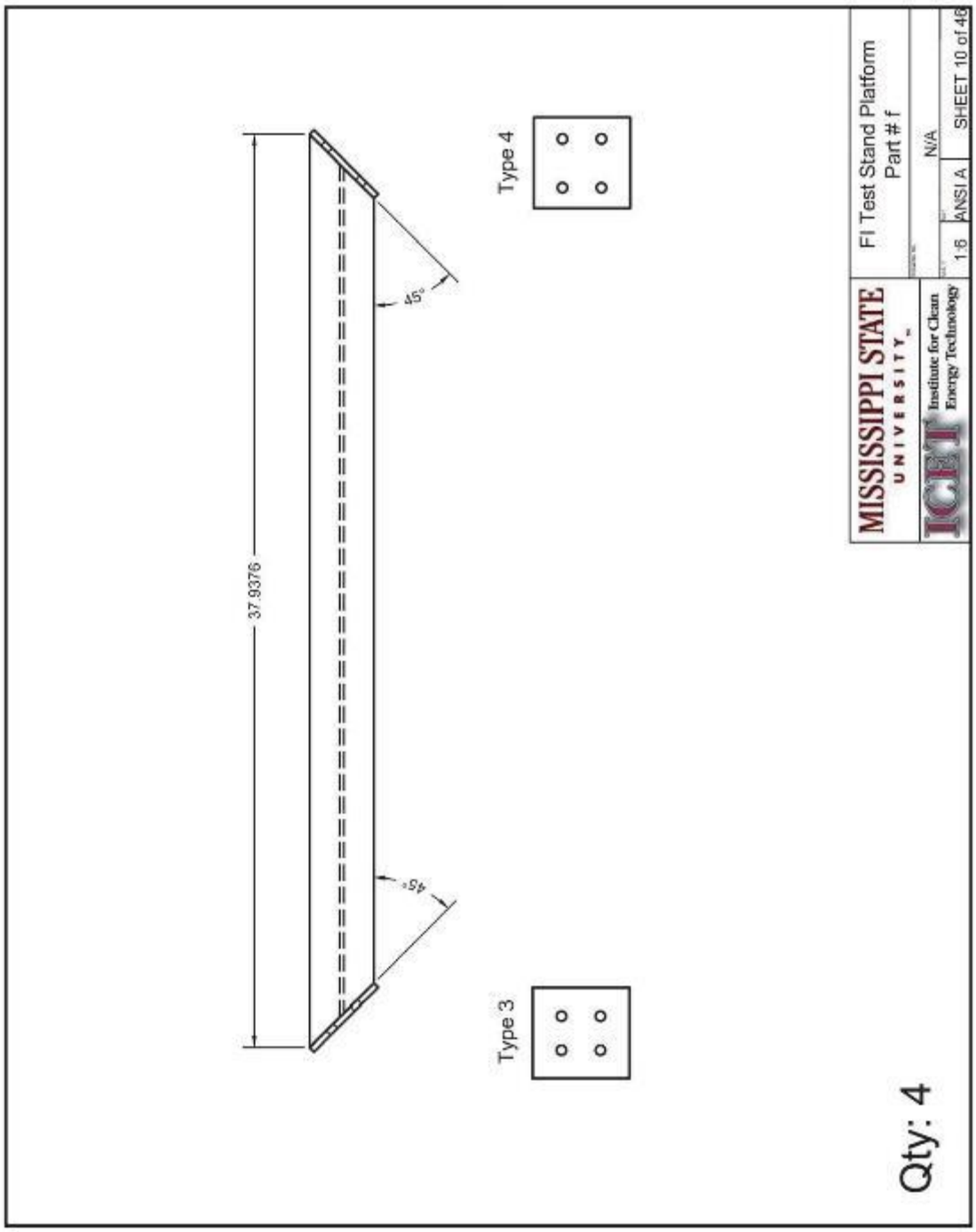

Figure 82 FI test stand platform part # f

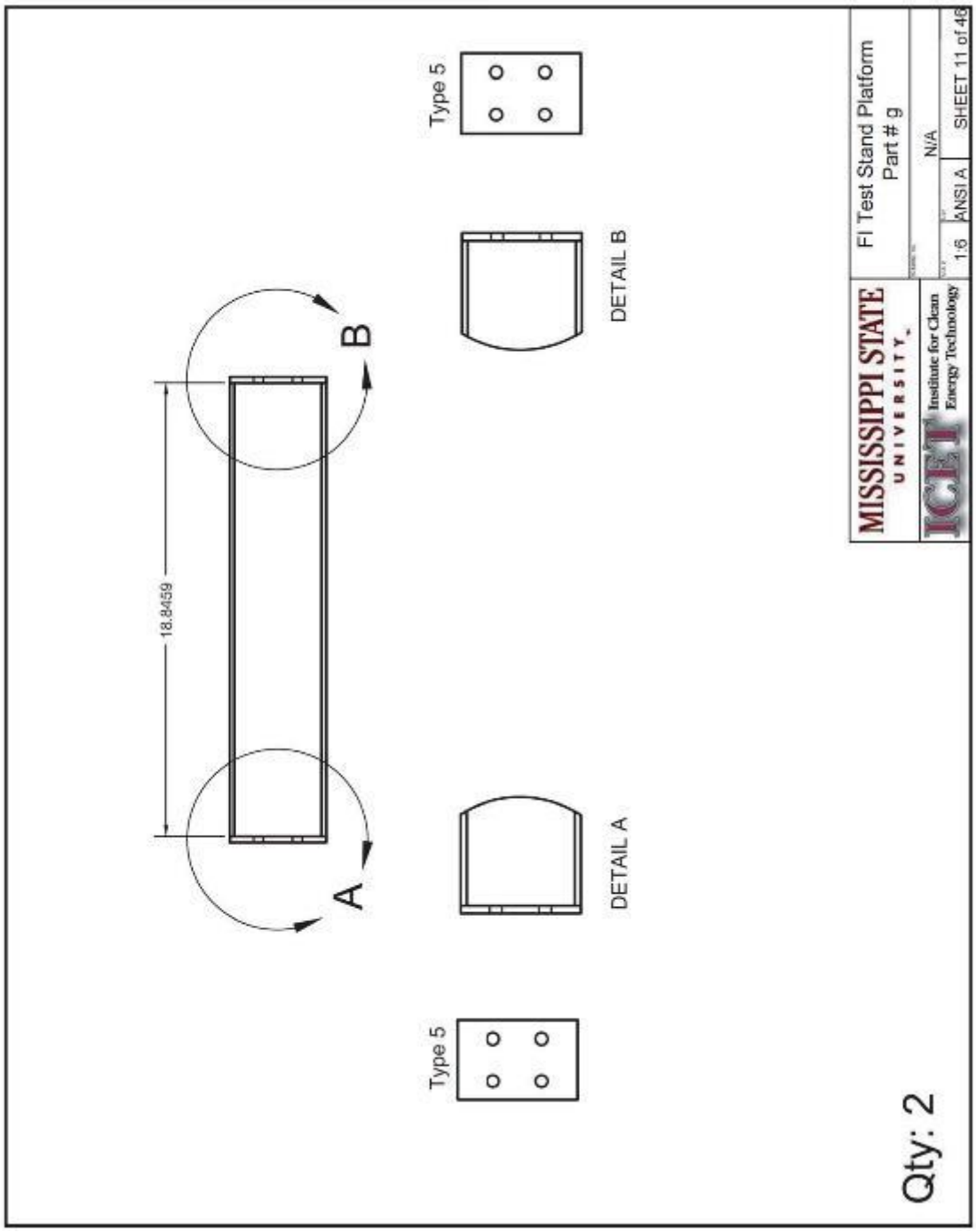

Figure 83 FI test stand platform part # g

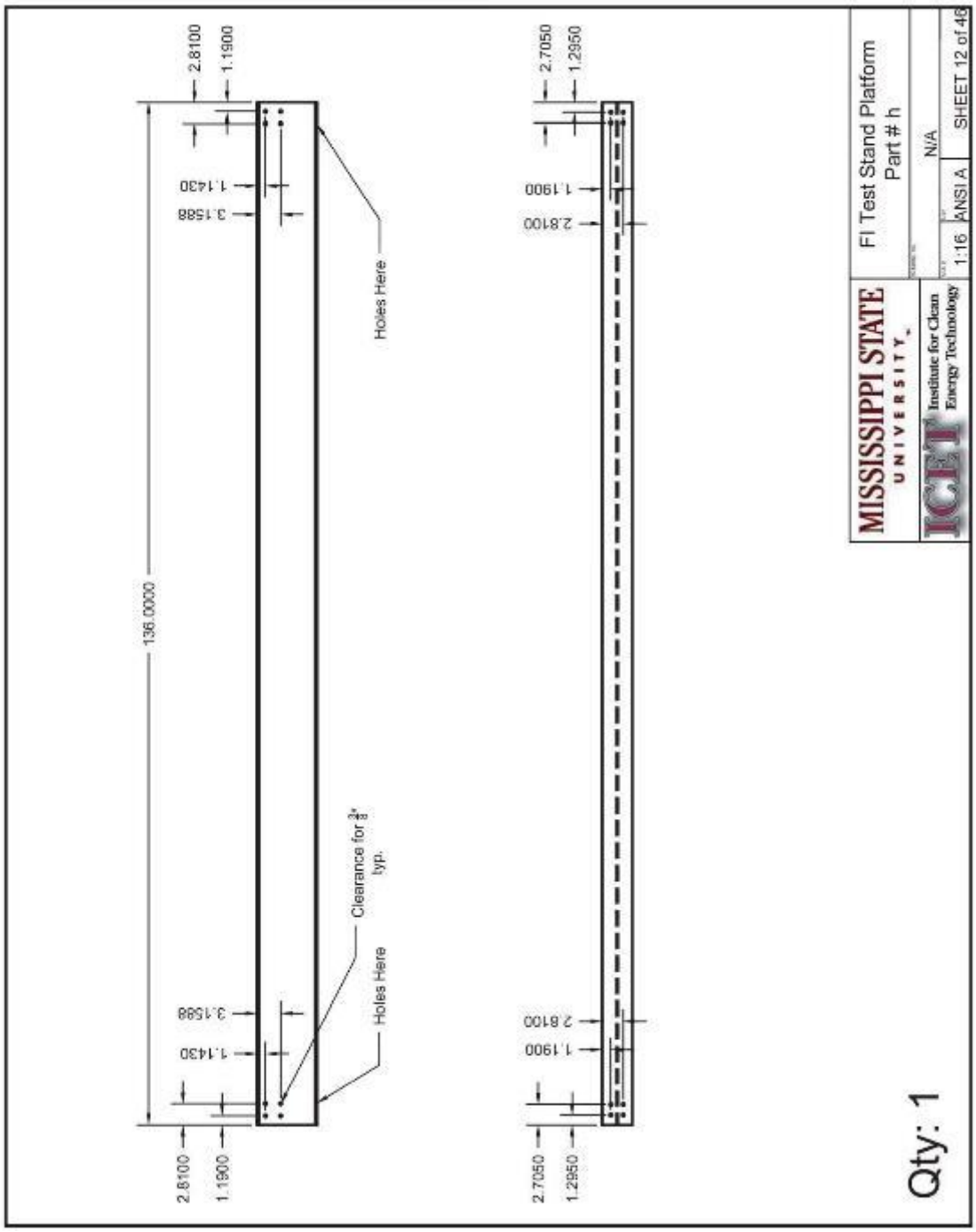

Figure 84 FI test stand platform part # h

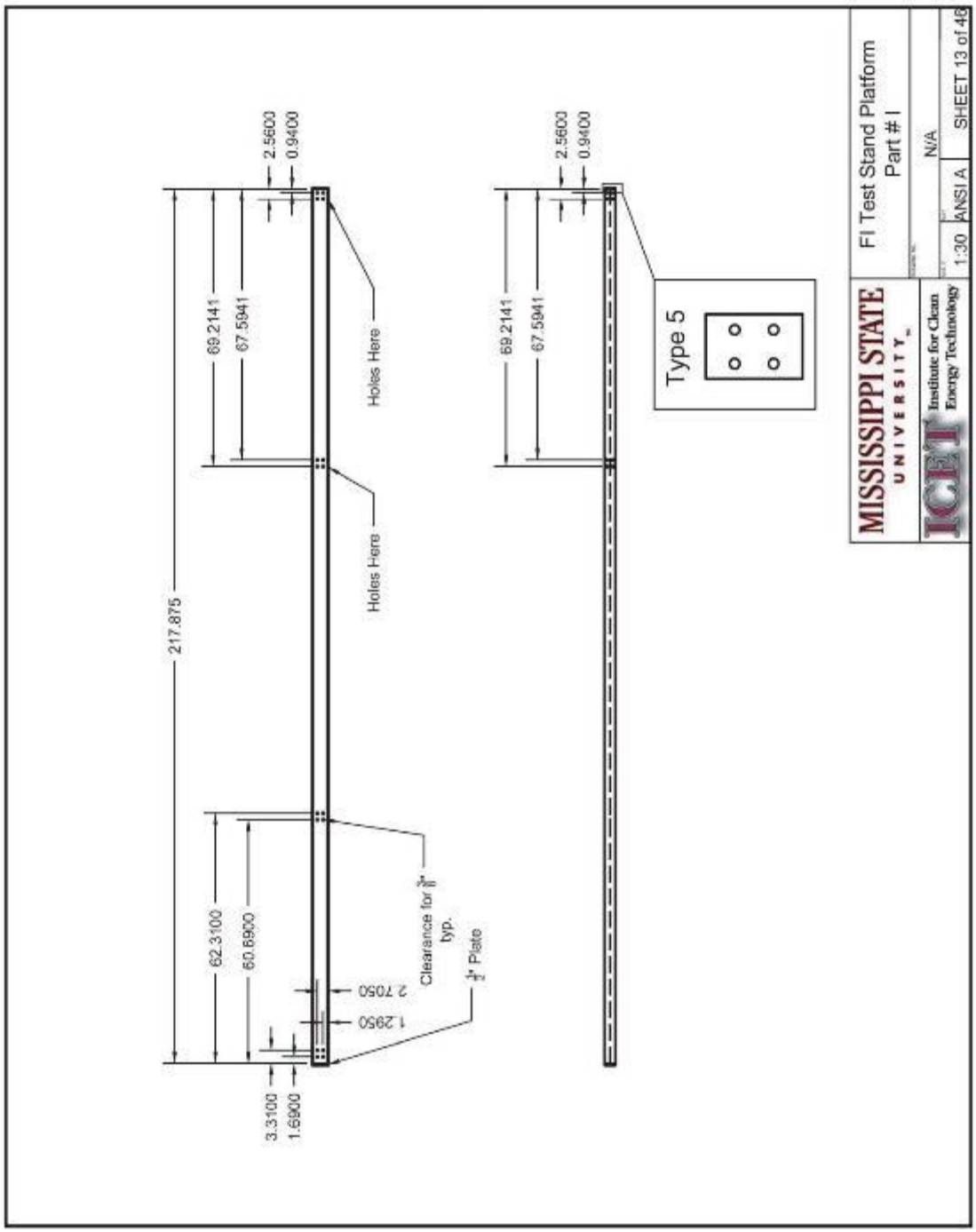

Figure 85 FI test stand platform part # 1

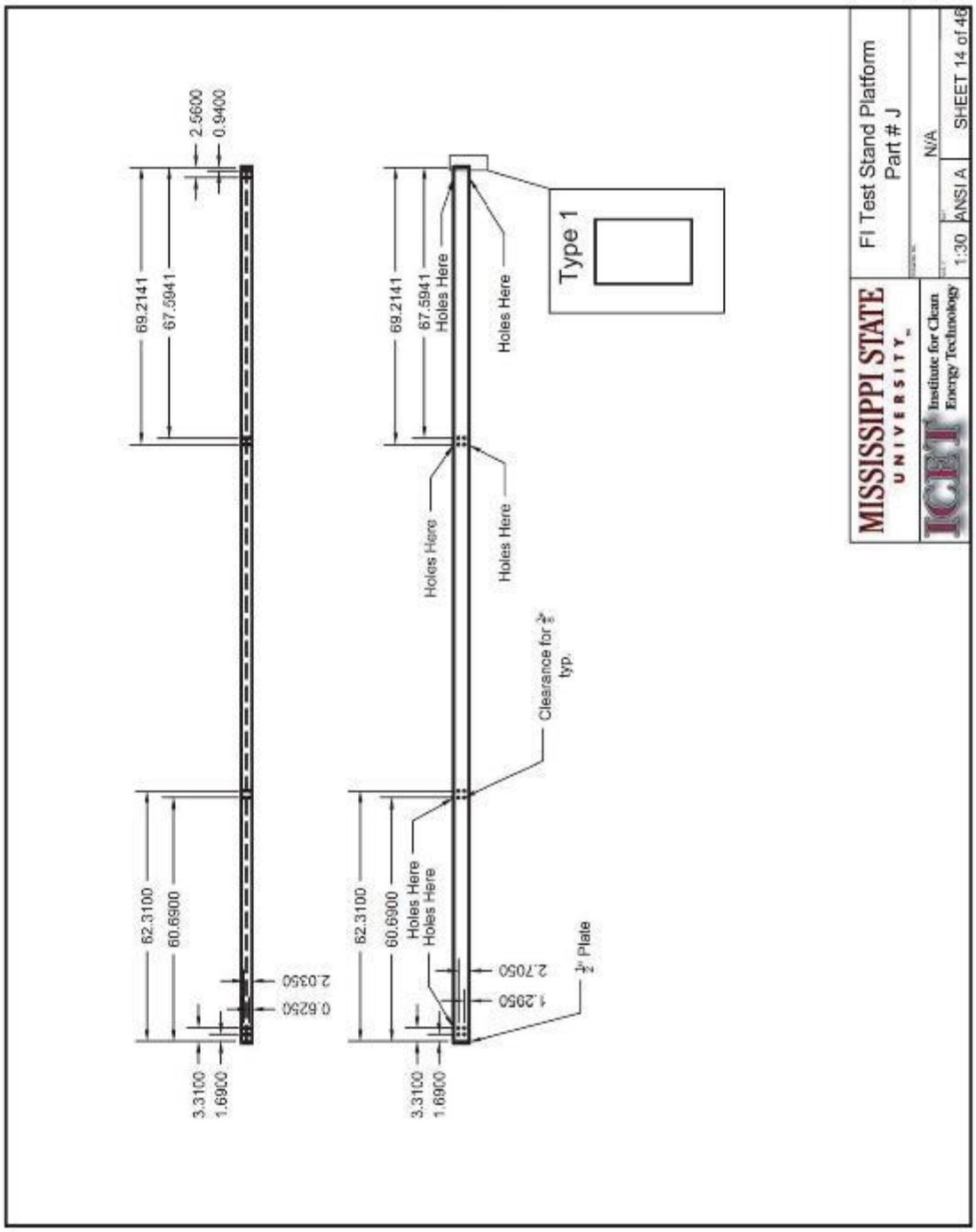

Figure 86 FI test stand platform part # J

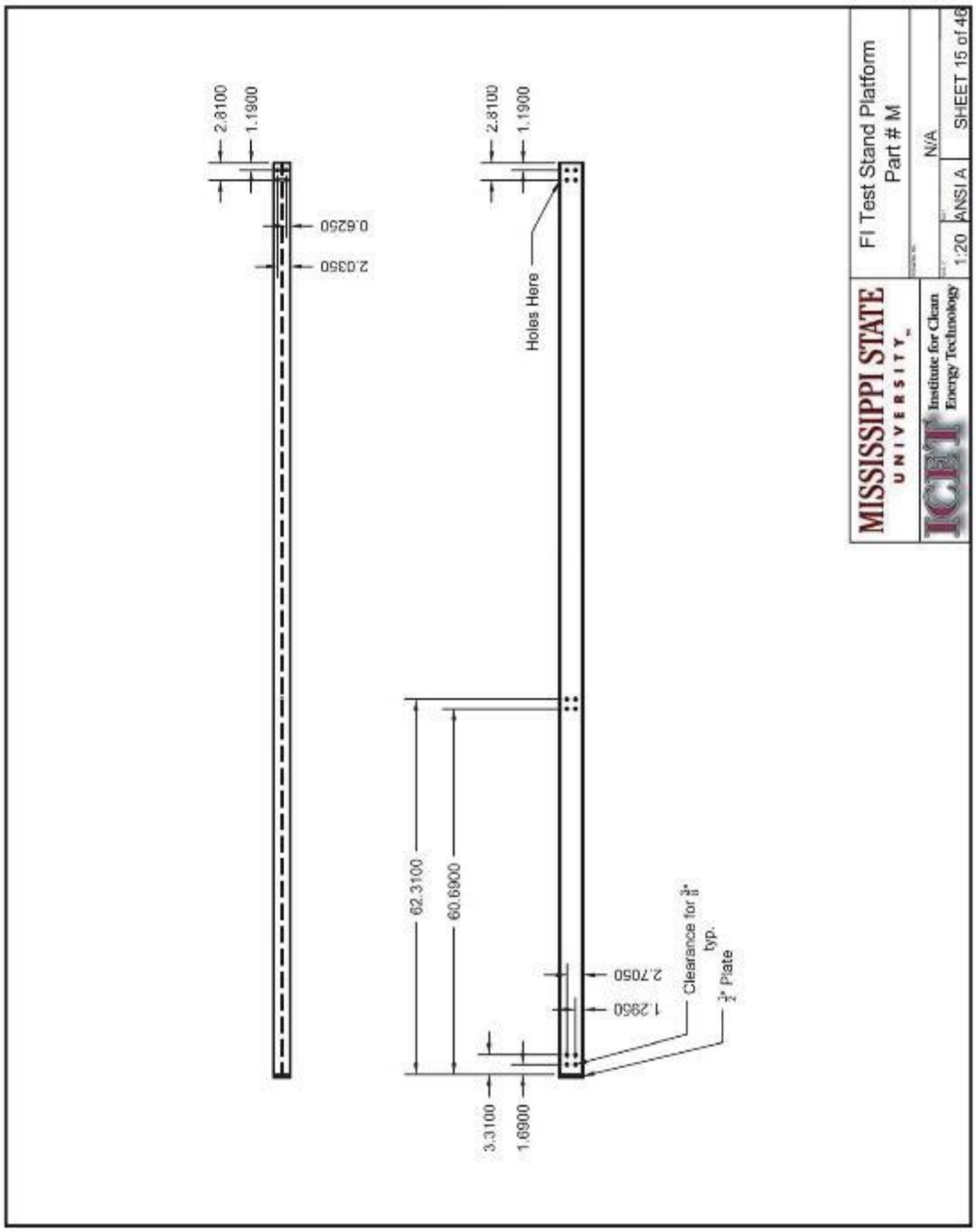

Figure 87 FI test stand platform part # M

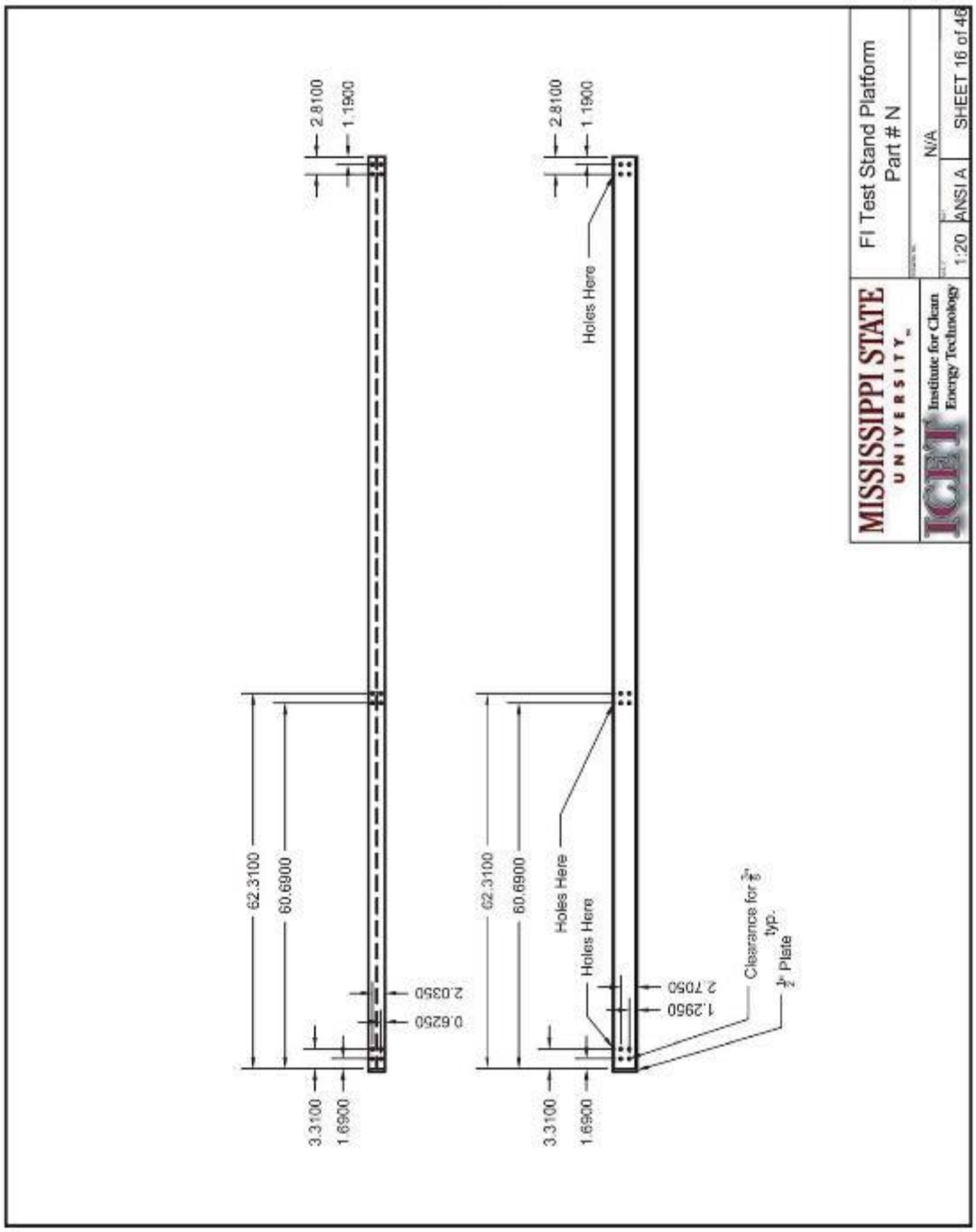

Figure 88 FI test stand platform part # N

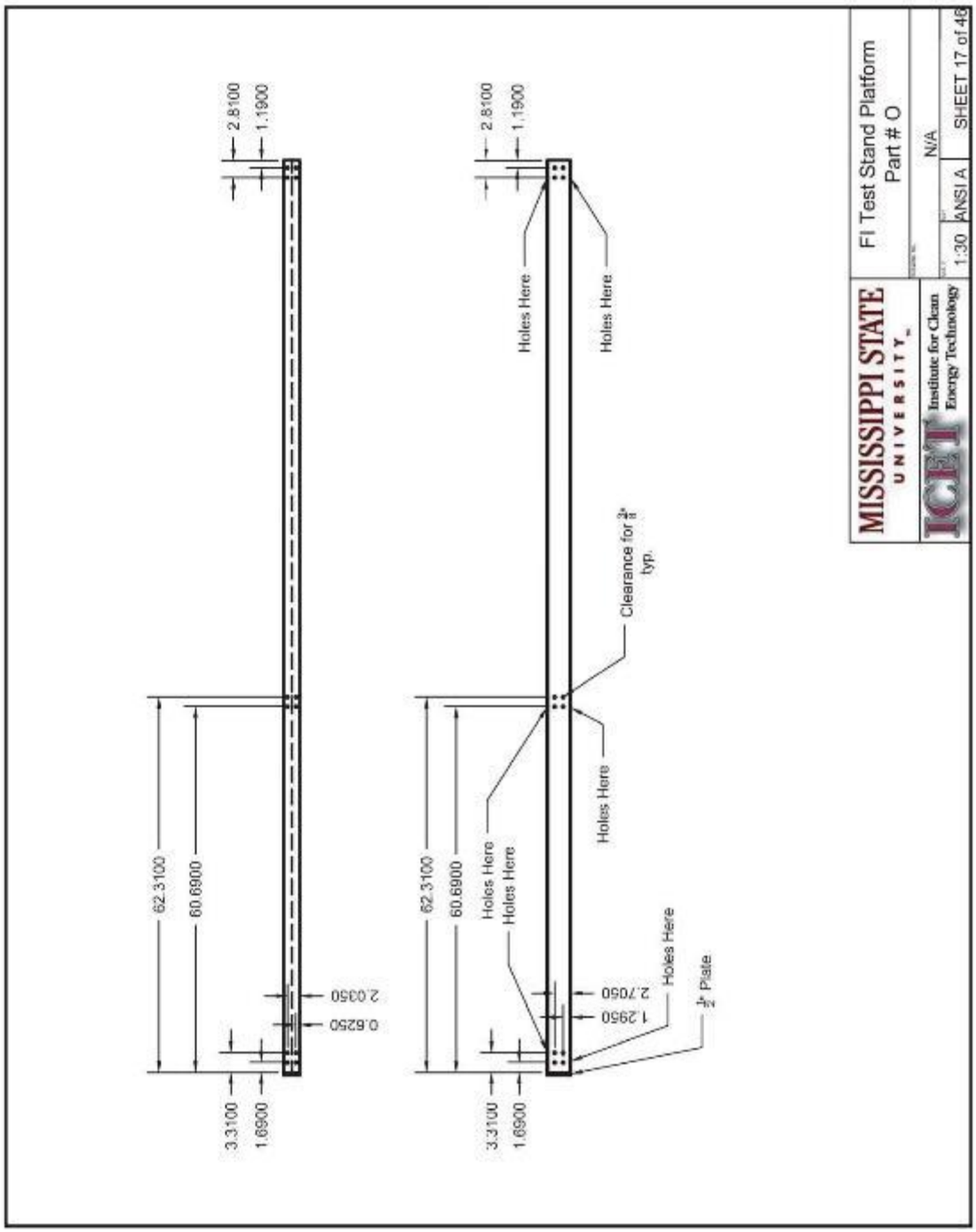

Figure 89 FI test stand platform part # O

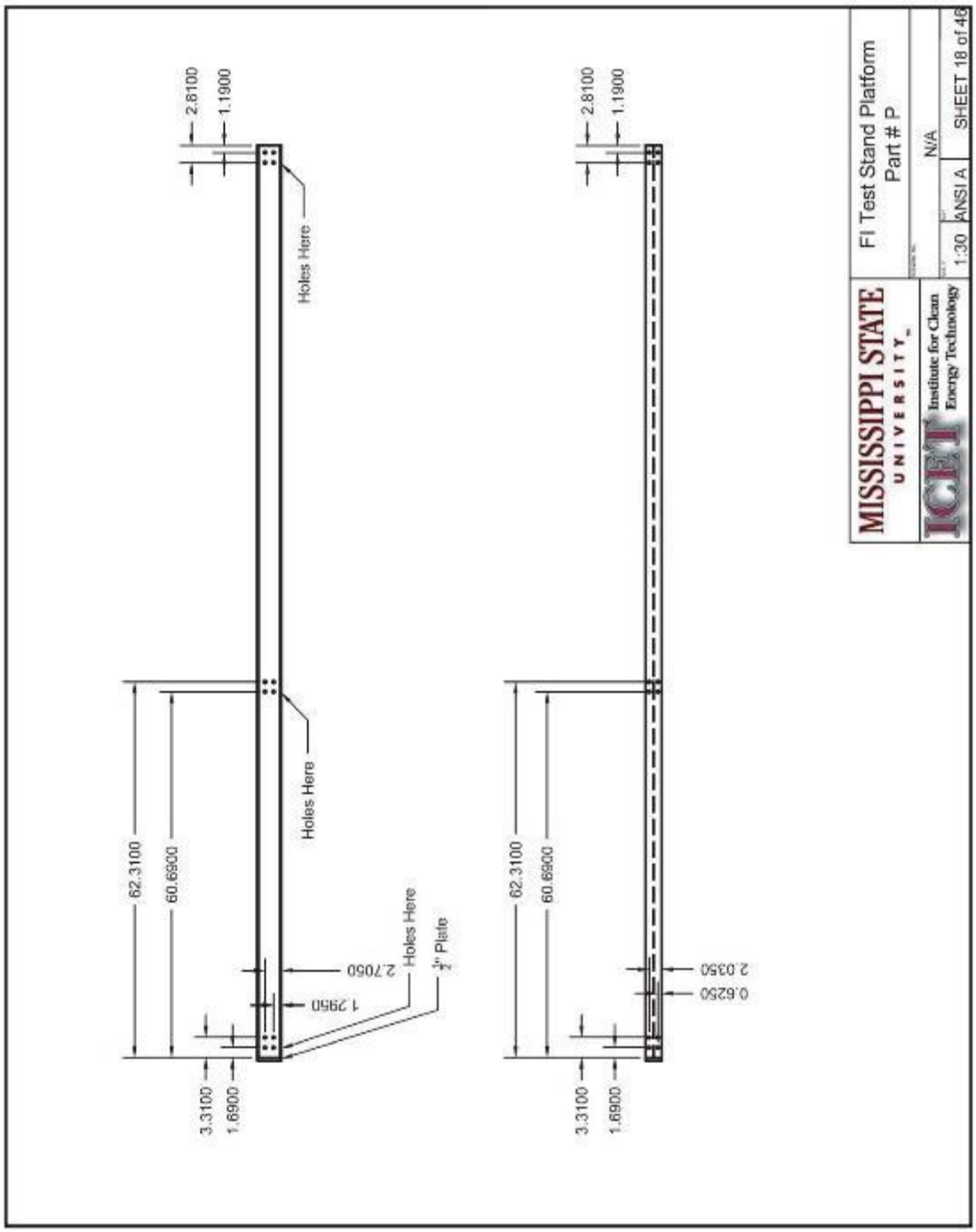

Figure 90 FI test stand platform part # P

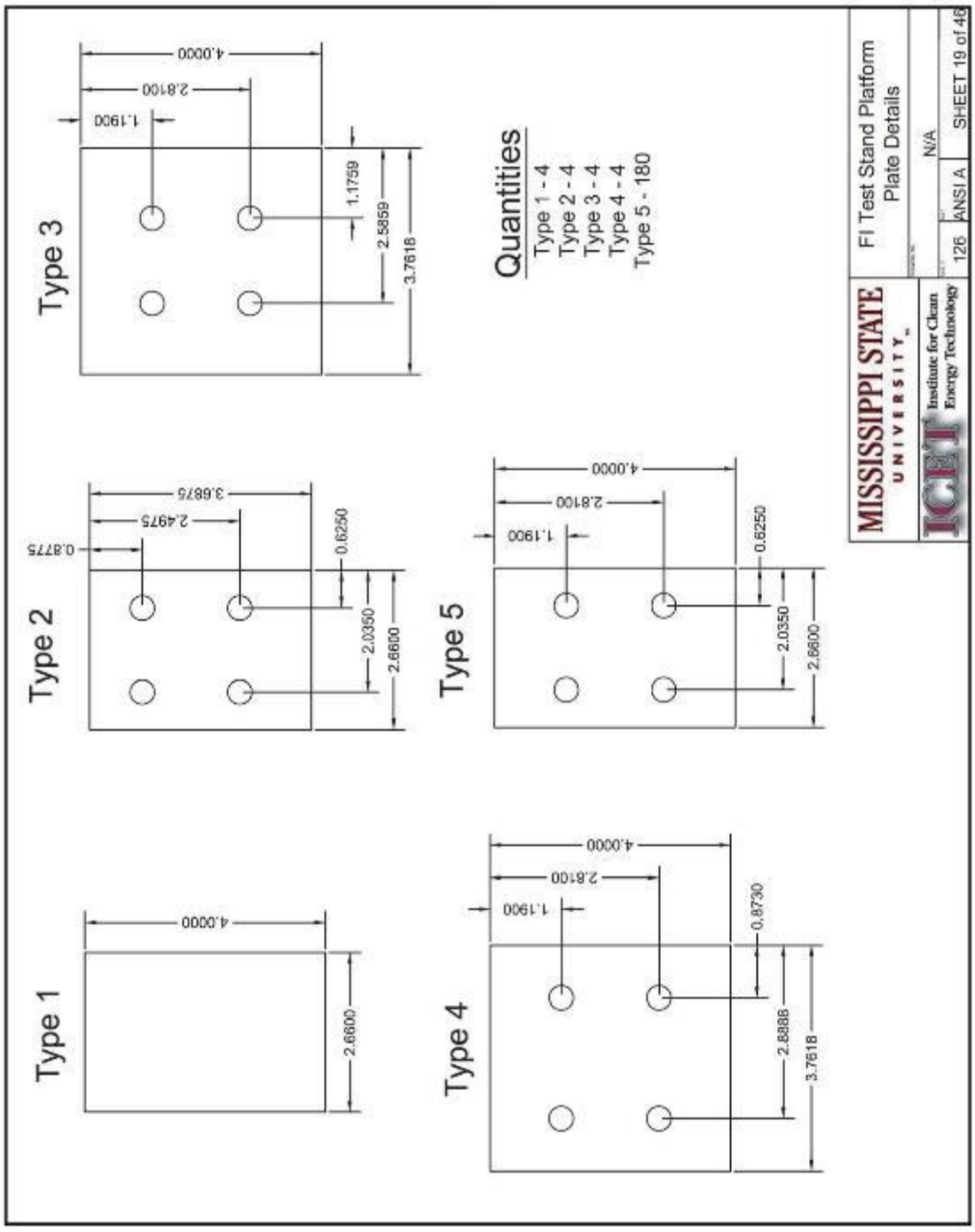

Figure 91 FI test stand platform plate details

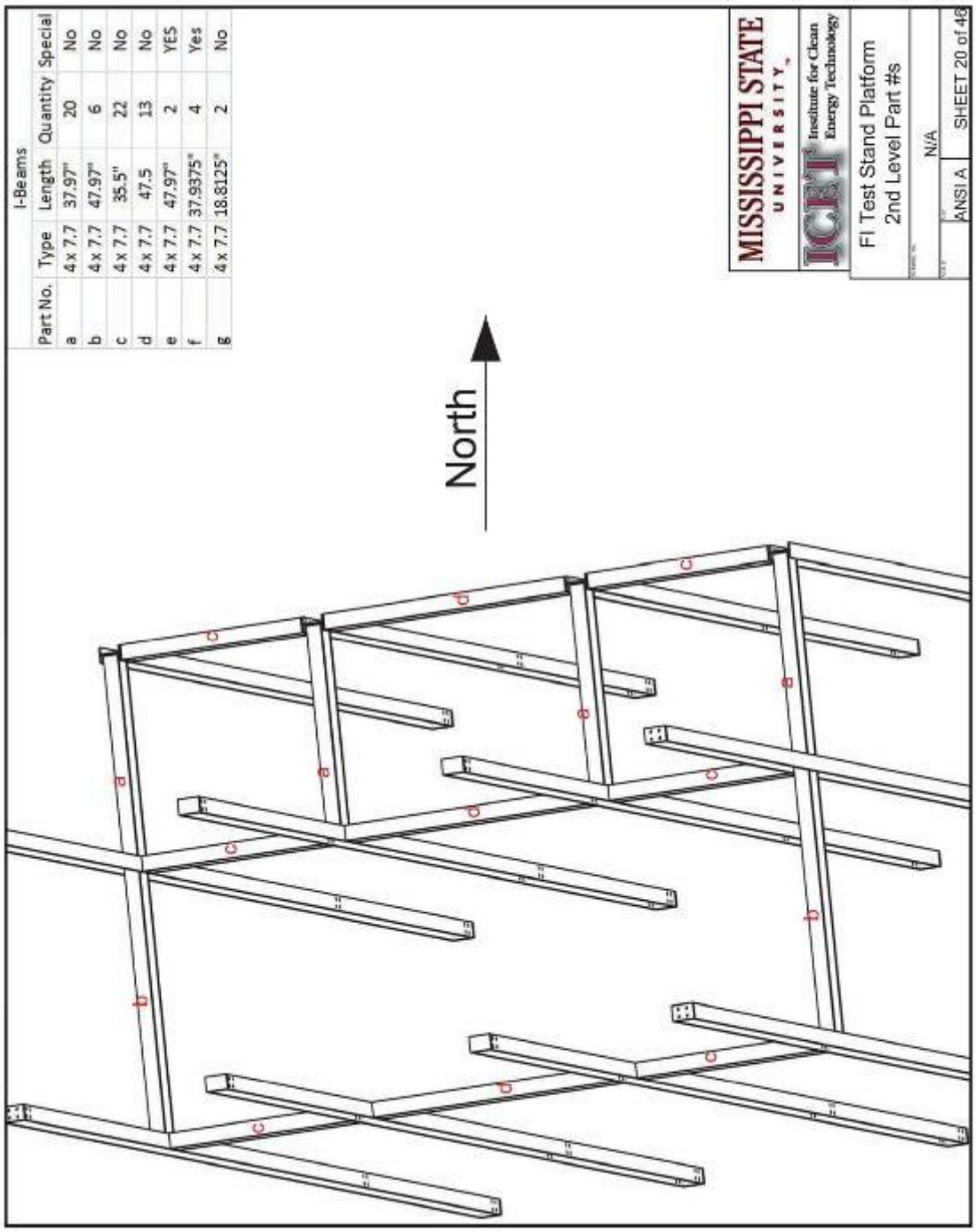

Figure 92 FI test stand platform 2nd level part #s

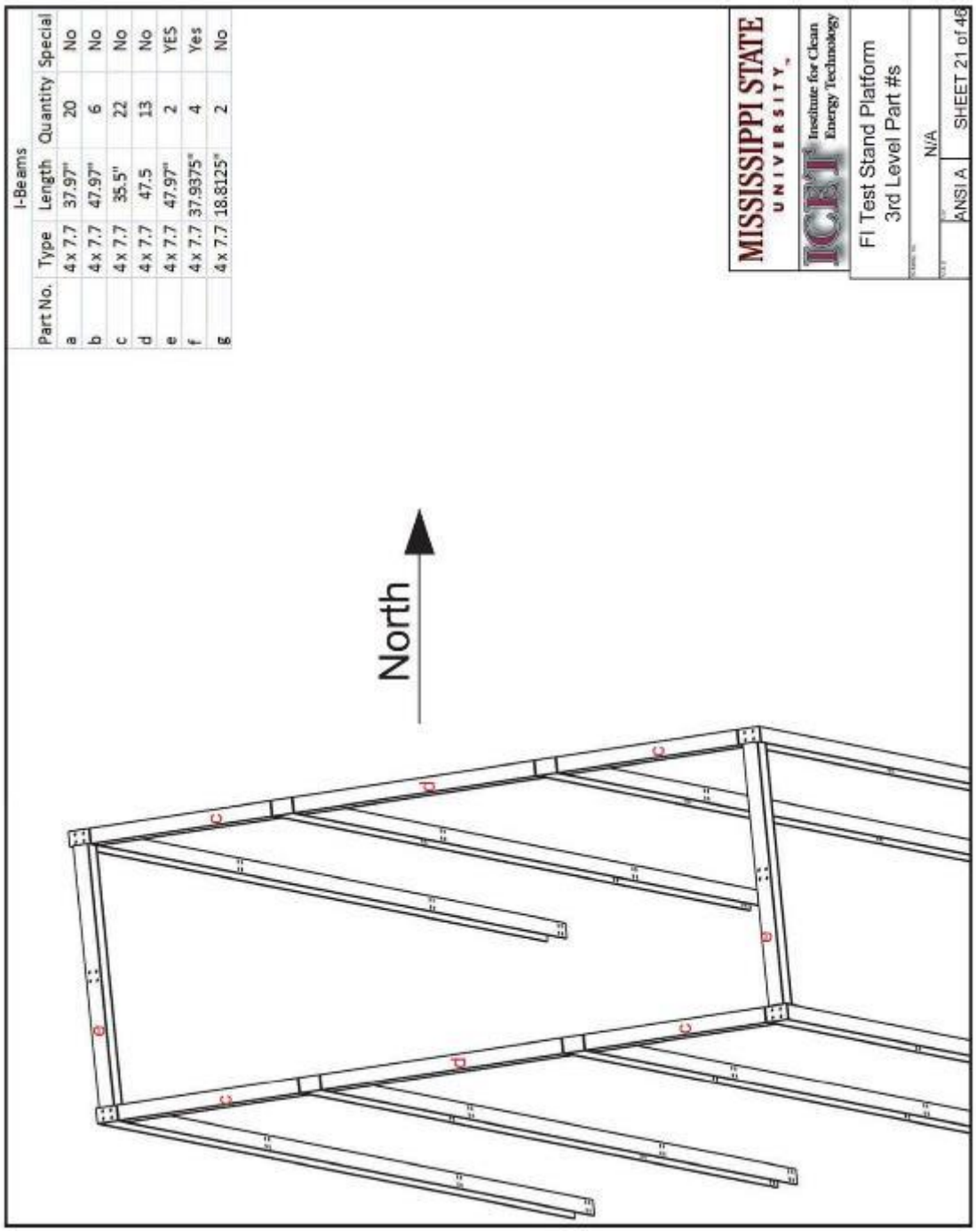

Figure 93 FI test stand platform 3rd level part #s

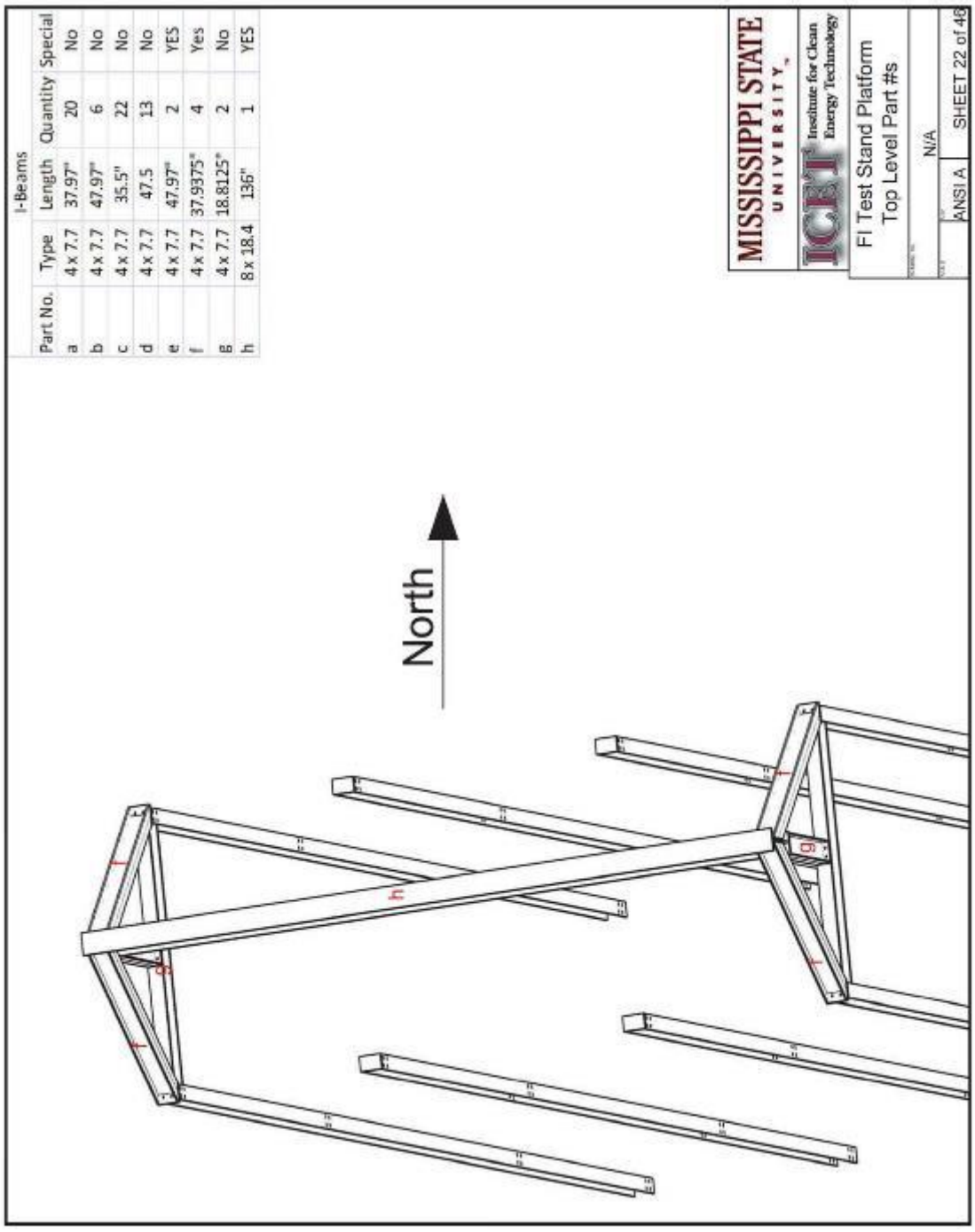

Figure 94 FI test stand platform Top level part #s

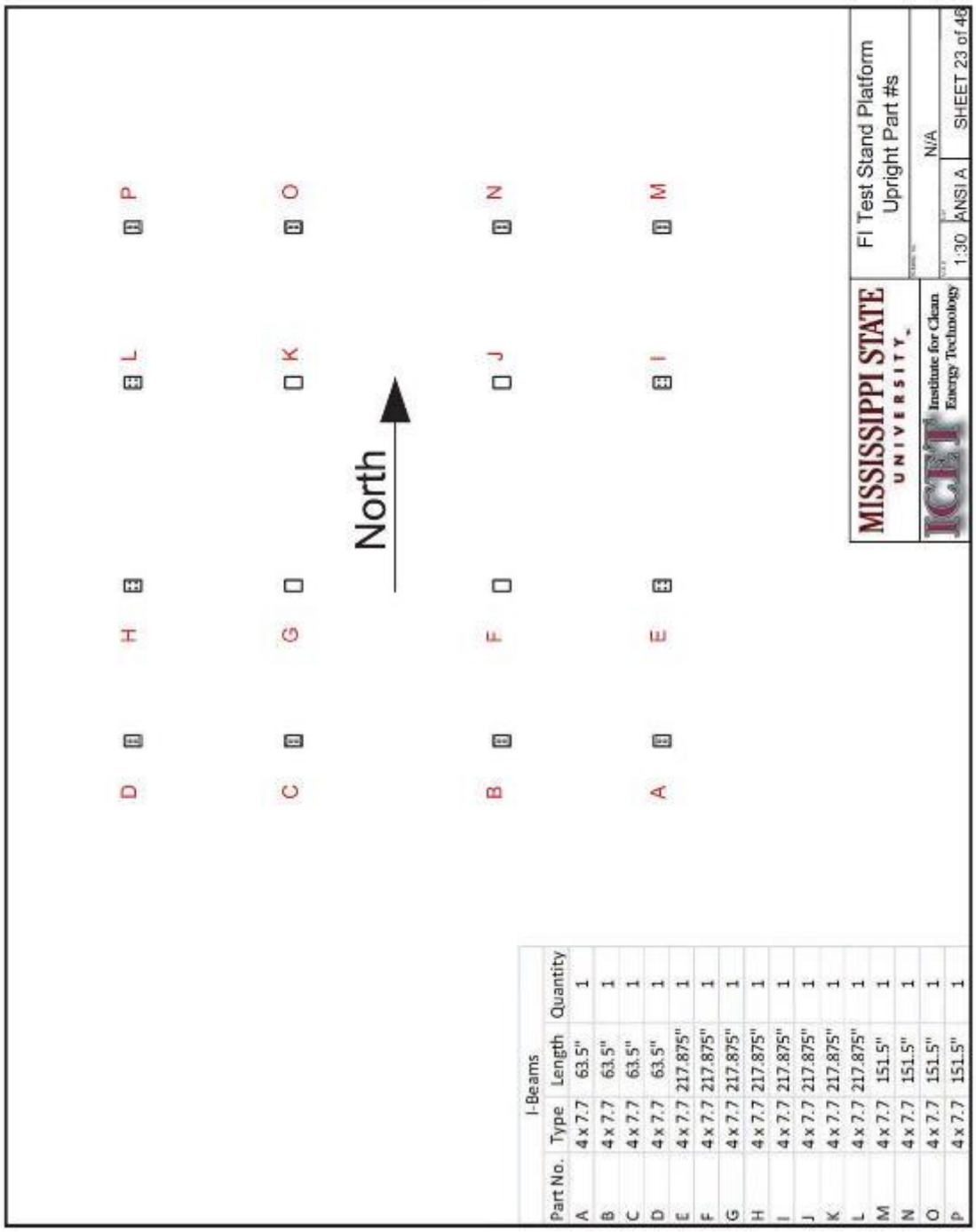

Figure 95 FI test stand platform upright part #s

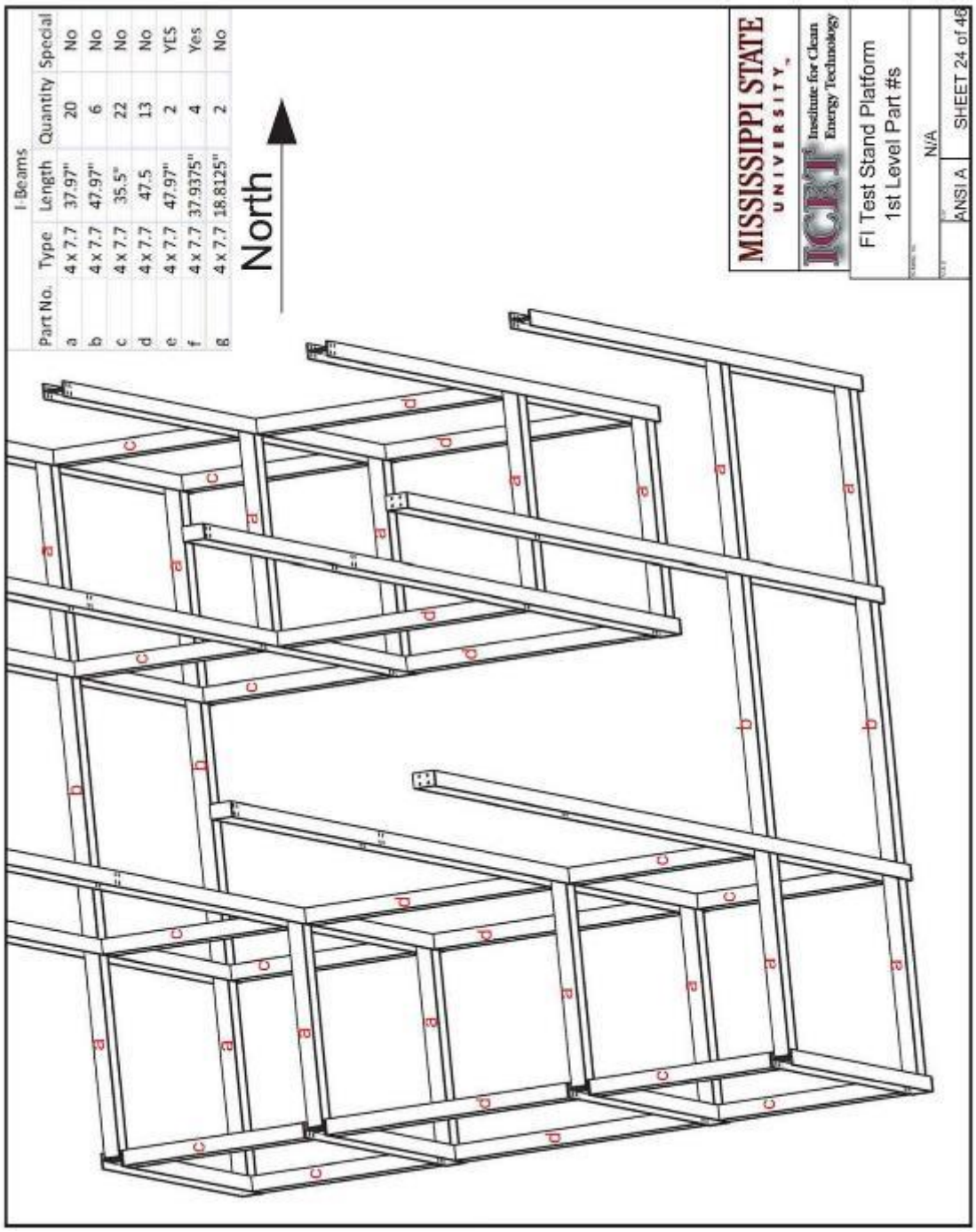

Figure 96 FI test stand platform 1st level part #s

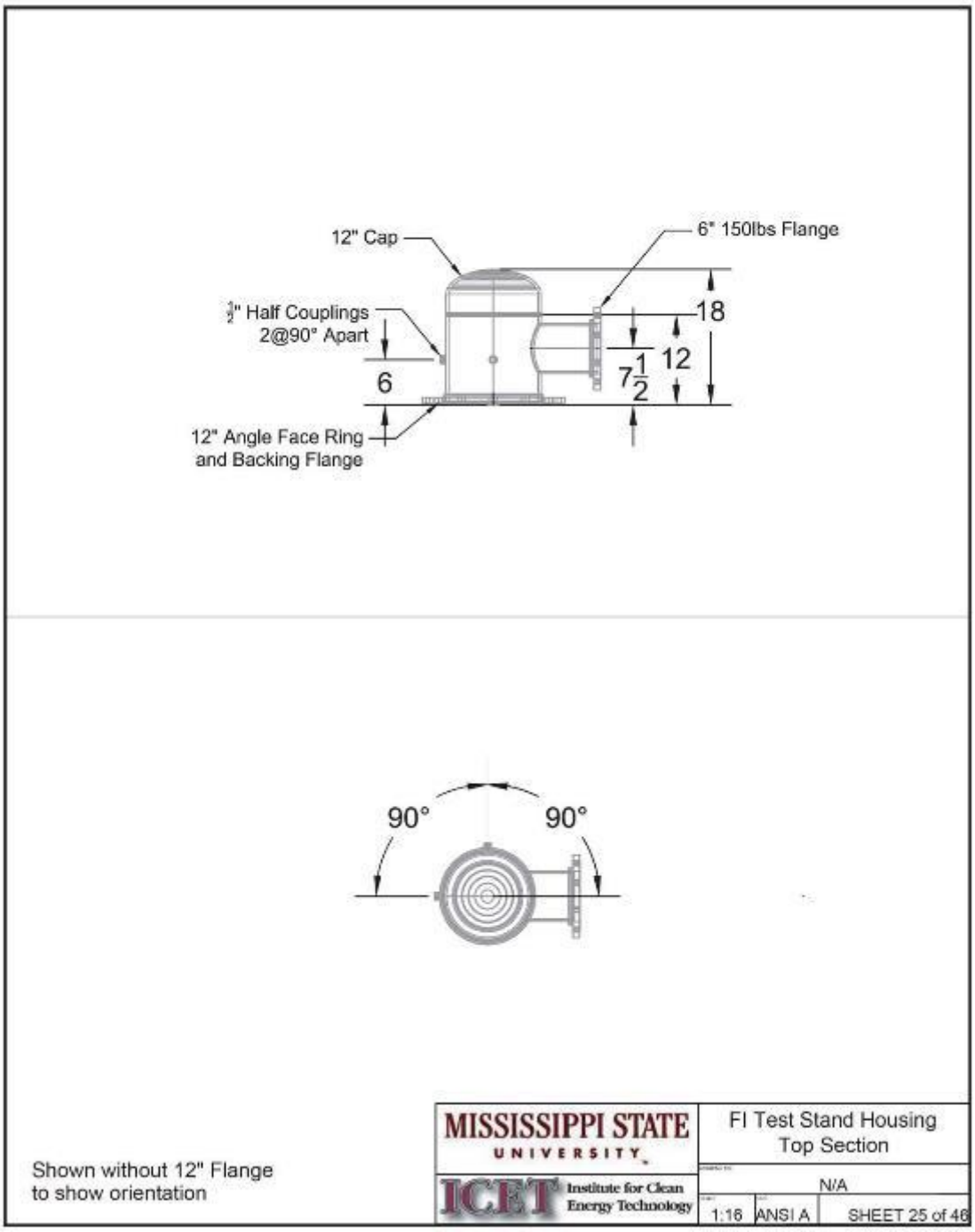

Figure 97 FI test stand housing top section

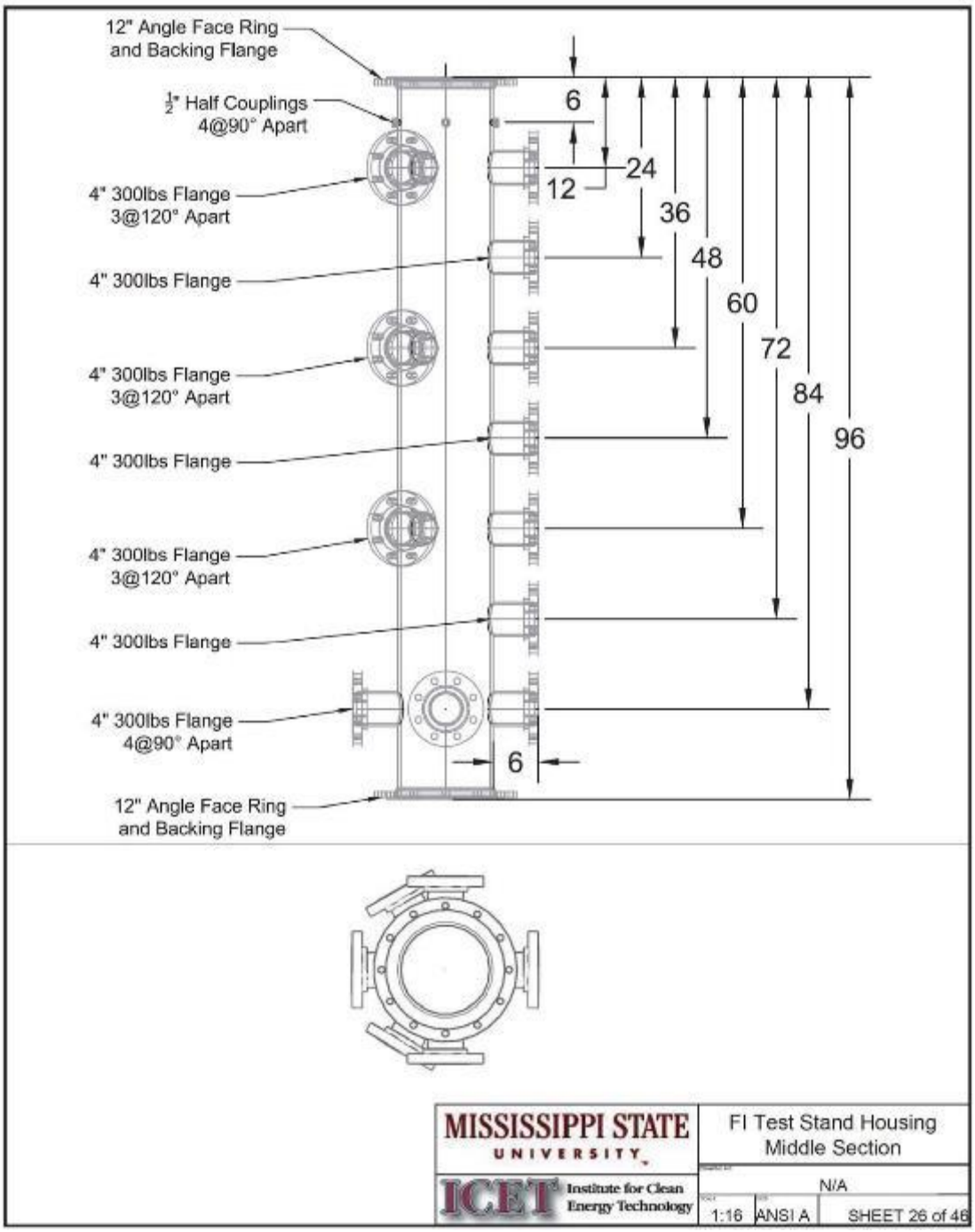

Figure 98 FI test stand housing middle section

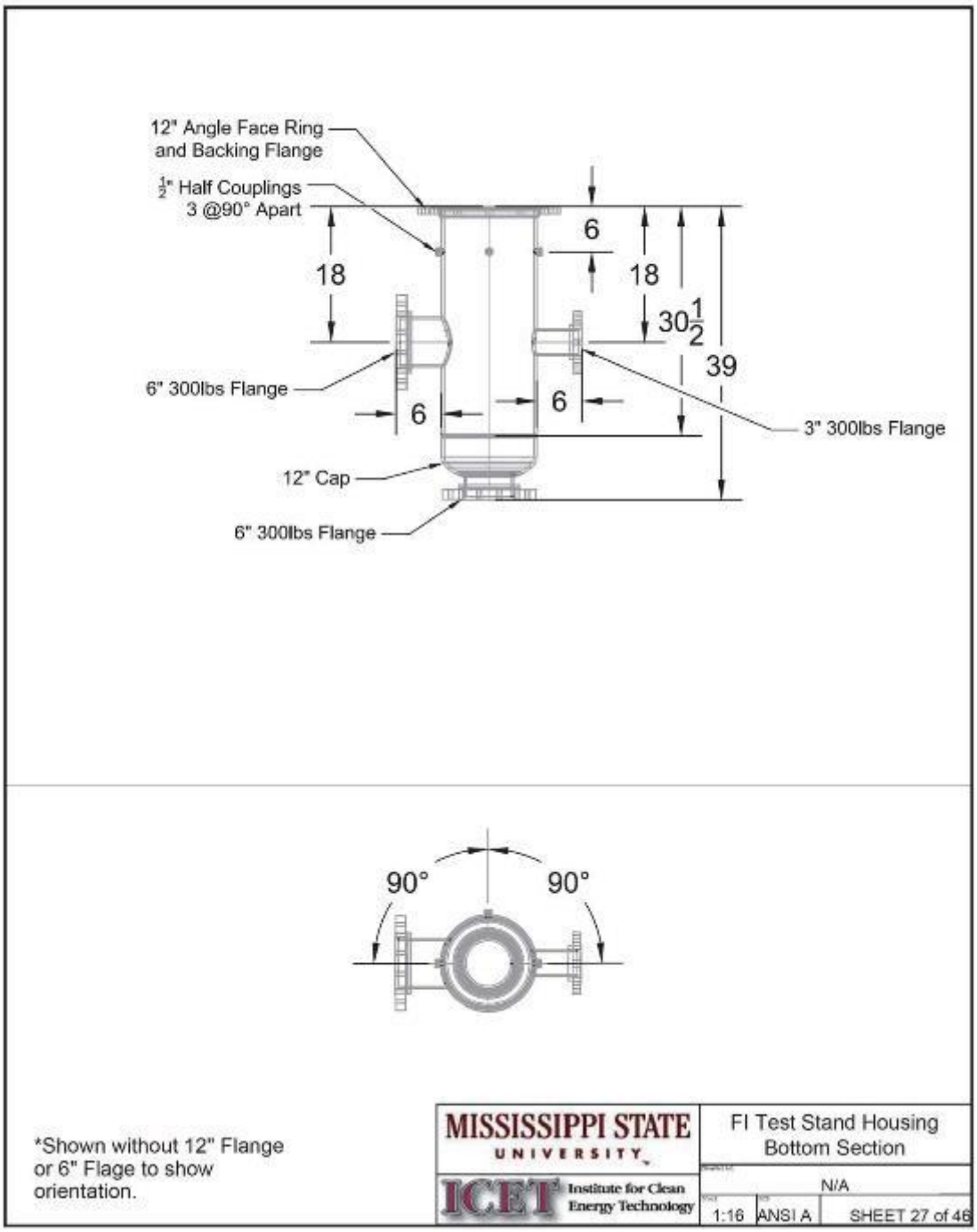

Figure 99 FI test stand housing bottom section

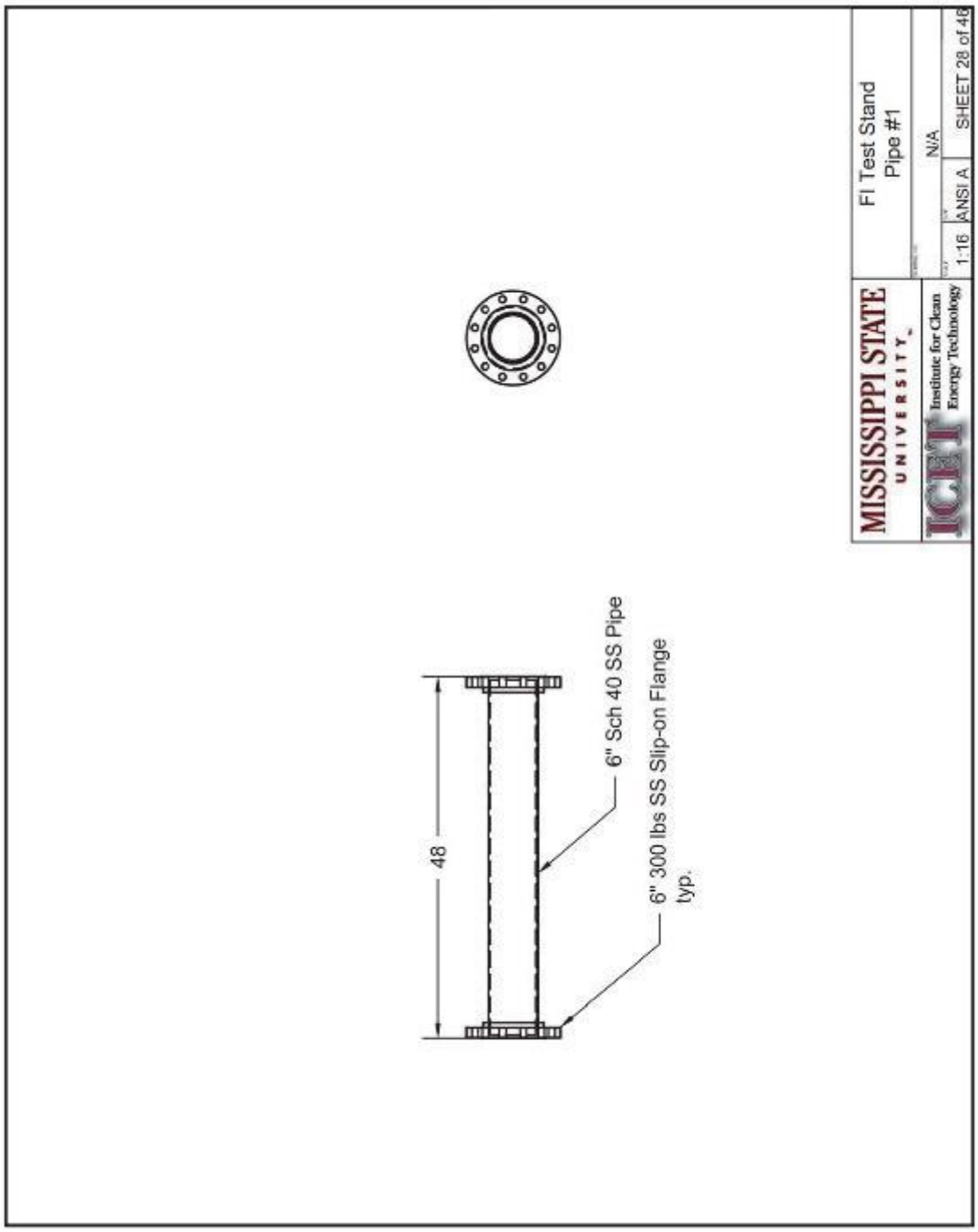

Figure 100 FI test stand pipe #1

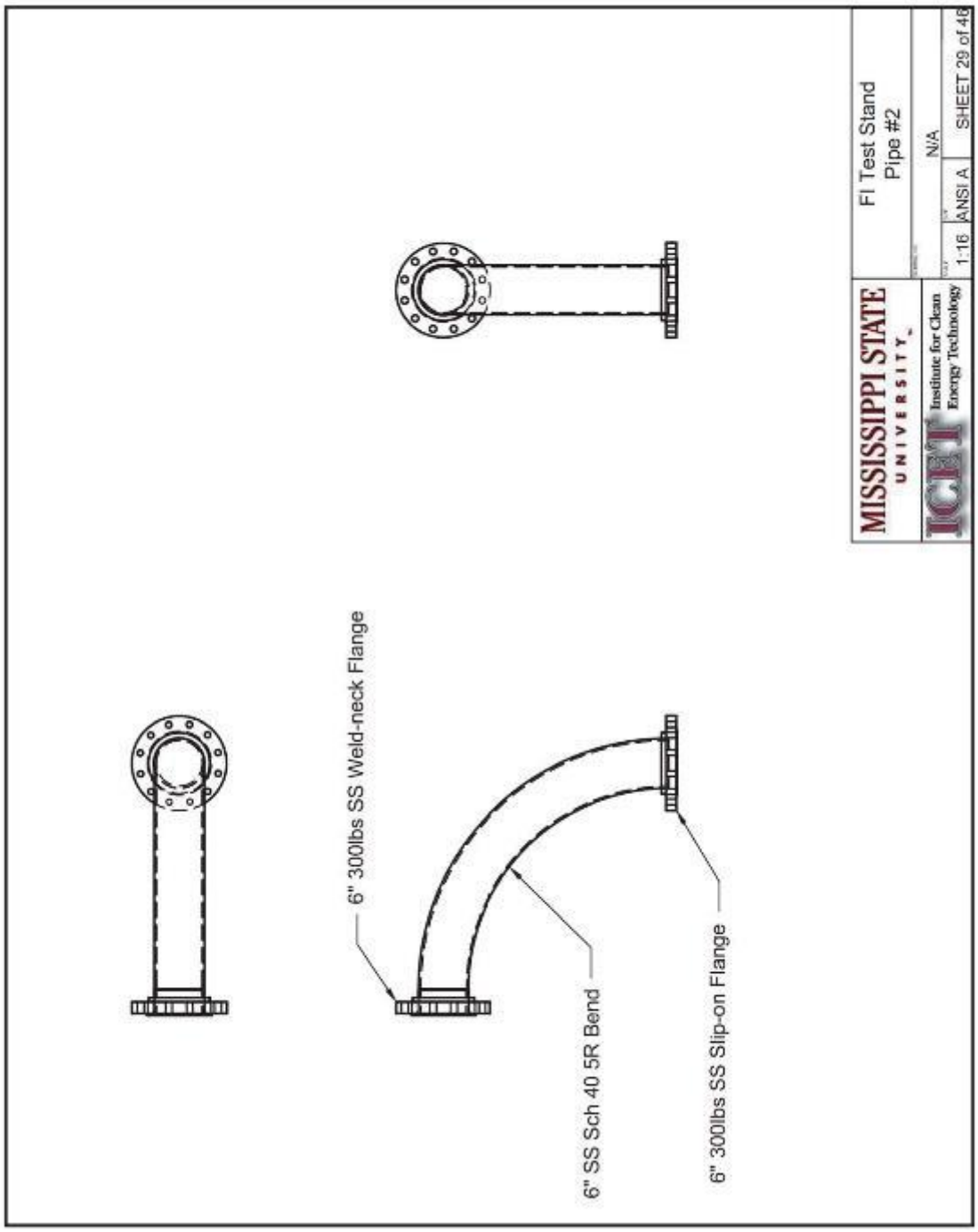

Figure 101 FI test stand pipe #2

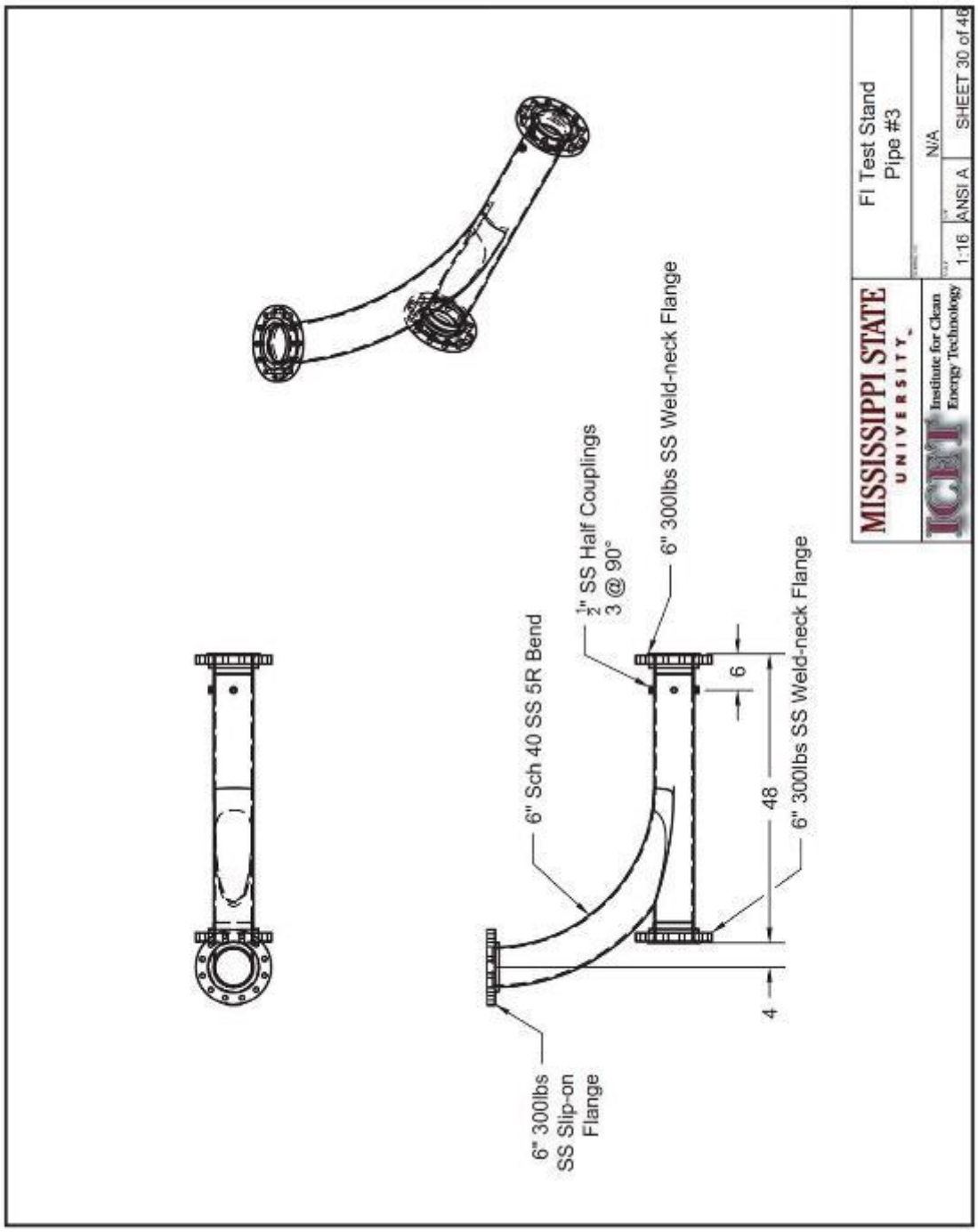

Figure 102 FI test stand pipe #3

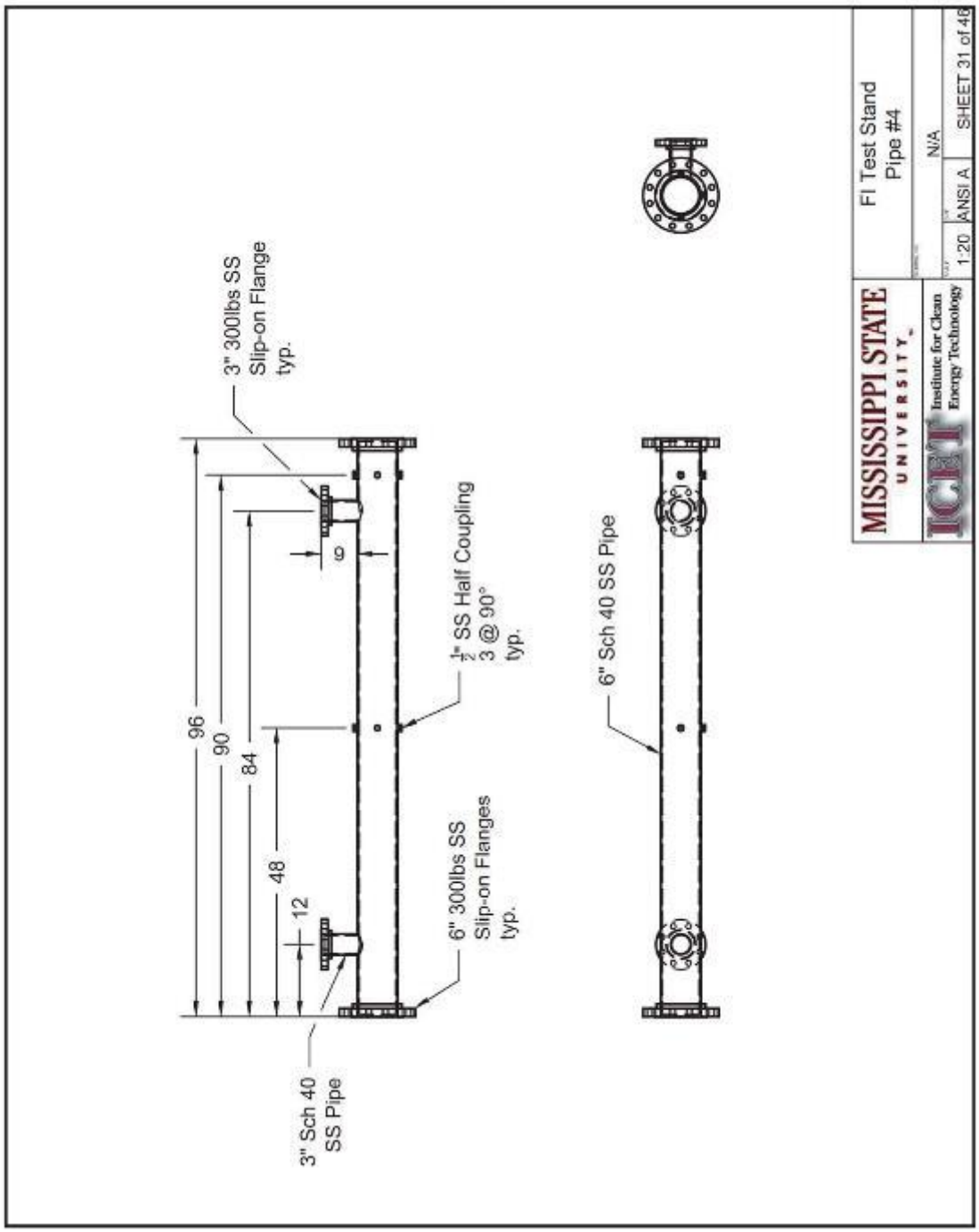

Figure 103 FI test stand pipe #4

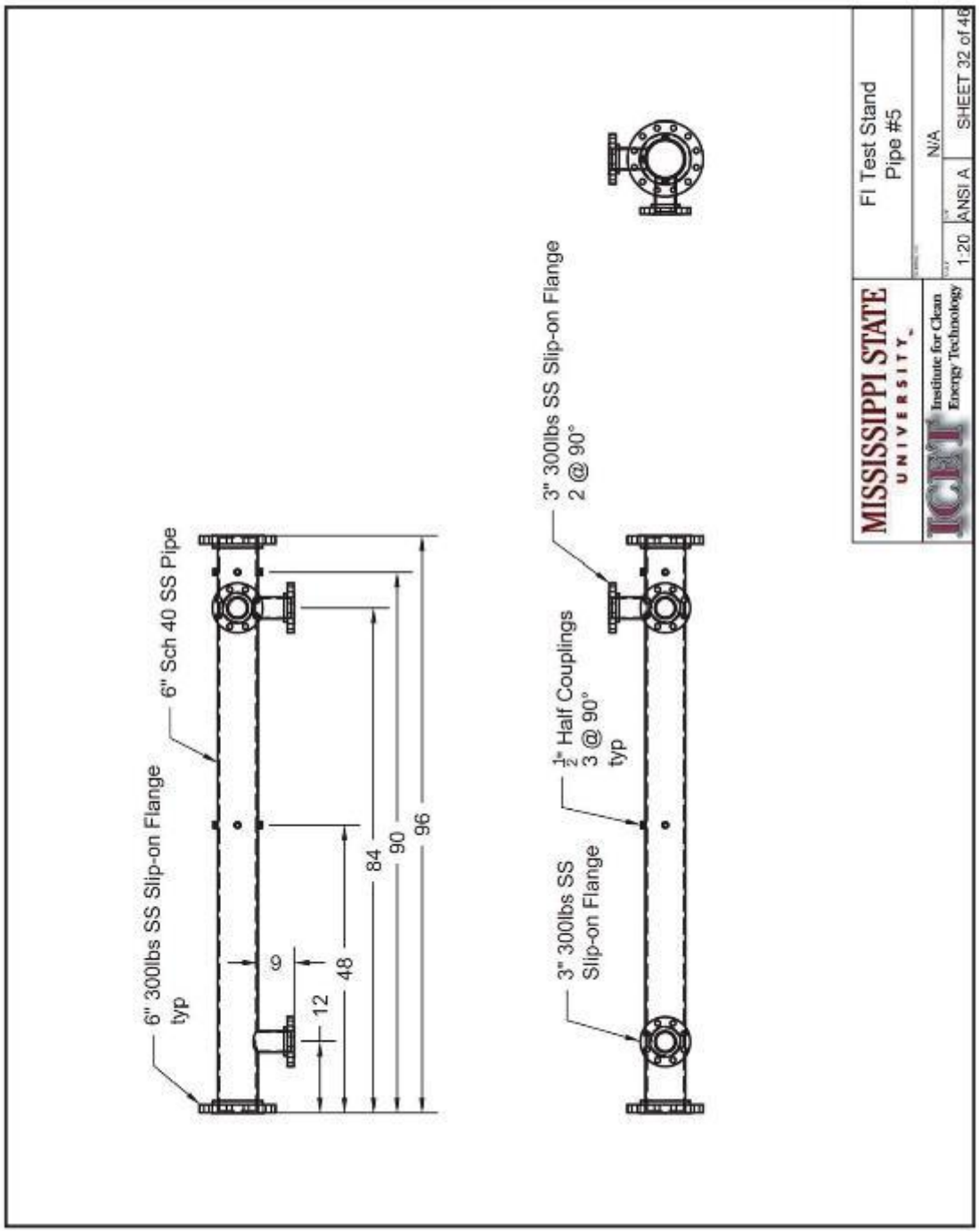

Figure 104 FI test stand pipe #5

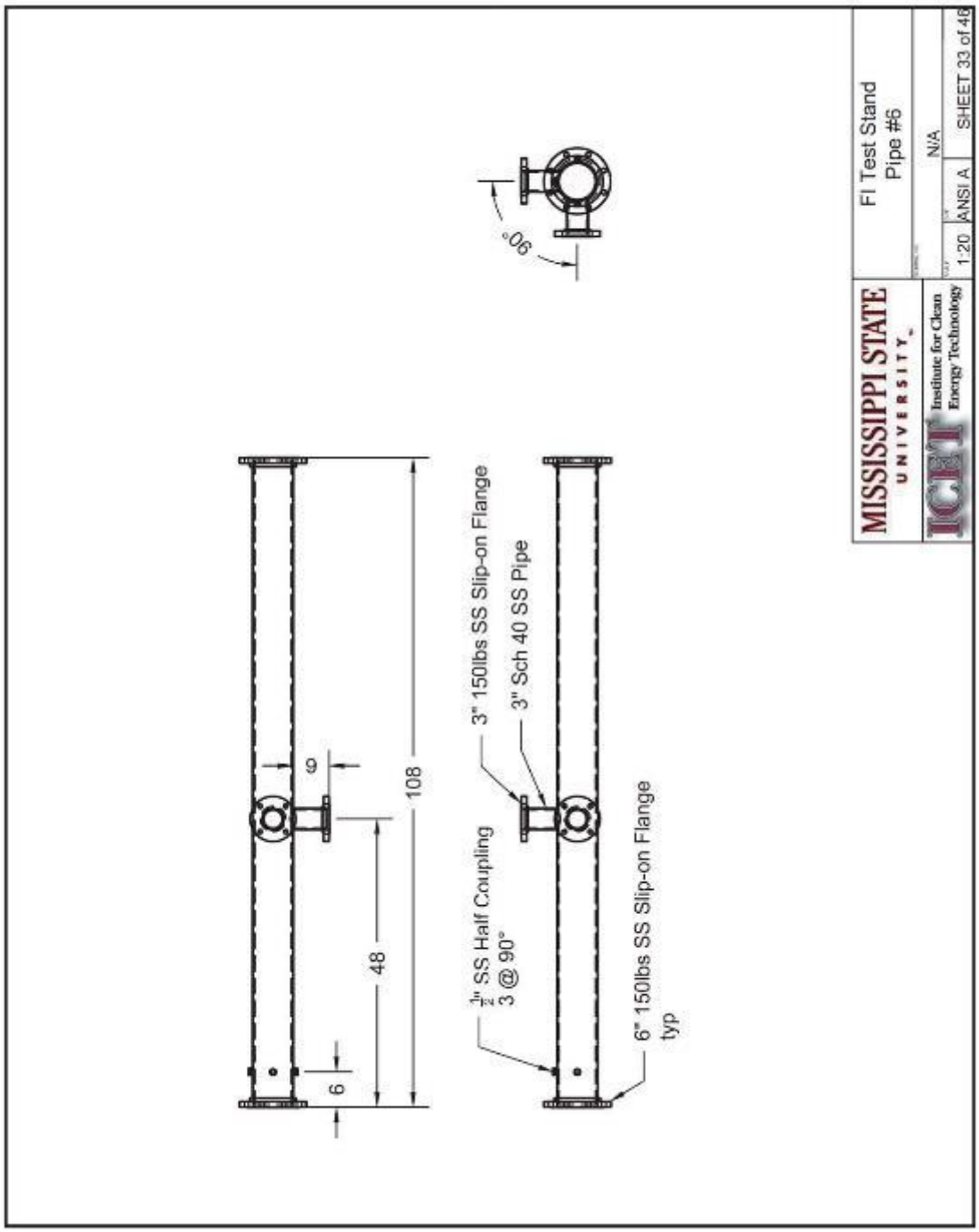

Figure 105 FI test stand pipe #6

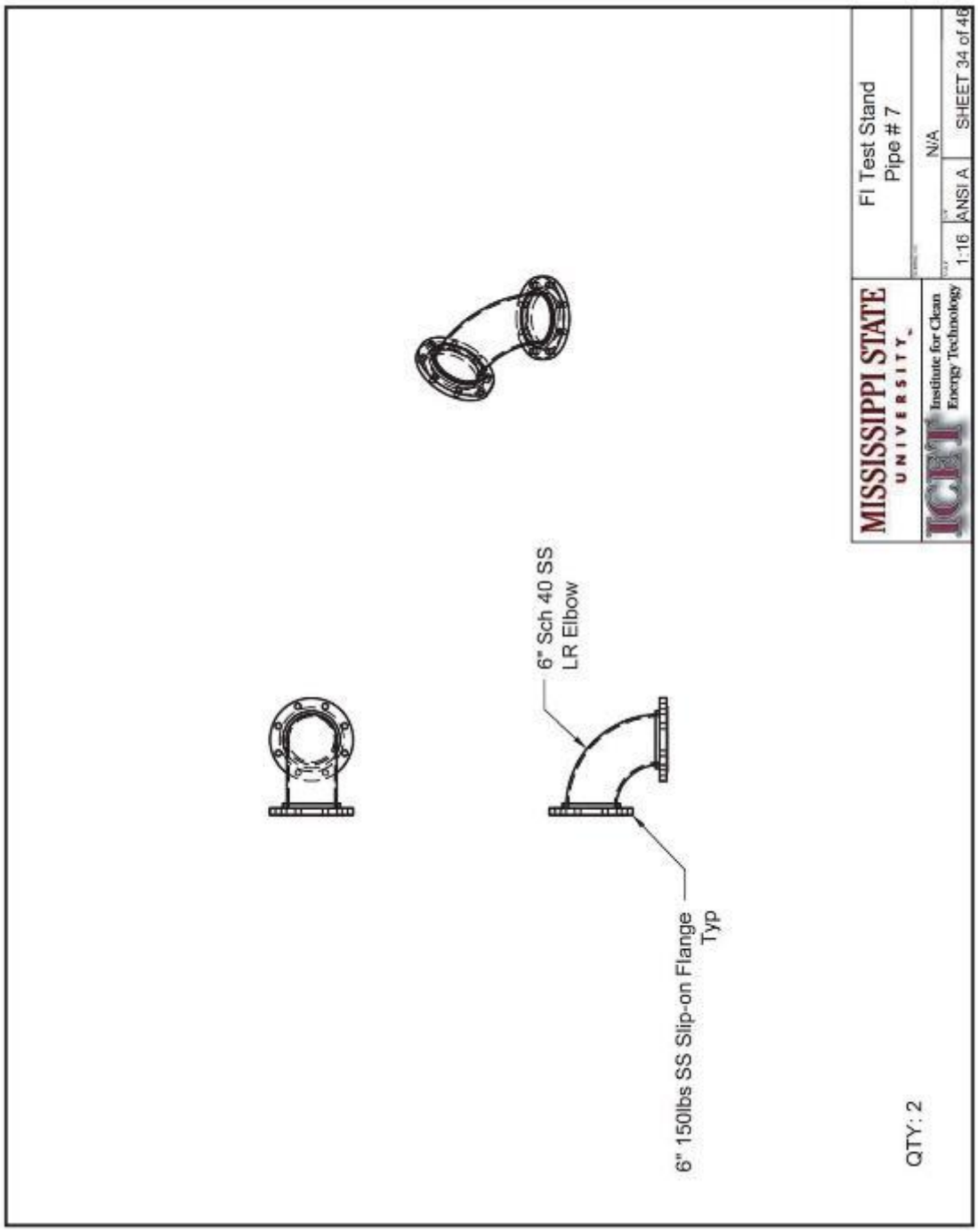

Figure 106 FI test stand pipe #7

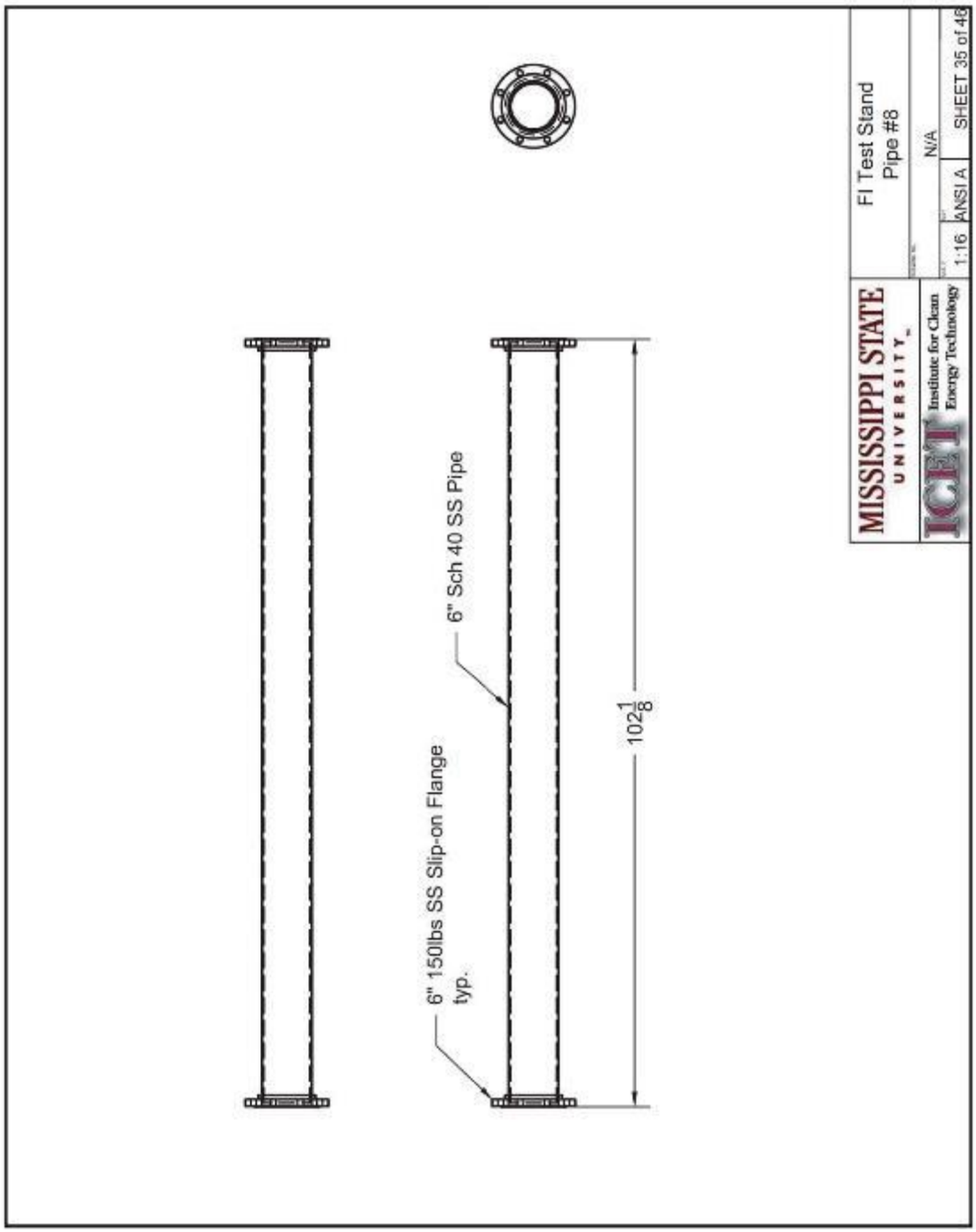

Figure 107 FI test stand pipe #8

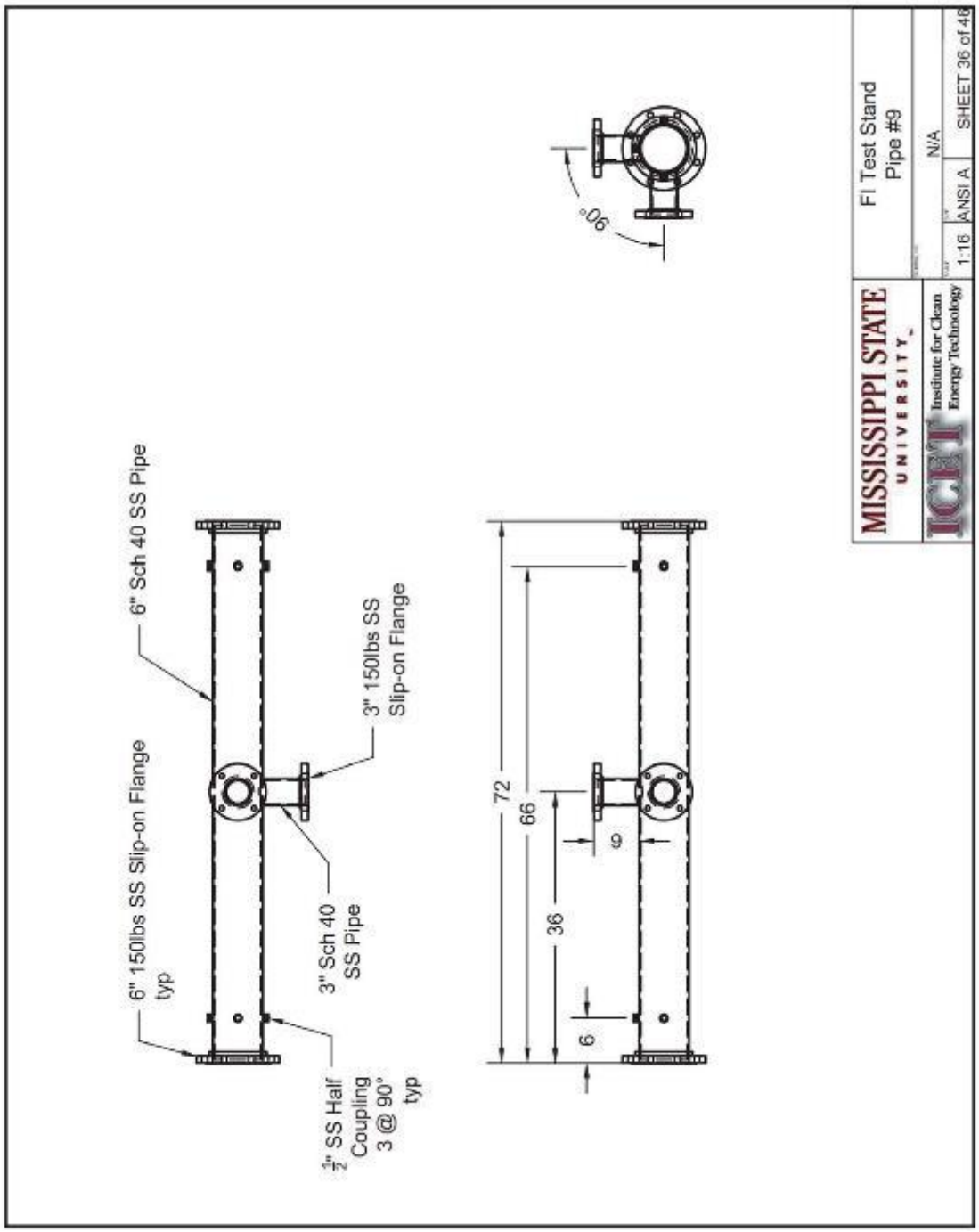

Figure 108 FI test stand pipe #9

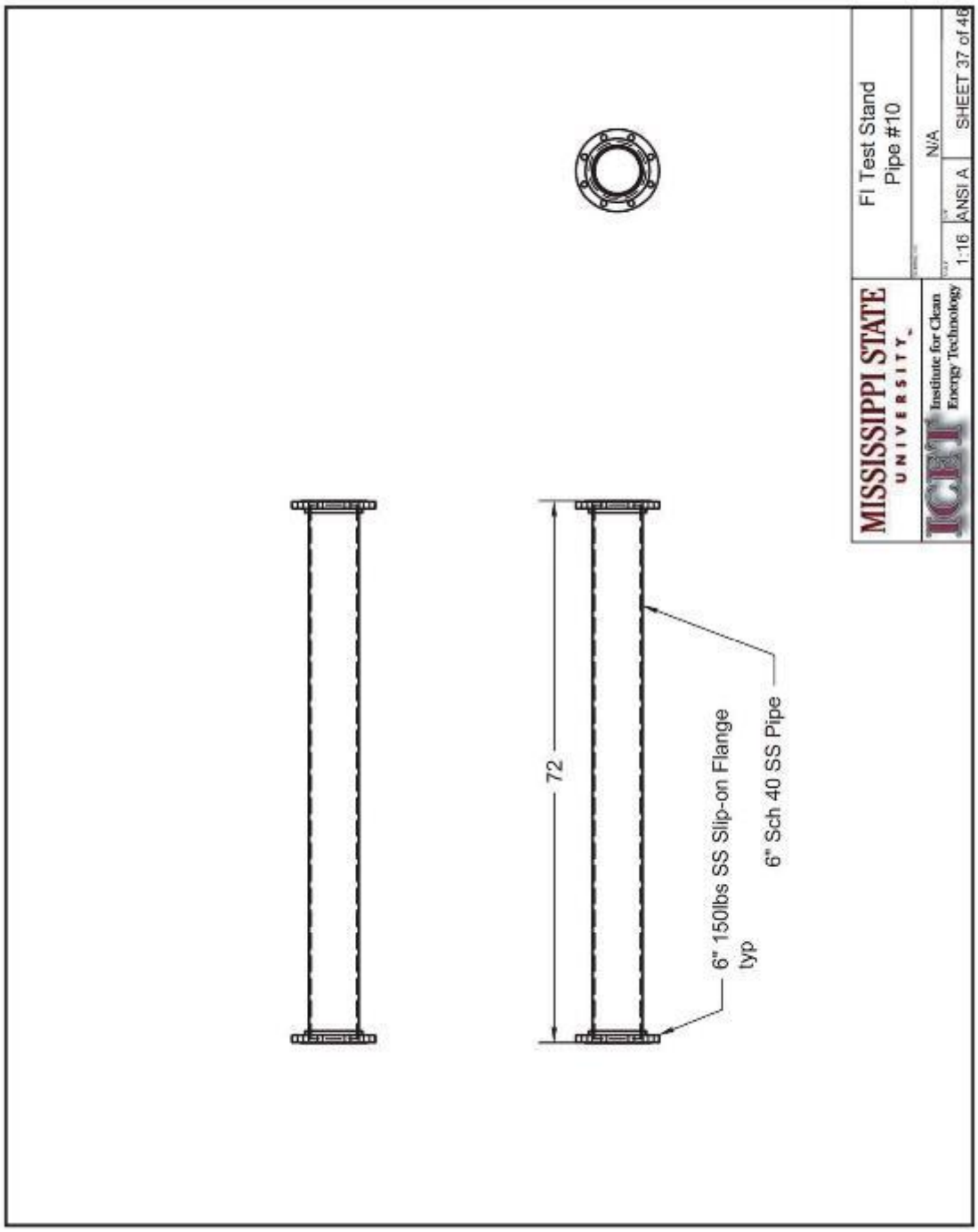

Figure 109 FI test stand pipe #10

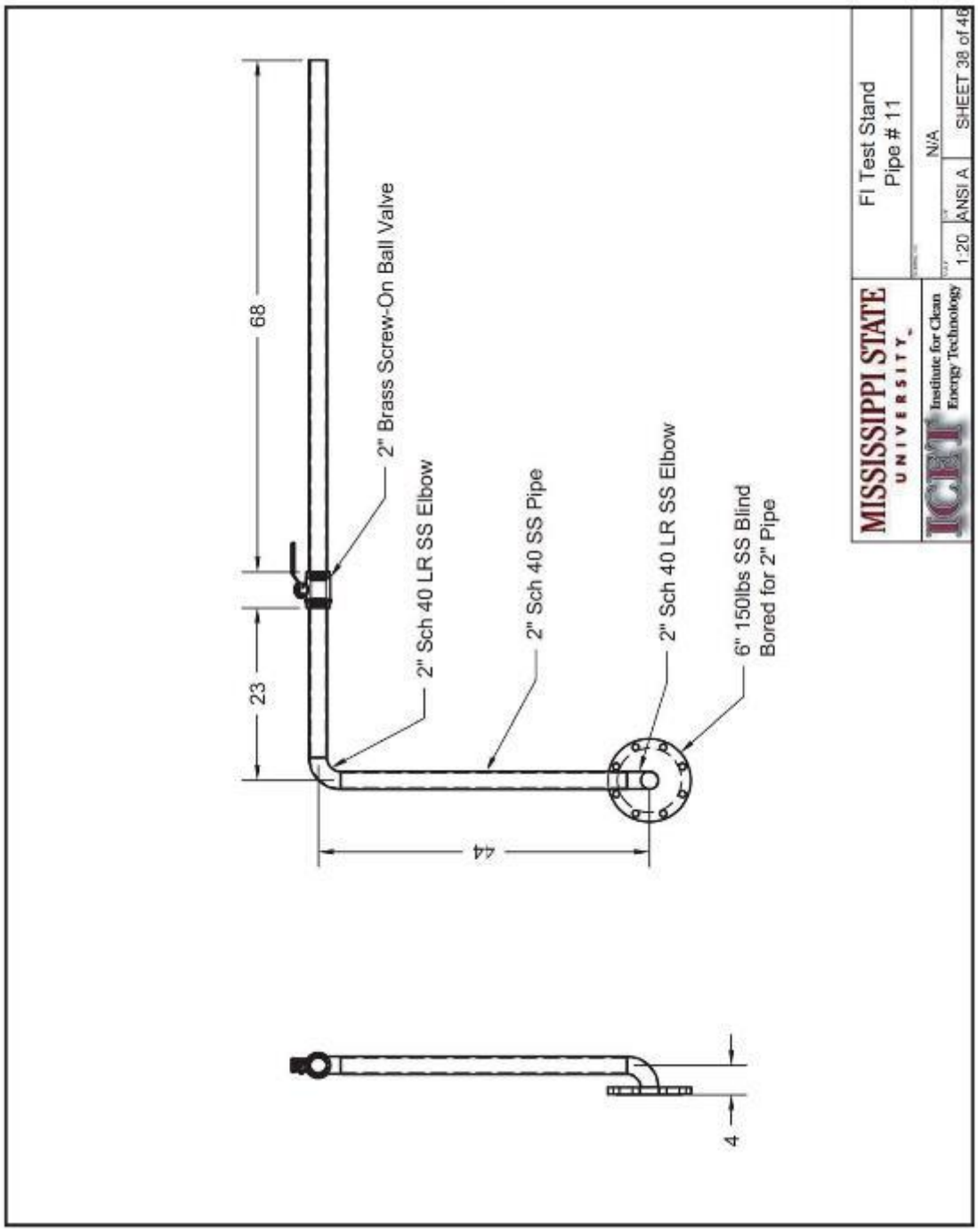

Figure 110 FI test stand pipe #11

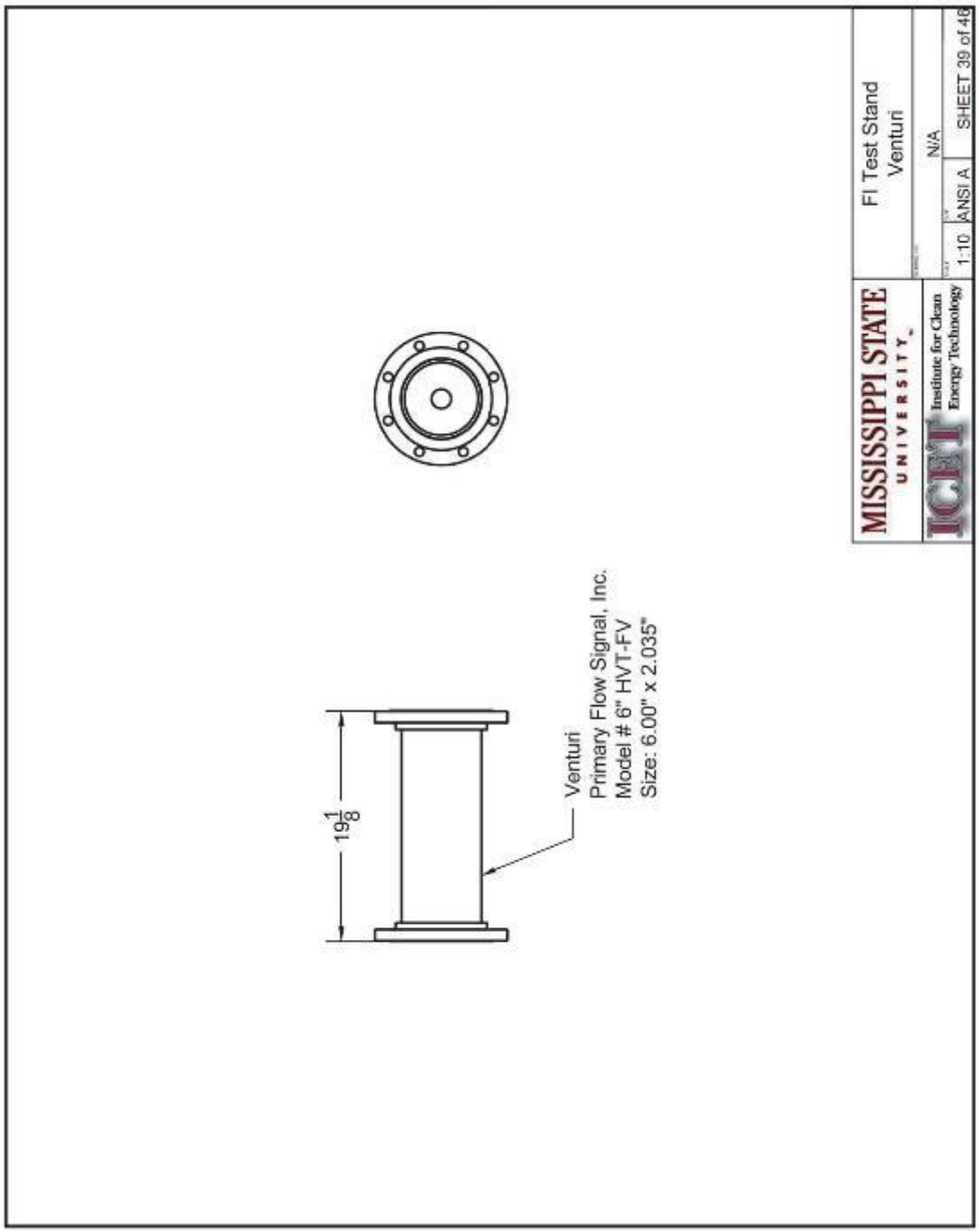

Figure 111 FI test stand venturi

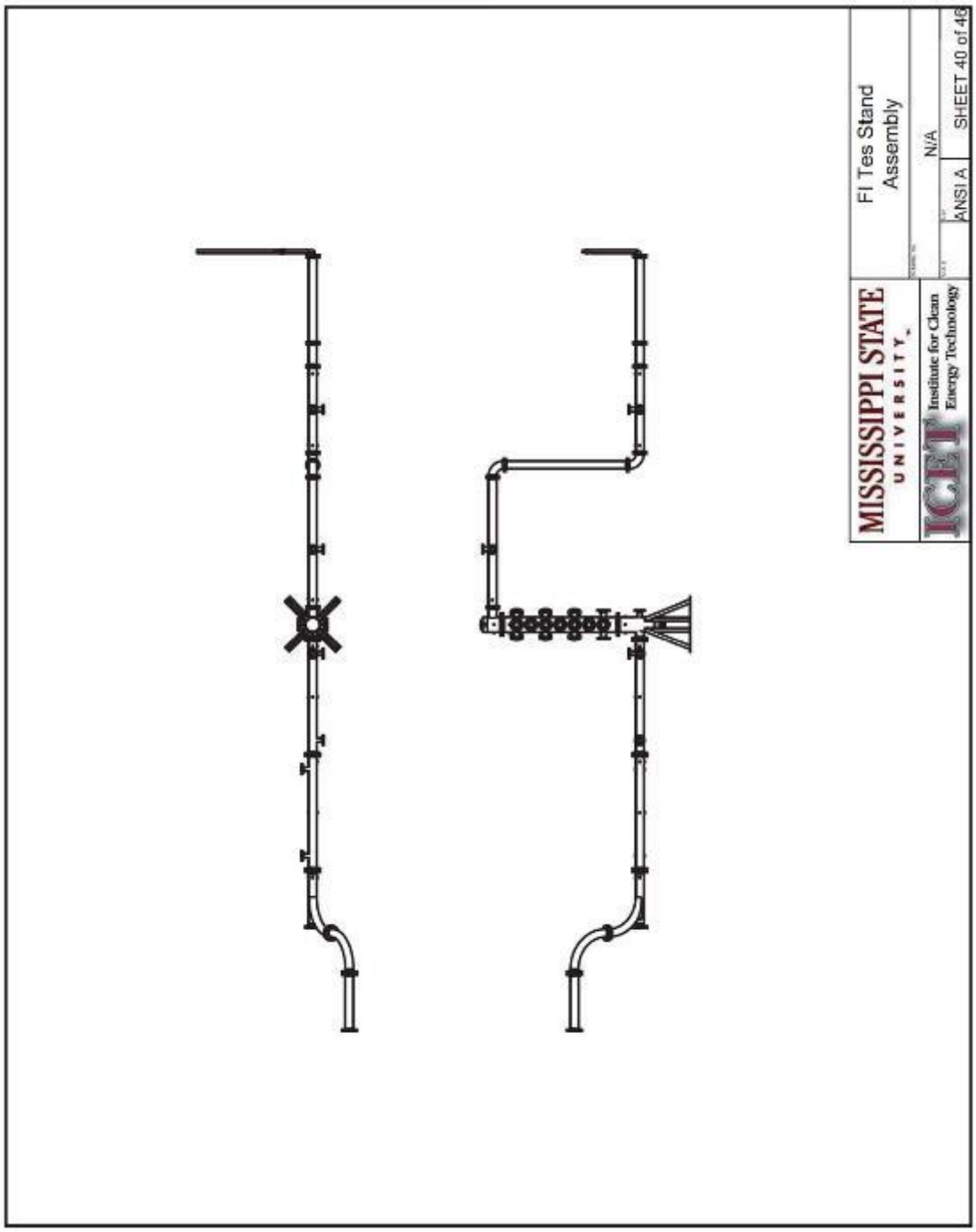

Figure 112 FI test stand assembly

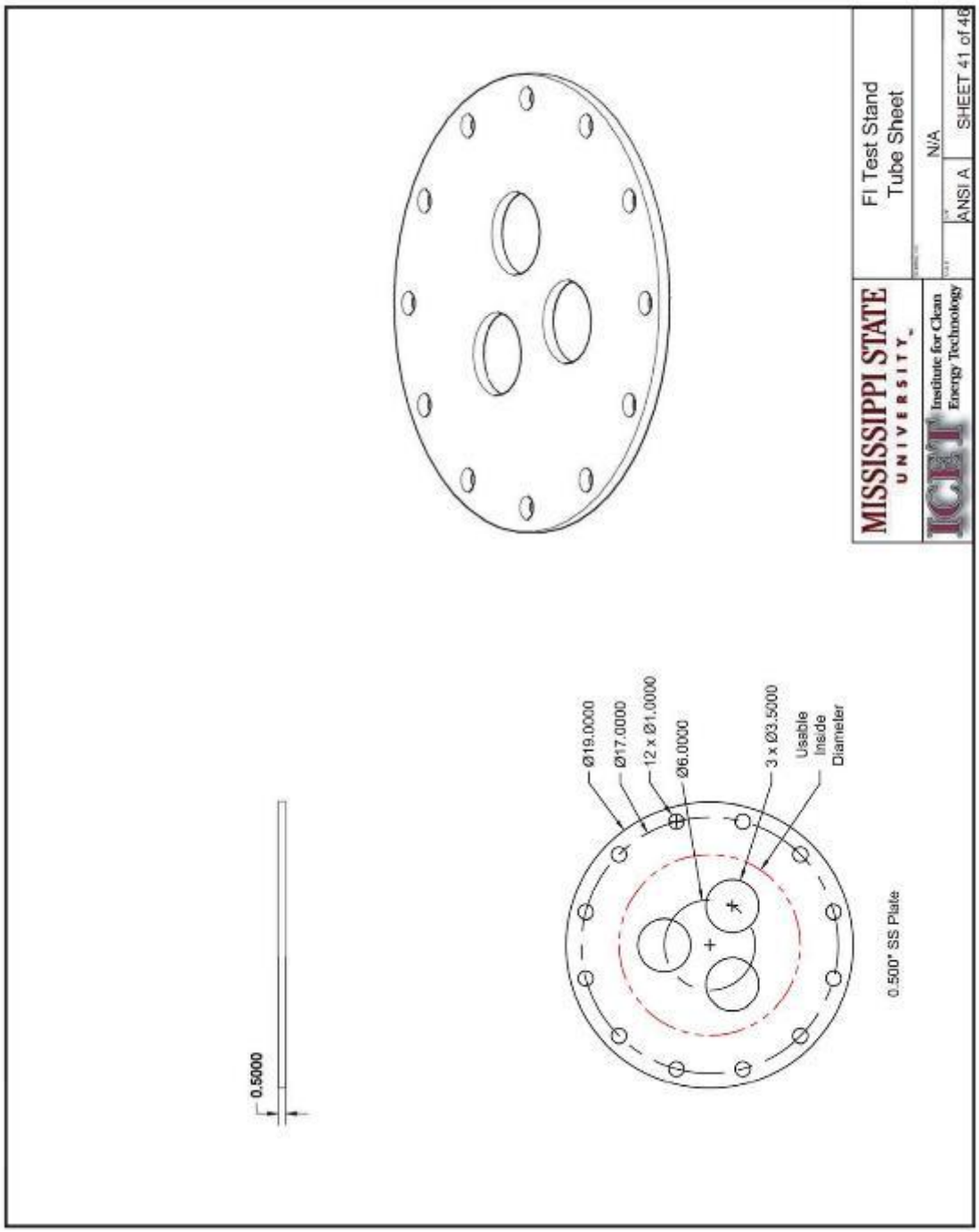

Figure 113 FI test stand tube sheet

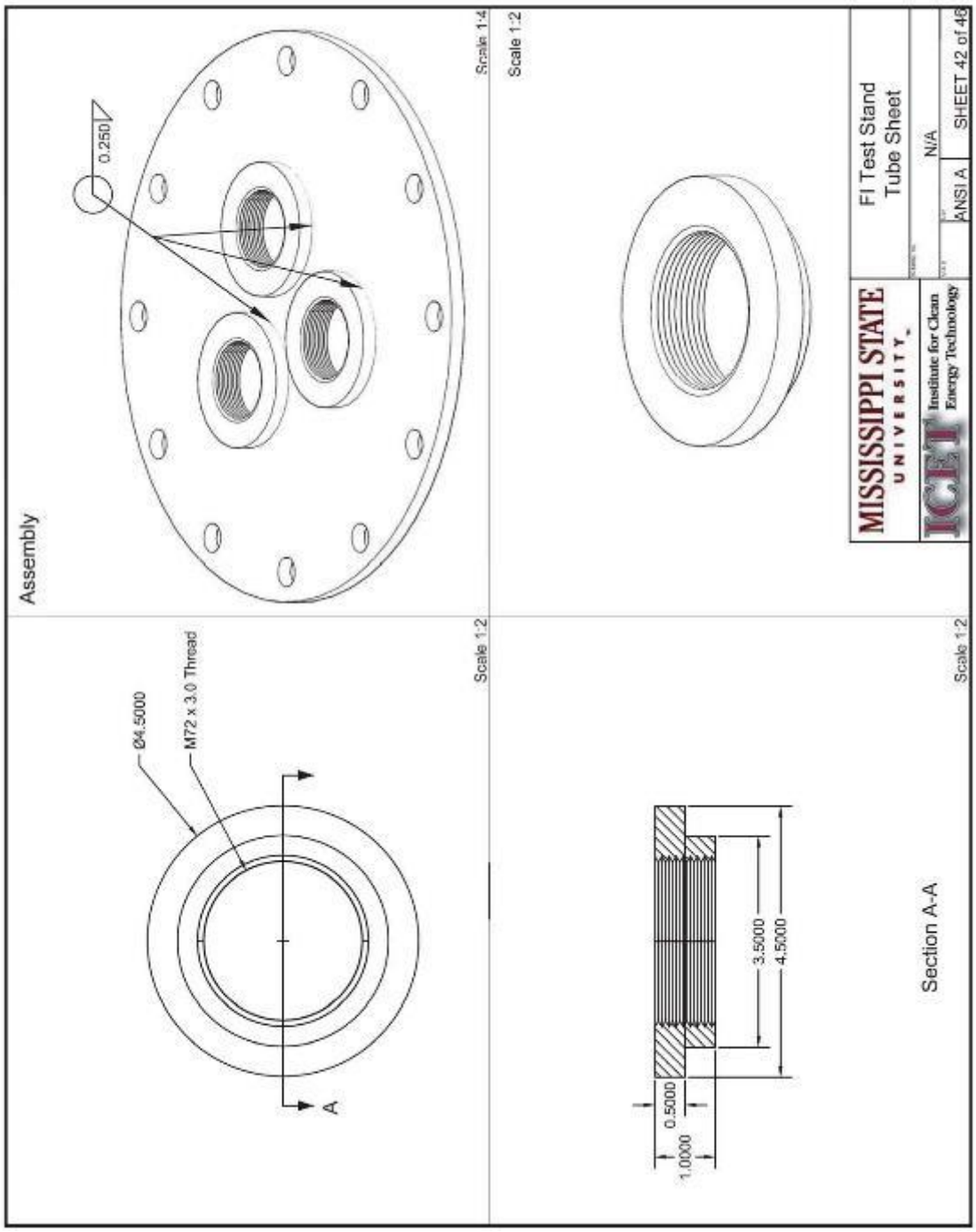

Figure 114 FI test stand tube sheet drawing 2

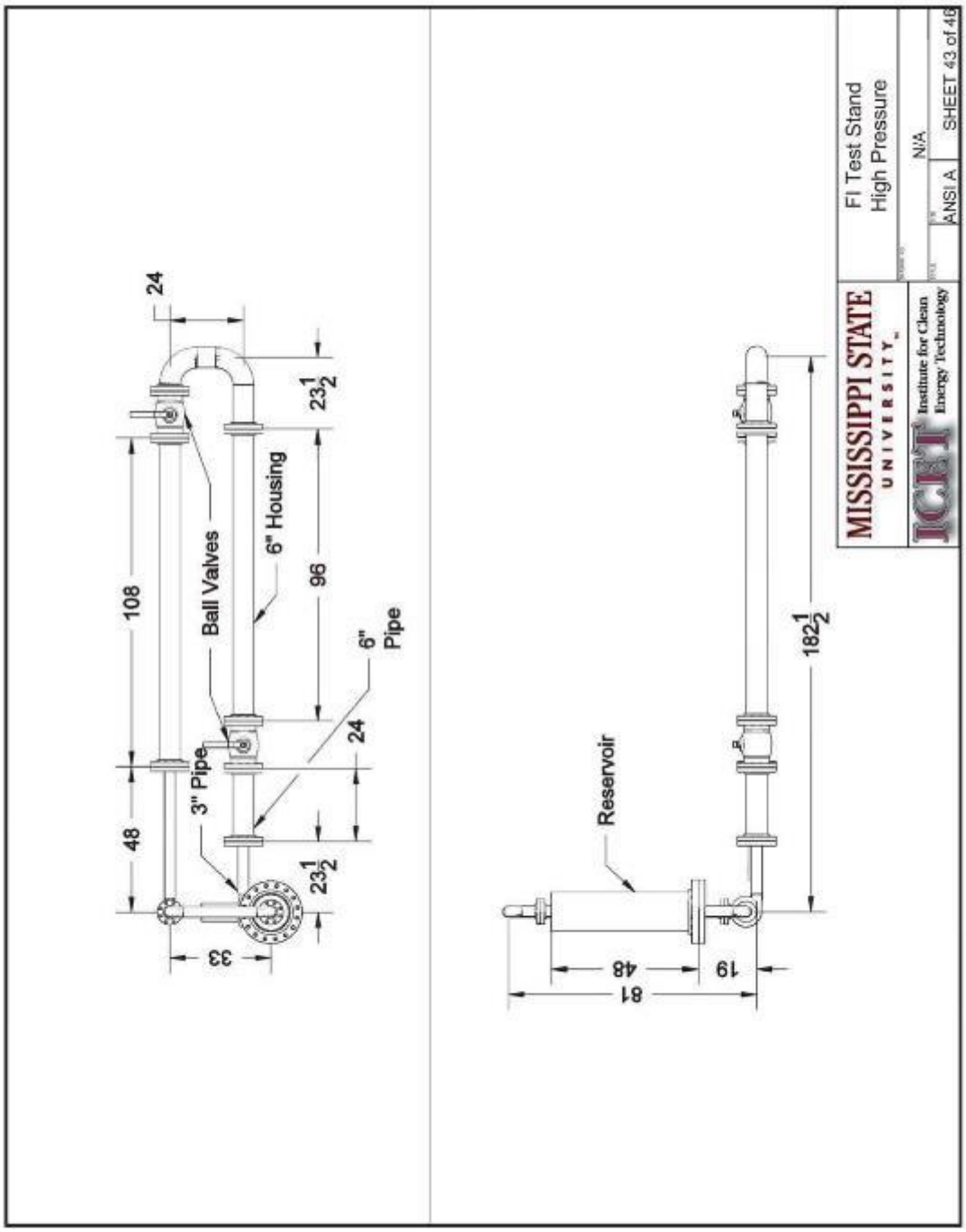

Figure 115 FI test stand high pressure

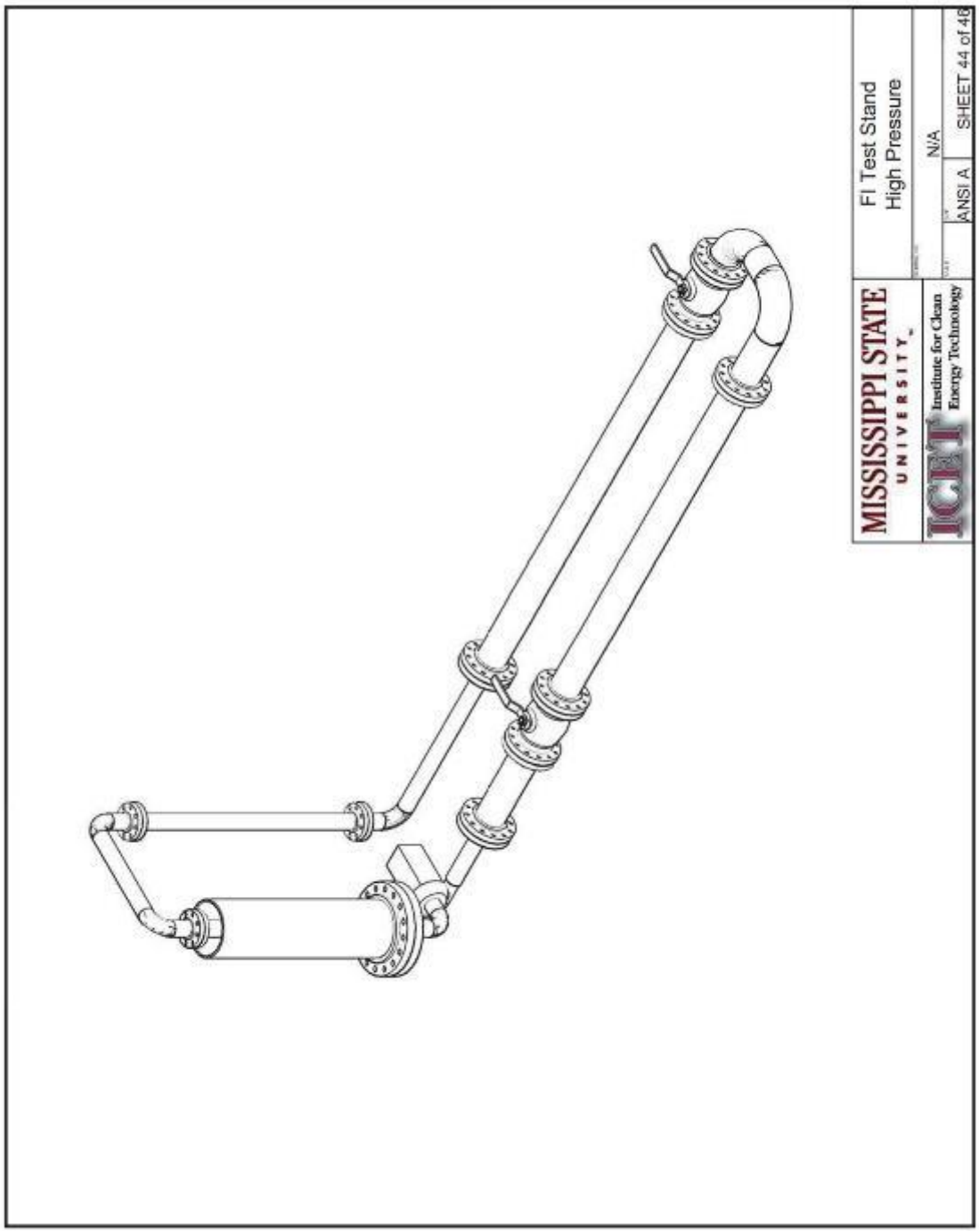

Figure 116 FI test stand high pressure drawing 2

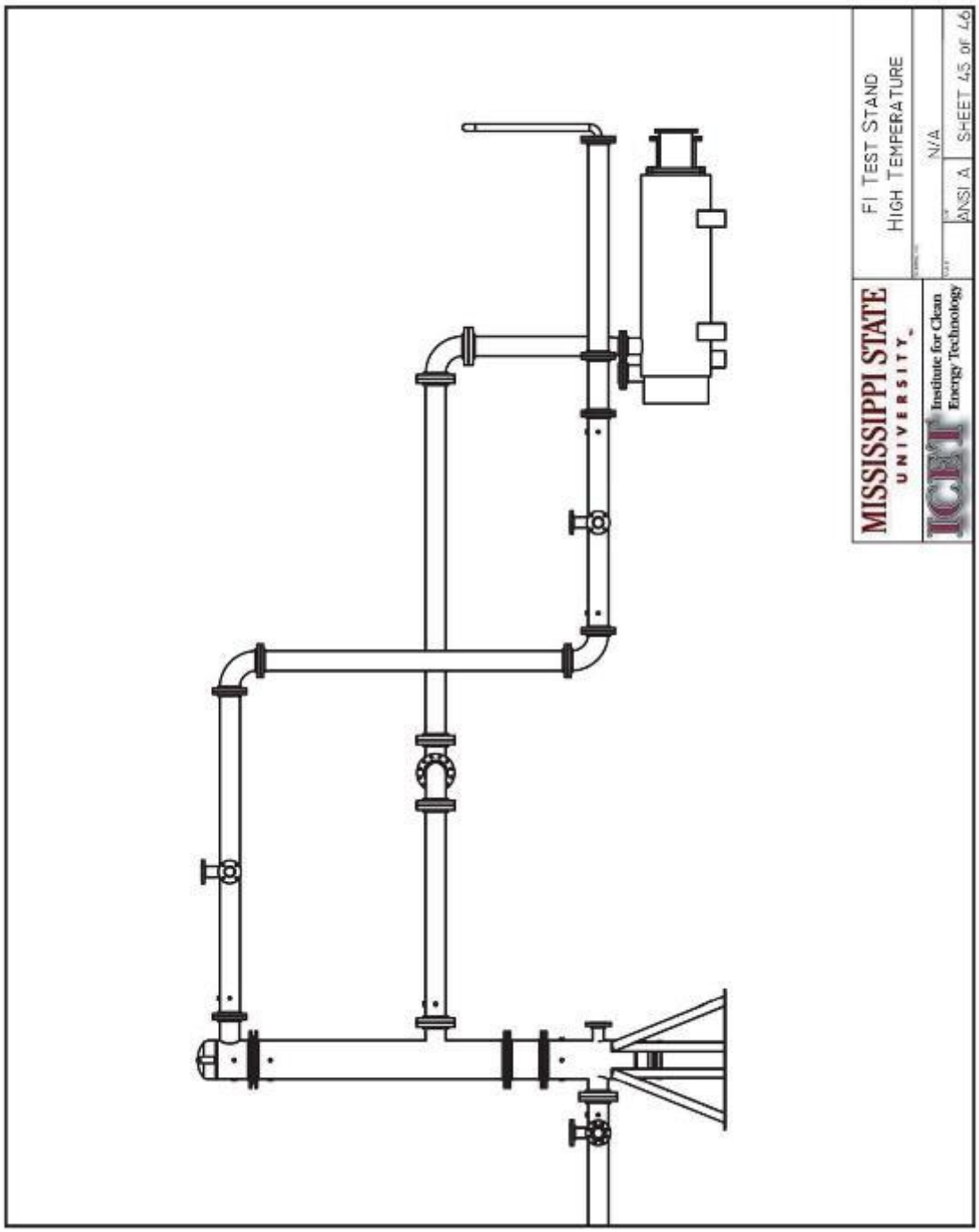

Figure 117 FI test stand high temperature

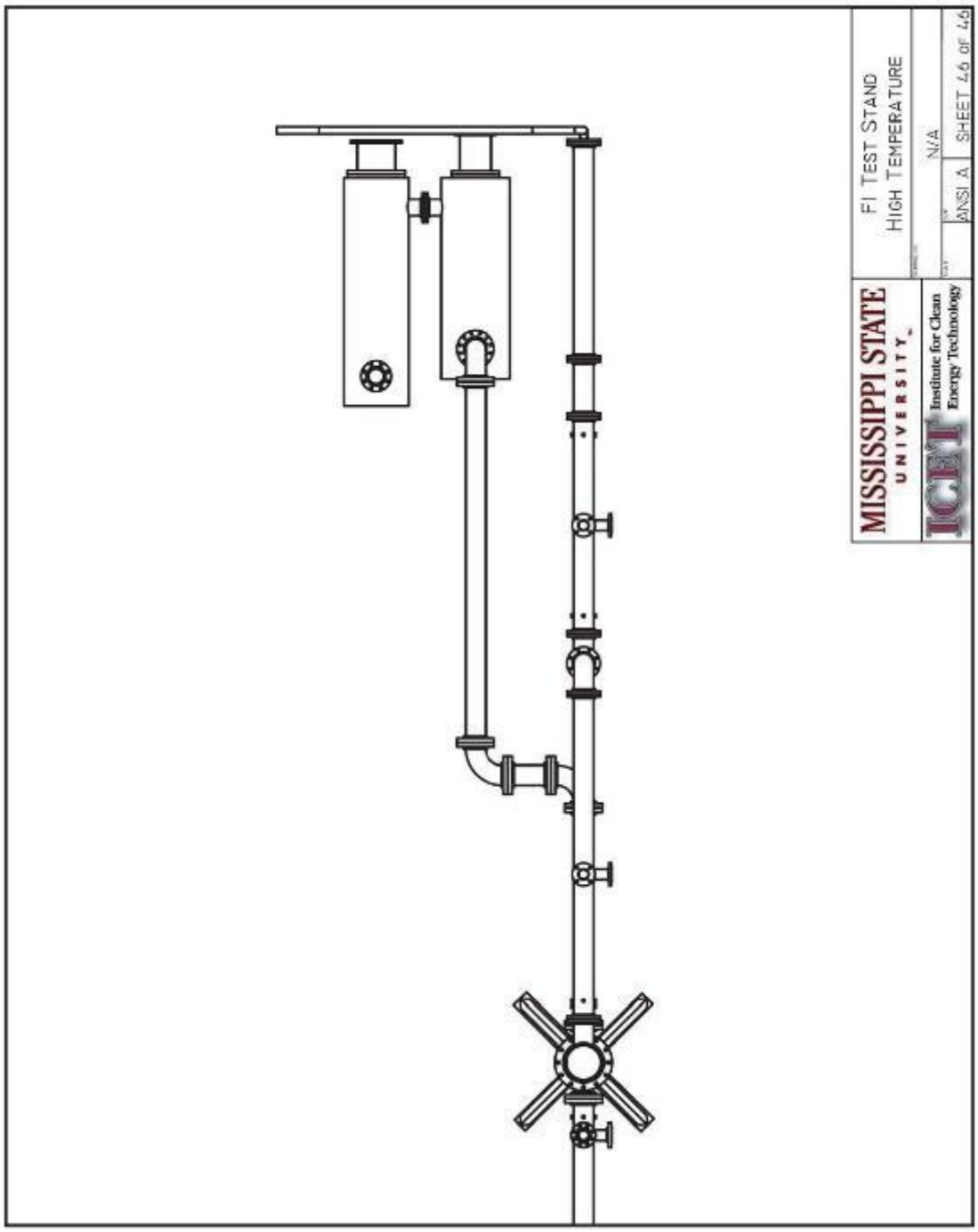

Figure 118 FI test stand high temperature drawing 2

APPENDIX C

FI TEST STAND TEMPERATURE AND RELATIVE HUMIDITY CONTROL INSTRUCTIONS

FI test stand temperature and relative humidity control instructions

1.0 Ensure that the test stand is ON and filters installed properly.
2.0 Operate test stand for 1 hour
3.0 Record temperature and relative humidity
4.0 Determine parameter that is outside of specified range (Temperature 60-80^{o}F and relative humidity 40-60%)
5.0 Adjust heat bypass, chiller bypass, or chiller temperature according to the following troubleshooting procedure.
    5.1 **Problem:** Problem: Temperature too low
        5.1.1 **Fix:** Reduce bypass on reheat heat exchanger or raise temperature on chiller
    5.2 **Problem:** Temperature too high
        5.2.1 **Fix:** Increase bypass on reheat heat exchanger or decrease temperature on chiller
    5.3 **Problem:** Relative Humidity too low
        5.3.1 **Fix:** Increase temperature on chiller
    5.4 **Problem:** Relative Humidity too high
        5.4.1 **Fix:** Decrease temperature on chiller
    5.5 **Problem:** Temperature too low relative humidity too low
        5.5.1 **Fix:**Increase Chiller temperature if temperature still low decrease reheat heat exchanger bypass
    5.6 **Problem:** Temperature too low relative humidity too high
        5.6.1 **Fix:** Decrease chiller temperature and decrease reheat heat exchanger bypass
    5.7 **Problem:** Temperature too high relative humidity too low
        5.7.1 **Fix:** Bypass reheat heat exchanger and increase chiller temperature (Most difficult problem to fix)
    5.8 **Problem:** Temperature too high relative humidity too high
        5.8.1 **Fix:** Decrease chiller temperature and decrease reheat heat exchanger bypass
6.0 Adjust suggested parameter and allow test stand to operate for 10 minutes.
7.0 Parameter Adjustment
    7.1 Parker Hyperchill (Chiller) Follow instructions in hyperchill user manual
8.0 Record temperature and relative humidity
9.0 If out of range repeat step 5. If within range begin testing
10.0 Monitor conditions throughout testing.

APPENDIX D

FI HEPA FILTER TEST STAND ASSEMBLY AND DISASSEMBLY

INSTRUCTIONS

FI HEPA filter test stand assembly and disassembly

Assembly

1.0 Using chain hoist and slings insert tube sheet with filter elements into middle section of the housing which is standing up right on the ground (not on base) and use bolts to secure into place
2.0 Lift middle section of housing and tube sheet with filters from the ground onto base of housing using chain hoist attached to slings.
3.0 Bolt the middle section of housing to the base of the housing at the connecting flanges
4.0 Remove Chain hoist and slings once middle section of the housing is attached.
5.0 Attach the chain hoist and slings to the cap of the filter housing and lift and set in place on top of the middle section.
6.0 Using the connection flanges bolt the cap to the base of the housing and the downstream section of piping. Loosen the tension from the chain hoist slings and leave attached to housing cap.
7.0 Check all bolts and connections to ensure the housing is securely bolted down.

Disassembly

1.0 Turn test stand flow OFF.
2.0 Connect cap to chain hoist and remove bolts connecting cap to middle section and downstream piping.
3.0 Using chain hoist lift and remove cap of housing.
4.0 Secure the tube sheet to the middle section of housing with bolts.
5.0 Lift middle section of housing and tube sheet with filters from base of housing using chain hoist attached to slings and lower to the ground next to the test stand.
6.0 Remove bolts securing tube sheet to housing and remove slings from middle section of housing
7.0 Using chain hoist and slings remove tube sheet with filter elements attached from the middle section of the housing and place on stand.
8.0 Unscrew and remove individual filter elements from tube sheet

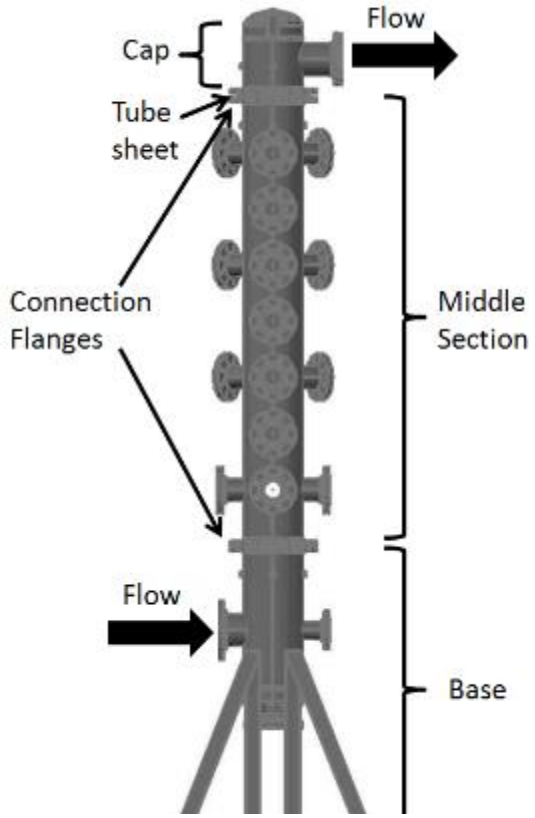

Figure 119 Housing of FI test stand showing sections and connection points

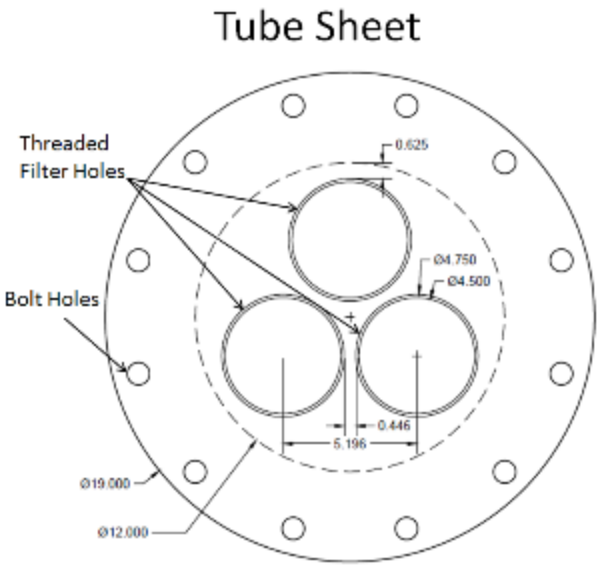

Figure 120 Tube sheet for FI metal media elements